THESIS

NEAR-PROTOTYPE TESTING OF WEDGE-BLOCK OVERTOPPING PROTECTION

Submitted by

Gustav George Slovensky Jr.

Department of Civil Engineering

In partial fulfillment of the requirements

for the Degree of Master of Science

Colorado State University

Fort Collins, Colorado

Spring, 1993

COLORADO STATE UNIVERSITY

APRIL 5, 1993

WE HEREBY RECOMMEND THAT THE THESIS PREPARED UNDER OUR SUPERVISION BY GUSTAV GEORGE SLOVENSKY JR. ENTITLED NEAR-PROTOTYPE TESTING OF WEDGE-BLOCK OVERTOPPING PROTECTION BE ACCEPTED AS FULFILLING IN PART, THE REQUIREMENTS FOR THE DEGREE OF MASTER OF SCIENCE.

Committee on Graduate Work

Advisor

Department Head

ABSTRACT

NEAR-PROTOTYPE TESTING OF WEDGE-BLOCK OVERTOPPING PROTECTION

Thousands of embankment dams in the U.S. presently have insufficient storage and/or spillway capacity to accommodate the Probable Maximum Flood (PMF). This situation is the result of a growth of historical flood and precipitation records which has improved estimates of the PMF. The two most obvious solutions to the problem, raising dam heights or increasing spillway capacities, are often prohibitively expensive. A promising alternative to these is to place a protective overlay on the downstream face of the dam which will allow it to be safely overtopped.

Previous research has investigated a variety of protection measures ranging from geotextiles to concrete blocks. In the present study, overlapping wedge blocks were tested on a near prototype scale. The tested blocks were approximately 1.25 feet (0.38 meters) long, 2 feet (0.61 meters) wide, and had an average thickness of 0.23 feet (0.07 meters). Drain holes were located beneath the overlapping lip of each block to facilitate the removal of seepage flows moving through the 6 inches (152 mm) of coarse drain material beneath the blocks. Testing took place in a 5 foot (1.5 meter) wide flume constructed on a 2H:1V slope which provided approximately 50 feet of vertical drop. The overlay was subjected to five unit discharges ranging from 2.8 to 31.6 ft^2/s (0.26 to 2.94 m^2/s) for four hours each and was stable in all cases.

Available results of previous model and prototype scale tests are presented to

facilitate comparison of the abilities of different protection systems and to illustrate the superiority of wedge and stepped-block designs.

The theoretical dependency of hydrodynamic pressures on such flow parameters as depth, velocity, and degree of aeration are discussed and used to explain variations in pressures observed in the near-prototype testing results.

Pressure data from piezometers located on the blocks and in the drainage layer are used to quantify the variation of block stability with location. Explanations are offered for observed variations. The pressure data is also used to present a qualitative picture of how movement of water through overlay drains varies with location on the embankment and unit discharge.

Finally, pressure data from the near-prototype study are compared to data obtained in an a smaller scale model study conducted by the U.S. Bureau of Reclamation. Froude criterion was used to scale model pressures up for comparison to near-prototype values. Pressure profiles at corresponding locations and discharges were found to compare quite well.

Gustav George Slovensky Jr.
Department of Civil Engineering
Colorado State University
Fort Collins, CO 80523
Spring 1993

To Kathy
Working on this
Enjoyed
with you

George S.
May, 1993

TO

MY PARENTS

BARBARA AND GUS SLOVENSKY

WITH GRATITUDE AND APPRECIATION

GUSTAV GEORGE SLOVENSKY JR.
SPRING, 1993

TABLE OF CONTENTS

CHAPTER ONE
INTRODUCTION 1
Objectives 5

CHAPTER TWO
REVIEW OF LITERATURE 7
Non-Stepped Protection Measures 7
Model Tests of Stepped Protection Measures 20
Prototype Installations of Stepped Protection Measures 38
Results of Russian Model and Prototype Testing 40

CHAPTER THREE
WEDGE-BLOCK FLOW CHARACTERISTICS AND THEORETICAL CONSIDERATIONS 46
General Characteristics of Flow Over a Wedge-Block Overlay 46
Theoretical Discussion of Recirculation Region 48
Theoretical Discussion of Impact Region 50
Theoretical Discussion of Overlay Failure 51

CHAPTER FOUR
DESCRIPTION OF NEAR-PROTOTYPE TESTING OF WEDGE-BLOCK PROTECTION 57
Description of Testing Facility 57
Testing Procedures and Setup 60

CHAPTER FIVE
RESULTS OF NEAR-PROTOTYPE TESTING OF WEDGE-BLOCK PROTECTION 72
Analysis of Pressure Data 72
Depth Data 97
Velocity Data 97
Block Movements 99
Comparison of Model and Near-Prototype Results 100

CHAPTER SIX
SUMMARY AND CONCLUSIONS 106

LIST OF FIGURES

Figure 2.1.	Cellular Concrete Protection Units Used in SLA Phase II Tests	18
Figure 2.2.	Salford University Test Block Shapes	22
Figure 2.3.	Impact Pressure as a Function of Step Height to Length Ratio (Baker, 1990)	25
Figure 2.4.	Drainage Layer Pressures as a Function of Unit Discharge and Drainage Hole Area (Baker, 1990)	25
Figure 2.5.	Pressure Profiles for Horizontal Steps, q = 6.71 ft^2/s (0.62 m^2/s), Overtopping Head = 1.67 feet (0.51 meters) (Frizell, 1992)	29
Figure 2.6.	Pressure Profiles for 15 Degree Steps, q = 6.71 ft^2/s (0.62 m^2/s), Overtopping Head = 1.67 feet (0.51 meters) (Frizell, 1992)	29
Figure 2.7.	USBR Model Test Velocity Profiles, Step 23, q = 6.71 ft^2/s (0.62 m^2/s), Overtopping Head = 1.67 feet (0.51 meters) (Frizell, 1992)	31
Figure 2.8.	Variation of Energy Dissipation with Unit Discharge for 15 Degree Steps (Frizell, 1992)	32
Figure 2.9.	Comparison of Energy Dissipation Characteristics for Smooth Surfaces and Stepped Surfaces with Horizontal and 15 Degree Steps, q = 6.71 ft^2/s (0.62 m^2/s), Overtopping Head = 1.67 feet (0.51 meters) (Frizell, 1992)	33
Figure 2.10.	Recommended Average Block Thickness (Grinchuk and Pravdivets, 1977)	43
Figure 2.11.	Recommended Average Block Thickness (Pravdivets et al, 1980)	43
Figure 2.12.	Correction Factor Φ Used for Stepped Spillway Depth Calculations, Yc = critical depth, L = downslope distance (Pravdivets and Bramley, 1989)	45
Figure 3.1.	Flow Over a Wedge-Block Overlay	47
Figure 3.2.	Theoretical Nappe Equation Superimposed on CSU Near-Prototype Embankment	56
Figure 4.1.	Plan View of CSU/USBR Dam Safety Overtopping Facility	58
Figure 4.2.	Profile of CSU/USBR Dam Safety Overtopping Facility	59
Figure 4.3.	Rating Curve for CSU/USBR Dam Safety Overtopping Facility	60
Figure 4.4.	Drain Material Size Distribution Range	62
Figure 4.5.	Typical Section of Wedge-Block Overlay and Drainage Layer	63
Figure 4.6.	Completed CSU/USBR Dam Safety Overtopping Facility and Wedge-Block Overlay	64
Figure 4.7.	CSU/USBR Dam Safety Overtopping Facility Operating at a Unit Discharge of 8 ft^2/s (0.74 m^2/s)	65
Figure 4.8.	Wedge-Block Dimensions and Tap Locations	67
Figure 5.1a.	Average Step Pressure Distributions, Unit Discharge = 2.8 ft^2/s (0.26 m^2/s)	74

Figure 5.1b. Differences of Maximum and Minimum Step Pressure Heads from Average Values, Unit Discharge = 2.8 ft^2/s (0.26 m^2/s) 74
Figure 5.2a. Average Step Pressure Distributions, Unit Discharge = 8 ft^2/s (0.74 m^2/s) 75
Figure 5.2b. Differences of Maximum and Minimum Step Pressure Heads from Average Values, Unit Discharge = 8 ft^2/s (0.74 m^2/s) 75
Figure 5.3a. Average Step Pressure Distributions, Unit Discharge = 14.8 ft^2/s (1.37 m^2/s) 76
Figure 5.3b. Differences of Maximum and Minimum Step Pressure Heads from Average Values, Unit Discharge = 14.8 ft^2/s (1.37 m^2/s) 76
Figure 5.4a. Average Step Pressure Distributions, Unit Discharge = 22.8 ft^2/s (2.12 m^2/s) 77
Figure 5.4b. Differences of Maximum and Minimum Step Pressure Heads from Average Values, Unit Discharge = 22.8 ft^2/s (2.12 m^2/s) 77
Figure 5.5a. Average Step Pressure Distributions, Unit Discharge = 31.6 ft^2/s (2.94 m^2/s) 78
Figure 5.5b. Differences of Maximum and Minimum Step Pressure Heads from Average Values, Unit Discharge = 31.6 ft^2/s (2.94 m^2/s) 78
Figure 5.6. Impact Force Per Unit Step Width 80
Figure 5.7. Variation of Pressure Distribution with Unit Discharge at Step Number 14 Below the Crest 80
Figure 5.8. Variation of Pressure Distribution with Unit Discharge at Step Number 84 Below the Crest 81
Figure 5.9a. Average Drainage Layer Pressures 84
Figure 5.9b. Differences of Maximum and Minimum Drainage Layer Pressure Heads from Average Values 84
Figure 5.10. Block Pressure Forces Considered in Stability Analysis 87
Figure 5.11. Summation of Step Tread Pressure Forces Per Unit Width 88
Figure 5.12. Summation of All Pressure Forces Per Unit Width Acting on Wedge Blocks 90
Figure 5.13. Pressure Head Difference Between Bottom and Top Block Surfaces Near the Overlay Drains, Unit Discharge = 2.8 ft^2/s (0.26 m^2/s) 92
Figure 5.14. Pressure Head Difference Between Bottom and Top Block Surfaces Near the Overlay Drains, Unit Discharge = 8 ft^2/s (0.74 m^2/s) 92
Figure 5.15. Pressure Head Difference Between Bottom and Top Block Surfaces Near the Overlay Drains, Unit Discharge = 14.8 ft^2/s (1.37 m^2/s) 93
Figure 5.16. Pressure Head Difference Between Bottom and Top Block Surfaces Near the Overlay Drains, Unit Discharge = 22.8 ft^2/s (2.12 m^2/s) 93
Figure 5.17. Pressure Head Difference Between Bottom and Top Block Surfaces Near the Overlay Drains, Unit Discharge = 31.6 ft^2/s (2.94 m^2/s) 94
Figure 5.18. Calculated Unaerated Flow Depths 98
Figure 5.19. Flow Depths (Aerated) Obtained Using the DMI Distance Probe 98
Figure 5.20. Flow Depths Obtained by Point Gage 99

Figure 5.21a. Comparison of Model Pressure Profile at Step 15 with Bracketing Near-Prototype Profiles at Step 14 101
Figure 5.21b. Comparison of Model Pressure Profile at Step 15 With Bracketing Near-Prototype Pressure Fluctuation Bands at Step 14 (Band Width = 2 Standard Deviations) 101
Figure 5.22. Difference Between Expected Model Pressures and Those Actually Recorded at Model Step 15 for Four Scaled Up Model Unit Discharges 103
Figure 5.23a. Comparison of Model Pressure Profile at Step 15 with Bracketing Near-Prototype Profiles at Step 44 103
Figure 5.23b. Comparison of Model Pressure Profile at Step 47 With Bracketing Near-Prototype Pressure Fluctuation Bands at Step 44 (Band Width = 2 Standard Deviations) 104
Figure 5.24. Difference Between Expected Model Pressures and Those Actually Recorded at Model Step 47 for Four Scaled Up Model Unit Discharges 104

LIST OF TABLES

Table 2.1.	CIRIA Tests On Erosion Protection of Steep Grassed Waterways	9
Table 2.2.	SLA Phase I Tests of Highway Embankment Protection Measures	11-12
Table 2.3.	SLA Phase II Tests of Highway Embankment Protection Measures	14-16
Table 2.4.	Geotextiles Used In SLA Testing	17
Table 2.5.	USBR Testing of Small Embankment Overtopping Protection	19
Table 2.6.	Dimensions of Salford University Test Blocks	22
Table 2.7.	Model Testing of Stepped Spillways (CIRIA, 1992)	36-37
Table 2.8.	Prototype Installations of Stepped Block Protection (CIRIA, 1992)	41
Table 4.1.	Five Discharges Tested at the CSU/USBR Near Prototype Facility	66
Table 5.1.	Negative Pressure Zone Size as a Function of Unit Discharge	96
Table 5.2.	Measured Flow Velocities	99

CHAPTER ONE

INTRODUCTION

For hundreds of years, dams have provided mankind with irrigation and drinking water, flood control, recreation, and hydropower. It is not an overstatement to say that in many parts of the world, dams are an essential part of society's infrastructure (NRC, 1983).

In recent decades, the focus of water resources engineers and entities managing water resources has moved away from new construction and toward the safety and rehabilitation of existing dams. A number of factors have been responsible for this trend.

One of these factors is the high level of utilization to which many of the world's rivers are already subjected. Rivers, such as the Colorado River in the United States, are heavily developed and most of the best sites for large dams have already been exploited. Heavy development has also been a factor because it has made evident some adverse environmental impacts which accompany large dams. Groups concerned with the preservation of our natural environment have reacted to this and have made environmental issues a force to be reckoned with when planning a new impoundment.

Also contributing to the trend is the constant growth of historical flood and precipitation records. These have significantly increased estimates of the Probable Maximum Flood (PMF) in many areas. The net result is that many dams previously

thought to be safe are now deemed to have inadequate storage and/or spillway capacity to pass the PMF. Embankment dams are especially vulnerable to this deficiency because, generally, they will not withstand significant overtopping flows. The erosion that results from overtopping, has been identified as a principal cause of failure of embankment dams. Consequently, most members of the water resources engineering community assume that an embankment dam will fail if overtopped by a PMF or near-PMF event (Powledge et al, 1989).

In recent decades, evidence of this danger has been brought to light as a number of embankment dams have failed or nearly failed due to overtopping. Three examples of such failures can be taken from the month of June, 1972. On the ninth day of that month a single storm, estimated to be of a 100 year frequency, caused the overtopping and destruction of two embankment dams in South Dakota. Canyon Lake Dam, a small earth-fill structure, was overtopped and failed when hit with a flash flood from the western hills. The waters it released contributed to the costly flooding of Rapid City, South Dakota. Fort Mead Dam, a 56 foot (17 meter) high rock-fill structure near Sturgis, South Dakota also fell victim to the storm. It was overtopped by 1.5 feet (0.5 meters) for several hours and so badly eroded that what remained of the weakened structure had to be demolished (ASCE/USCOLD, 1975).

Ten days later, the northeastern region of the United States was experiencing extremely heavy rainfall from Tropical Storm Agnes. The resulting floods were of unprecedented magnitude and a number of dams were overtopped and damaged. Notable among these was the 69 foot (21 meter) high Lake Barcoft Dam located in northern

Virginia. This dam had a gravity center section with earth embankments on either side. On June 21, an overtopping depth of 1.3 feet (0.4 meters) eroded a 10 foot (3 meter) breach in the right embankment. Thankfully, the breach developed slowly and the left embankment held, so, impounded water was discharged gradually rather than all at once. The event was near catastrophic, though, for the one thousand people living downstream from the dam (ASCE/USCOLD, 1975).

Dam failures, such as the three examples given, helped to bring the issue of dam safety into the public eye and to the attention of legislators in the early 1970's. The Army Corps of Engineers' National Program for Inspection of Non-Federal Dams (PL 92-367) was partially an outgrowth of such events. The Corps inspection program, initiated in 1972, included all non-Federal dams over 25 feet (7.6 meters) high or with impoundment capacity over 50 acre-feet (61.7×10^3 m^3). Excluded were all structures less than 6 feet (1.8 meters) high and all structures with impoundment capacity less than 15 acre-ft (18.5×10^3 m^3). These size criteria was met by 63,367 dams. Of these, 8,639 were deemed to be high-hazard, meaning, that failure would cause loss of life or severe economic damage. Of the high-hazard dams, 2,884 were found to be potentially unsafe, and, in 2,687 of these, inadequate spillway capacity was at least a contributing factor. This in itself constitutes an enormous problem, but further, it is reasonable to assume that the 54,728 dams not deemed high-hazard were designed for less than the PMF. Therefore, the potential exists for these dams to be overtopped and as our population expands, more and more of them will fall into the high hazard category. Summarizing the results of the Corps' inspection program, the total number of non-

federal dams which may potentially experience overtopping exceeds 57,000. This number includes all dam types but a non-comprehensive survey, published jointly by ASCE and the U.S. Committee on Large Dams (USCOLD), indicates that the majority are of the embankment variety. That report states that, as of 1972, 73 percent of dams in the U.S. were earth-fill.

The USCOLD report also provides a history of dam failures in the U.S. It states that there have been 18 failures of embankment dams in the U.S. as a result of overtopping between 1900 and 1979. Further, this number constitutes 26 percent of reported failures in all dam type categories (ASCE/USCOLD, 1975 and NRC, 1983).

The results of another non-comprehensive survey of dams over 49 feet (15 meters) high, published by the International Committee on Large Dams (ICOLD), contains a history of international dam failures. That report indicates that overtopping has been responsible for 35 percent of all embankment dam failures between 1900 and 1975 in responding countries (NRC, 1983).

One estimate suggests that the correction of all unsafe dams could cost over 6.8 billion dollars (Bivins, 1984). Given that 73 percent of U.S. dams are earth-fill, a very large percentage of the correction cost estimate must be attributable to this dam variety. Obviously, financing this work presents a huge problem. In 1982 the Army Corps of Engineers reported that no remedial measures had been instituted at 64 percent of the unsafe dams found during its four year inspection program, principally, because of owners lack of resources (Corps, 1982). This statistic makes obvious the need for a lower cost alternative to raising dam heights or increasing spillway capacities.

At present, the most attractive alternative appears to be placement of an overlay on the downstream slope of the embankment dam which protects the underlying fill in the event of overtopping. A good deal of research, including the present study of wedge-block protection, has been conducted in this area. To date, this research indicates that planned overtopping of embankment dams is a viable alternative to increasing spillway capacities or raising dam heights.

OBJECTIVES

The U. S. Bureau of Reclamation, as the owner of over 250 dams in the U.S, has taken a great interest in overtopping protection. They have been conducting research in this area since the early 1980's. The research results indicate that overlapping concrete blocks covering the downstream embankment face may be a viable option for protection against overtopping flows. The present study of wedge-block protection was conducted by the USBR in two phases and began in January of 1990. The first phase consisted of laboratory tests, carried out at the USBR Hydraulics Laboratory, which were intended to identify the geometry of overlay blocks which produced an optimum balance of energy dissipation and separation zone pressure reduction. To this end, three different geometries were tested for application on an embankment slope of 2H:1V. It was found that a block with a step height to length ratio of 1:4.6 and a tread surface sloped downward from horizontal by 15 degrees, provided the desired combination of characteristics for an embankment slope of 2H:1V. Further tests are planned to determine how block geometry should be changed for other embankment slopes.

The second phase of the USBR study consisted of near-prototype modeling of an embankment protected with the chosen block geometry. It was accomplished through a cooperative agreement between the Bureau of Reclamation and Colorado State University. This phase of the study was carried out at an outdoor facility constructed for this purpose by Colorado State University at the Engineering Research Center on the Foothills Campus. This near-prototype experimentation is the subject of the current report and its objectives were as follows:

1. Investigate, on a near-prototype scale, the hydraulic characteristics of flow down an embankment protected with wedge-blocks of the chosen geometry.
2. Investigate hydraulic characteristics of the filter-layer.
3. Verify the stability of the overlay under near-prototype conditions and in the presence of a filter-layer.
4. Identify areas of the overlay which have lower hydrodynamic stability and suggest explanations.
5. Compare results of the model and near-prototype studies to see if extrapolation of tests results to larger embankments is possible.

CHAPTER TWO

REVIEW OF PREVIOUSLY RESEARCHED EMBANKMENT PROTECTION MEASURES

During recent years, many studies of measures designed to protect embankments during overtopping events have been conducted. Much of this research has taken place on large scale models because of the inaccuracies inherent in the scaling of complex hydraulic and erosional processes which take place in an overtopping flow (Powledge et al, 1989). In this chapter, a summary of the testing of measures other than stepped-block type protection is presented first. Then, experiences dealing specifically with stepped-block protection, both model studies and prototype installations, are presented. The presentation of data derived from testing of protection measures other than stepped blocks is intended to facilitate some general comparison of the abilities of different protection systems and to illustrate the superiority of the stepped block design. Note that this is not a comprehensive presentation of overtopping flow research because tests involving flow over unprotected (bare soil or grass) embankments have generally not been included.

NON-STEPPED PROTECTION MEASURES

CIRIA Full Scale Tests at Jackhouse Reservoir, Lancashire, England

In 1983, the Construction Industry Research and Information Association (CIRIA) commissioned a study on the use of concrete and geotextile products as erosion protection for steep, grassed waterways. Ten trapezoidal channels, 82 feet (25 meters) long and at

a slope of 2.5H:1V, were constructed on the face of a 33 foot (10.06 meter) high disused earthfill dam at Jackhouse Reservoir. Five channels were lined with precast concrete block products, four with geotextiles and one, the control channel, was lined with grass. All of the protected channels were then topsoiled, seeded and maintained for approximately 20 months before testing. The facility had a maximum discharge capacity of 40 ft^3/s (1.133 m^3/s) and a corresponding maximum channel velocity of approximately 26 ft/s (7.92 m/s) (Hewlett. 1987).

The tests conducted at Jackhouse Reservoir differed from others that will be presented in that, a true overtopping flow was never developed. Water was discharged directly onto the protected channel rather than allowing it to flow freely over a crest. This approach precluded the development of a region of reduced pressure near the crest that occurs with overtopping flows (Powledge et al, 1989). Additionally, in an overtopping situation, a destabilizing uplift pressure can develop beneath the overlay as a result of hydraulic connection of the overtopping head and the underside of the overlay. This also was not an element in the CIRIA sponsored tests. Rather, the intended focus of these tests was the stability of protection measures when subjected to erosive, high velocity flows on a steep grade. The results, therefore, will not be strictly comparable to the results of subsequent testing programs that will be discussed. The CIRIA tests at Jackhouse Reservoir have been summarized and are presented in Table 2.1.

Table 2.1. CIRIA Tests On Erosion Protection of Steep Grassed Waterways

PROTECTION MEASURE	DISCHARGE (ft^3/s)	TEST DURATION (hr)	VELOCITY	PERFORMANCE
Armorflex 140	12.2	1	15.4	Good
	13.2	1.25	15.7	Good
	11.7	3	15.1	Good
	26.0	0.75	22.6	Limited damage
	26.5	2, 2.5	23.0	Limited damage
	34.4	.75, 2, 2.5	26.2	Further damage
	35.6	.25, .25	26.6	Limited damage
Petraflex	6.1	0.75	13.1	Good
	5.8	1.5	13.1	Good
	6.3	3	13.8	Good
	27.4	1, 1.75, 2.5	23.3	Good
	37.5	0.75	25.9	Good
	38.7	1.5, 3	25.9	Limited damage
	4.8	1.75	11.5	Limited damage
Dycel	8.1	0.75	14.8	Good
	8.3	1.75	15.1	Good
	9.7	2.75	16.7	Good
	25.6	.75, 1.5, 3	22.6	Limited Damage
	33.5	0.25	24.9	Further damage
	36.7	.25, 1.5, 3	25.9	Further damage
	36.7	1	25.9	Limited damage
Dymex	5.8	0.75	13.1	Good
	6.2	1.75	13.5	Good
	4.9	1.50	12.8	Good
	5.8	0.50	13.1	Good
	4.4	0.50	11.8	Good
	10.6	1.00	14.8	Limited damage
	10.6	1.50	15.1	Further damage
	14.3	2.50	16.4	Failed
Grasscrete	4.6	0.75	14.4	Good
	6.5	1.5, 3	15.1	Good
	21.4	0.75	22.3	Good
	36.0	.5, .75, 3	25.9	Slight damage
	36.3	.5, .75	26.2	Further damage
	33.9	3	25.6	Further damage

NOTE: 1 ft^3/s = .0283 m^3/s

Simons, Li and Associates, Inc., Fort Collins, Colorado

Full scale tests of protection measures for overtopping of highway embankments have been conducted by Simons, Li & Associates, Inc. (SLA). Testing was accomplished in two phases. Phase I was jointly sponsored by the Federal Highway Administration (FHWA) and the U.S. Forest Service (USFS). The flume used for testing measured 4 feet (1.22 meters) wide, 11 feet (3.35 meters) high and, 90 feet (27.43 meters) long. The embankment height for all Phase I tests was 6 feet (1.83 meters) and downstream slopes of 2H:1V and 3H:1V were investigated. Crest widths, measured in the direction of flow, varied between 10 and 22 feet (3.05 and 6.71 meters). Overtopping depths tested ranged from 0.5 to 4 feet (0.15 to 1.22 meters) and the range of discharges was 1 to 25 ft^3/s (0.03 to 0.71 m^3/s). A variety of tailwater conditions were tested which ranged from only a 10 percent water surface drop to complete freefall. Protection measures tested included grass, soil cement, gabions and, geotextile type products. A summary of Phase I testing conditions and results is presented in Table 2.2. Descriptions of geotextiles used in both phases of testing is given in Table 2.4. Full details of Phase I testing can be found in Chen and Anderson (1986).

Phase II of the testing program was jointly sponsored by the FHWA and the USBR. The same flume, embankment height, range of slopes, and range of overtopping depths were used. Tailwater conditions ranged from 20 percent water surface drop to complete freefall. The crest width in the direction of flow was 20 feet (6.1 meters) in all cases. This second phase of testing investigated the stability of soil cement, gabions, geotextile type products and, precast cellular concrete block products. A summary of

Table 2.2. SLA Phase I Tests of Highway Embankment Protection Measures

PROTECTION TYPE	SLOPE (H:V)	OVERTOPPING HEAD (FT)	TAIL WATER DEPTH (FT)	TIME TO FAILURE OR END OF TEST (HR)	STABLE ?	PERFORMANCE REMARKS
Gabion Mattress	Mattress 6 in. thick and filled with 3-6 in rock. Dupont Typar 3401 filter fabric pined underneath mattress. Failure, defined as exposure of liner, did not occur.					
	2:1	1	0	2	YES	
	2:1	2	0	2	YES	
	2:1	4	0	2	YES	10-20% of upstream rocks migrated downstream.
Geoweb	Grid confinement system made of polyethylene. The 4 in. deep cells were filled with 1-2 in. rock. Typar 3401 was used as an underlayer. Failure occurs when flow boils rocks out of cells then impinges on cell walls. This results in impingement of flow on embankment and elongation of the system which exposes soil to erosion.					
	3:1	0.5	0	< 1	NO	
	3:1	1	0	< 1	NO	Elongation & washing out of rocks.
	3:1	2	0	< 1	NO	
	3:1	4	0	< 1	NO	
Enkamat	Soil reinforcement mat made of heavy monofilament fused at intersections. Thickness is .35 in. (9 mm). Enkamat pinned with metal staples every 3 ft. Failure mode is ripping and stretching then local scour at staples. Staples must be placed parallel to flow to minimize ripping/stretching and local scour.					
	3:1	0.5	0		YES	
	3:1	2	0		NO	Minor ripping/stretching and erosion of embankment material.

Table 2.2 cont.

PROTECTION TYPE	SLOPE (H:V)	OVERTOPPING HEAD (FT)	TAIL WATER DEPTH (FT)	TIME TO FAILURE OR END OF TEST (HR)	STABLE ?	PERFORMANCE REMARKS
Enkamat with grass	Enkamat covered with 1-2 in. soil and seeded with grass. Pinned with staples parallel to flow every 3 ft. Grass allowed to grow 1 year. Vegetation quickly removed by flow and had little effect. Failure mode was again ripping/stretching and erosion by local scour at staples.					
	3:1	0.5	0	2	YES	
	3:1	1	0	2	YES	
	3:1	2	0	2	NO	Minor ripping/stretching and erosion of embankment material.
	3:1	4	0	2	NO	Minor ripping/stretching and erosion of embankment material.
Soil Cement	Placed in 1 ft. thick layer on embankment. Best protection measure tested. No erosion of embankment soil or soil cement observed in any test. Failure mechanism is probably long-term weathering processes (freeze/thaw).					
	2:1	1	0	2	YES	
	2:1	2	0	2	YES	
	2:1	4	0	2	YES	
Grass	For overtopping depths greater than 0.5 ft. pockets of grass removed inducing local scour. Root system probably not fully established. Severe toe erosion also observed for overtopping depth of 2 and 4 ft.					
	3:1	0.5	0		YES	
	3:1	0.5	6.35		YES	
	3:1	2	0		NO	
	3:1	2	7.4		NO	
	3:1	4	0		NO	

NOTE: 1 foot = 0.3048 meters

testing conditions and results for Phase II can be found in Table 2.3 and Figure 2.1 provides specifications of the concrete block products tested. For full details of Phase II testing, Clopper and Chen (1988) should be consulted.

The SLA tests did produce a true overtopping flow, but, were limited by the fact that they were directed toward the analysis of highway embankments. Embankments tested provided only a 6 foot (1.83 meter) drop; therefore, SLA did not test any protection measures under the more extreme conditions that develop on a larger embankment.

Scale Model Studies, U.S. Bureau of Reclamation, Denver, Colorado

In 1983 the Bureau of Reclamation began a study of cost effective measures that could be used to protect small embankments during overtopping flows. Model tests were conducted in a flume that was 3 feet (0.91 meters) wide, 4 feet (1.22 meters) high, and 30 feet (9.14 meters) long. Froude scaling was employed and a length ratio of 1:15 (model:prototype) selected. The prototype embankment modeled was 32 feet (9.75 meters) high and had a crest length in the direction of flow that was approximately 24 feet (7.32 meters). The prototype unit discharge was 40 ft^2/s (1.133 m^2/s) for most tests. Slopes of 4H:1V and 6H:1V were tested.

These tests, by the USBR, were different from other research that has been discussed because protection measures were not extended down the full length of the

Table 2.3. SLA Phase II Tests of Highway Embankment Protection Measures

PROTECTION TYPE	SLOPE (H:V)	OVERTOPPING HEAD (FT)	TAIL WATER DEPTH (FT)	TIME TO FAILURE OR END OF TEST (HR)	STABLE ?	PERFORMANCE REMARKS
Soil Cement	Placed in 4 in x 3 ft x 4 ft lifts. Best protection system tested.					
	3:1	4	0	10	YES	
	2:1	4	0	10	YES	
Gabion Mattresses	Mattress was 6 in. thick, filled with 3 to 6 in. river rock, and anchored at the toe. Typar 3401 filter fabric was used as the underlayer. Some downslope movement of rock observed.					
	3:1	2	6	4	YES	
	3:1	4	8	4	YES	
	3:1	2	0	4	YES	
	3:1	4	0	1	NO	Poor anchoring at crest
	2:1	2	6	4	YES	
	2:1	4	8	4	YES	
	2:1	2	0	4	YES	
	2:1	4	0	4	YES	
Geoweb (4 in.)	Grid confinement system made of polyethylene. A single cell had an open area of 41 square inches & was 4 in. deep. Mirafi 1120N filter fabric was used as an underlayer. Cells were filled with 1 to 2 inch river rock. Tenax netting was placed over the system & hog ringed to the geoweb.					
	2:1	1	0	10	YES	
	2:1	2	0	1	NO	Crest anchor failed.
	2:1	4	0	0.167	NO	Stretched down embankment thus separating from flume walls & allowing erosion of soil.
Enkamat (7020)	Flexible soil reinforcement matting made of nylon monofilament fused at their intersections. Has a 90% open area. Was staked to embankment & secured at toe with an overlying steel bar. Least effective protection measure tested.					
	3:1	0.5	0		YES	
	2:1	1	6		NO	Tearing at stakes.
	2:1	2	6		NO	

Table 2.3 cont.

PROTECTION TYPE	SLOPE (H:V)	OVERTOPPING HEAD (FT)	TAIL WATER DEPTH (FT)	TIME TO FAILURE OR END OF TEST (HR)	STABLE ?	PERFORMANCE REMARKS
Enkamat (7020) w/1 in. asphalt	Same as above except with 1 in. of asphalt cover rolled into mat.					
	2:1	1	0	0.5	NO	Mat uplift & erosion of soil.
	2:1	1	6		NO	
Enkamat (7020) w/3 in. asphalt	Same as above except with 3 in. of asphalt cover rolled into mat.					
	3:1	2	6	4	YES	
	3:1	2	0	4	YES	
	3:1	4	8	1	NO	Mat uplift & erosion of soil.
Armorflex	Precast, interlocking concrete blocks reinforced with 2 cables running through each block in the direction of flow. Block has open cells & a unit weight of 36 pounds per square foot. Nicolon 70/06 woven fabric was used as an underlayer. Open cells filled with 3/4 in. crushed gravel which quickly washed away. Toe anchored with overlying steel bar. Researchers thought anchoring overlay to embankment & a better draining underlayer (to reduce pressure build up) would probably have improved performance.					
	2:1	1	0	N/A	YES	
	2:1	2	0	N/A	YES	
	2:1	4	0	N/A	NO	Block uplift, soil liquification.
	2:1	4	0	N/A	NO	
Petraflex	Precast interlocking concrete blocks reinforced with lateral & longitudinal cables. Unit weight is 42 pounds per square foot. Open cells filled with 1-1.5 in. river rock which quickly washed away. Polyfilter GB & Tensar DN1 made up double underlayer. For tests 1-3, system was anchored to the embankment by 2 sets of helix anchors. The toe was anchored by an overlying steel bar. The helix anchors were removed for tests 4 & 5. For test 6, the toe anchor was also removed.					
			0	10		
	2:1	1	0	10	YES	
	2:1	2	0	10	YES	
	2:1	4	0	4	YES	
	2:1	4	0	0-2	YES	
	2:1	4	3	2-6	YES	
			6	6-8		
			8	8-10		
	2:1	4	7	4	YES	

Table 2.3 cont.

PROTECTION TYPE	SLOPE (H:V)	OVERTOPPING HEAD (FT)	TAIL WATER DEPTH (FT)	TIME TO FAILURE OR END OF TEST (HR)	STABLE ?	PERFORMANCE REMARKS
Dycel 100	Interlocking concrete blocks with longitudinal cables. Bock unit weight is 33 pounds per square foot. UCO-SG 34 & Polyfilter GB made up double underlayer. In test 2 Tensar DN1 was also used. Overlay was secured to embankment by 2 sets of helix anchors. The toe was anchored with an overlying steel bar. Relative to Armorflex & Petraflex, Dycel blocks had over 60% higher surface area & 8-21% lower unit weight. Dycel blocks, therefore, thought more vulnerable to uplift pressures.					
	2:1 2:1	1 1	0 0	1.5 1.5	NO NO	Block uplift, soil liquification

NOTE: 1 foot = 0.3048 meters

Table 2.4. Geotextiles Used in SLA Testing

GEOTEXTILE TYPE	DESCRIPTION	UNIT WEIGHT (oz/yd^2)	THICK-NESS (mm)	PERCENT OPEN AREA	EFFECTIVE SIEVE OPENING
Typar 3401	Nonwoven filter fabric made of spun-bonded fiber.	4	N/A	N/A	N/A
Mirafi 1120N	Needle-punched, nonwoven filter fabric.	12	3	N/A	100
Enkamat 7020	Flexible soil reinforcement matting made from nylon monofilament fused at their intersections. Large open area is filled with specified material. Typically filled with soil and seeded with grass.	N/A	N/A	90	N/A
Nicolon 70/06	Woven fabric.	6.6	N/A	2-8	70
Polyfilter GB	Woven fabric made of polypropylene monofilament fibers.	6	N/A	20-30	40-50
Tensar DN1 (geonet)	A mesh structure consisting of 2 sets of parallel polyethylene strands providing multiple drainage channels.	23.2	6.4	N/A	N/A
UCO-SG 34/34	Woven fabric of polypropylene monofilament.	1.08	0.8	N/A	120

NOTE: 1 mm = 0.0397 inches

embankment. Thus, analysis of the effectiveness of a given protection measure is approached a bit differently and consists of two parts. First, is the stability of the protected portion of the slope. Second, is the amount of erosion that takes place on the unprotected portion of the slope relative to control tests of completely unprotected embankments. It should be noted that in all tests, significant scour was observed on the unprotected portions of embankments. A summary of the test results is presented in Table 2.5. For further details, the report by Dodge (1988) should be consulted.

Powledge et al (1989) discussed Dodge's work and concluded that because flow and erosional characteristics found with the model cannot be accurately extrapolated to

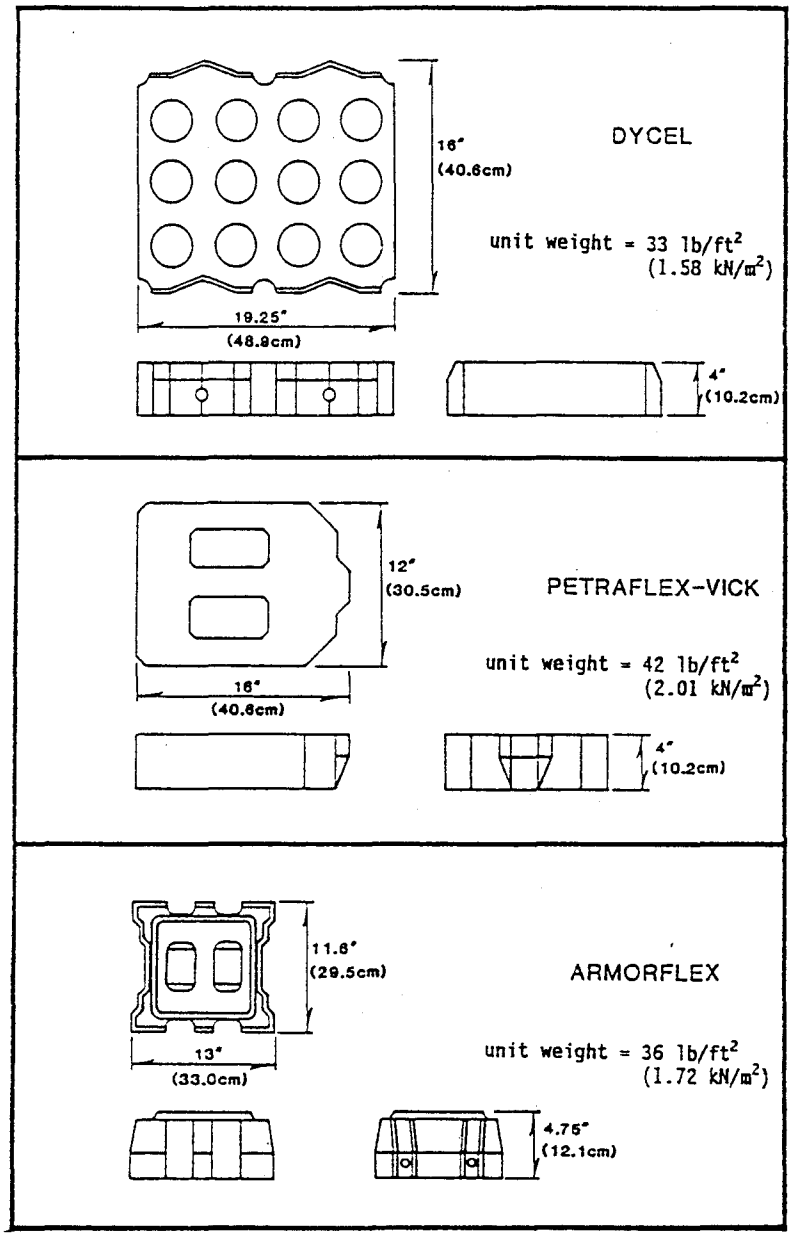

Figure 2.1. Cellular Concrete Protection Units Used in SLA Phase II Tests (Clopper and Chen, 1988)

Table 2.5. USBR Testing of Small Embankment Overtopping Protection

PROTECTION MEASURE	SLOPE (h:v)	PROTOTYPE OVERTOPPING HEAD (ft)	PROTOTYPE UNIT DISCHARGE (cfs/ft)	PROTOTYPE ELAPSED TIME (hr)	EROSION OF AVAILABLE VOLUME OF MODEL MATERIAL (%)	MAX. SCOUR DEPTH (ft)	LOCATION OF MAX. SCOUR DEPTH (ft)
Hard Crest Cap	The crest was protected with a hard cap which extended 10 ft. down the embankment face and ended with a 7 ft. vertical toe curtain.						
	6:1		40	1	15.8	10	15.2
Hard Crest Cap with Roughness	Pea gravel representing 3 to 6 in. prototype rock was epoxied to downslope 10 ft. of crest cap. Compared to first test, this resulted in increased flow depth, damping of vortex action, a decrease of erosion volume by 1/2 and more uniform erosion.						
	6:1		40	1	7.2	8.8	106.2
Rip rap	Hard crest cap with roughness from previous test was used and additionally a 30 ft. length of 6 to 24 in. (prototype) rip rap was placed immediately downslope of cap. A filter base was placed beneath the riprap. Stones fluidized and eroded out immediately.						
	6:1		40	1	13.4	8	10.1
Gabions	Riprap from previous test was replaced with 3x3x3 ft. (prototype) gabions which likewise extended 30 ft. downslope from hard cap with roughness. Gabions were filled with 12 in. rock and anchored to timbers buried in embankment and with epoxy to vertical toe curtain. A filter bed was placed under gabions. Gabions showed no sign of being dislodged.						
	6:1		40	1	2.4	1.9	83.7
	6:1		40	5	4.6	3.8	95.1
	4:1		40	1	11.7	3.4	59.2
Gabion Mattress	Prototype mattress was 18 in. thick and contained riprap of 9 in. maximum and 4 in. mean size. Both the crest and 50 ft. of the embankment face were covered with the mattress which was placed overtop of a filter layer. Mattress showed no sign of being dislodged.						
	4:1		40	1	3.8	6.3	104.3
	4:1		40	5	8.4	10	83.7
Bare Soil at 95% Proctor	Bare soil was used to construct the crest and the entire embankment face. Soil was compacted to 95% max. Proctor. Increasing unit discharge from 40 to 87 cfs/ft. caused a 40% increase in erosion.						
	4:1		40	1	9.1	5	77.3
	4:1		40	5	14.1	8.8	59.2
	4:1		87	1	12.7	3.4	Toe
Bare Soil at 102% Proctor	Bare soil was used to construct the flat crest and the entire embankment face. Soil was overcompacted to 102% max. Proctor. The increased compaction reduced the volume of soil eroded by approximately 1/2.						
	4:1		87	1	6.5	3.8	Toe
	4:1		87	5	6.5	5.6	Toe

NOTE: 1 ft. = .3048 m, 1 cfs/ft = ft^2/s = .093 m^2/s. Where not specified, soil was compacted to 90% max. Proctor.

larger embankments, the results of this study should be considered only qualitative in nature. In other words, which protection measures worked better may be ascertained, but, not how much better.

MODEL TESTS OF STEPPED PROTECTION MEASURES

A number of individuals have carried out tests on stepped protection measures under laboratory conditions. The results of these tests are presented in Table 2.7. In preparing this table and the summary of tests, the CIRIA report, Design of Stepped Block Spillways, (CIRIA, 1992) has been drawn upon heavily. For more detailed explanations of test conditions or results, the aforementioned CIRIA report or the references given in Table 2.7, located on pages 36 and 37, should be consulted.

King Faisal University, Saudi Arabia

El Khashab investigated both the flow resistance of fixed strips designed to have the same geometry as a stepped block overlay (El Khashab, 1986) and the stability of loose, wedge-shaped blocks (El Khashab et al, 1987). In the latter paper, the wedge blocks tested were 0.94 inches (24 mm) long and wide and had a mean thickness of 0.3 inches (7.5 mm). The upstream and downstream ends of the blocks butted together and interlocked but were not tied together. These blocks are said to have withstood a unit discharge of 1.08 ft^2/s (0.1 m^2/s) but it is unclear whether the blocks failed at that point.

University of Southampton, England

Noori also reported tests of both fixed strips and loose stepped-shaped blocks (Noori, 1985). The loose blocks, which were about twice as large as those tested by El Kashab, failed at a unit discharge of 1.7 ft^2/s (0.156 m^2/s). At this discharge, the blocks along with their underlayer began to slide down the sand embankment beneath.

Simons Li and Associates, Fort Collins, Colorado

As part of a larger study of methods for protecting overtopped embankments, Simons Li and Associates tested overlapping, wedge-shaped blocks in a 4 foot (1.22 meter) wide flume. A single block size was tested on downstream slopes of 3H:1V and 2H:1V. The maximum unit discharge tested was 22.9 ft^2/s (2.125 m^2/s) and the overlay was found to be stable under these conditions (Simons Li & Associates, 1989).

CIRIA Sponsored Tests, University of Salford, England

Research on precast concrete block protection of spillways was sponsored by CIRIA and carried out by Baker (1989,90,91) at the University of Salford. Both overlapping and non-overlapping wedge blocks were tested in a 2.0 foot (0.6 meter) wide recirculating flume set at a slope of 2.5H:1V. The maximum unit discharge available was 5.4 ft^2/s (0.5 m^2/s) and the maximum attainable velocity was 24.6 ft/s (7.5 m/s). The lower 6.6 feet (2 meters) of the 35.4 foot (10.75 meter) long flume constituted the test section where the wedge blocks were installed on top of a 0.16 inch (4 mm) thick

polyethylene core of proprietary fin drain called Trammel. The remainder of the flume was covered with wood strips that simulated the geometry of a wedge block overlay.

Three different sizes of overlapping and one size of non-overlapping wedge blocks were tested. These block shapes and sizes are presented in Figure 2.2 and Table 2.6.

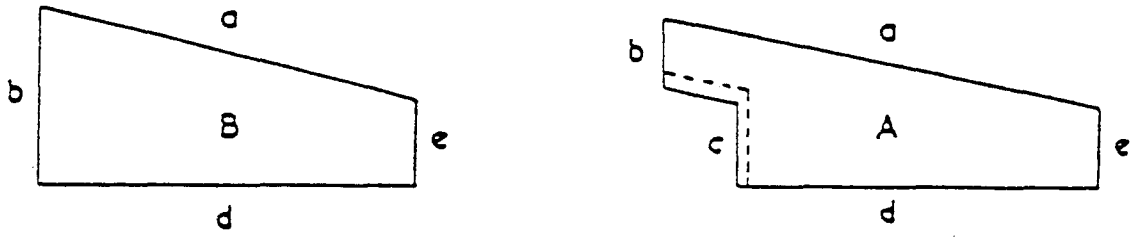

Figure 2.2. Salford University Test Block Shapes

Table 2.6. Dimensions of Salford University Test Blocks

Size	Block A			Block B
	Small	**Medium**	**Large**	**Medium**
a (mm)	30.0	60.0	180.0	50.0
b (mm)	4.5	9.0	31.0	23.0
c (mm)	5.5	11.0	29.0	-
d (mm)	24.0	48.0	146.0	49.0
e (mm)	5.0	10.0	30.0	11.0
Width (mm)	25.0	50.0	150.0	50.0
Average Block Thickness (mm)	8.5	17.0	50.0	17.0

All the blocks described in Table 2.6 were found to be stable at 5.4 ft^2/s (0.5 m^2/s), the maximum unit discharge of the facility. Specific results of the Salford University tests are presented in the following sections.

Arrangement of Blocks

Wedge blocks were installed in a stretcher-bond configuration. Arranged in this way, the longitudinal joints between adjacent blocks do not line up from row to row. This arrangement was chosen because tests on both flat and wedge-shaped blocks indicated it to be the most stable. When longitudinal joints were aligned, high velocity jets formed in them and produced increased pressures beneath the blocks. Additionally, it was found that these jets detrimentally effect the formation of a recirculation zone in the lee of the step. The recirculation was found to be weaker and, therefore, the pressure reduction was not as great in the presence of aligned joints (CIRIA, 1992). In light of these results, it has been recommended that, even in stretcher-bond configuration, the widths of longitudinal joints between blocks should be kept to a minimum (CIRIA, 1992).

Step Height to Length Ratio

The step height to length ratio of blocks was investigated by casting the bases of one row of blocks in concrete and attaching wooden sheets of different thicknesses to form the step tread. This special row was installed immediately upstream of a wedge block instrumented with 14 pressure taps. The test results are presented in Figure 2.3.

They indicate that flow ceases to reattach to the next block downstream for step height to length ratios less than approximately 1:3.5. On the other hand, maximum impact pressures were obtained when this ratio was approximately equal to 1:5. These results agree well with the recommendation by Pravdivets and Bramley (1989) that the step height to length ratio be between 1:4 and 1:6.

Plan Area of Drainage Holes

The Salford University tests also investigated the relationship between drainage hole area and pressures in the underdrain. The number of holes was varied from 0 to 14, where 14 holes constituted about 5 percent of the block surface area. The results of these tests are illustrated in Figure 2.4 (Baker, 1990). With no drainage holes at all, pressure in the underdrain rose steadily with increasing unit discharge. As the number of holes was increased this trend began to reverse. From the data, it appears that 7 holes, or a drainage area equal to 2.5 percent of the block's plan area, is sufficient to cause underdrain pressures to drop steadily, rather than rise, with increasing unit discharge. Additionally, it appears that there is not much reduction of underdrain pressures gained by increasing the drainage area over about 2.5 percent.

Note also from Figure 2.4 that, when drainage holes are present, the highest underdrain pressures are generally observed at the lowest flows. Such results were also found in the current set of tests carried out on a near prototype scale at CSU. The

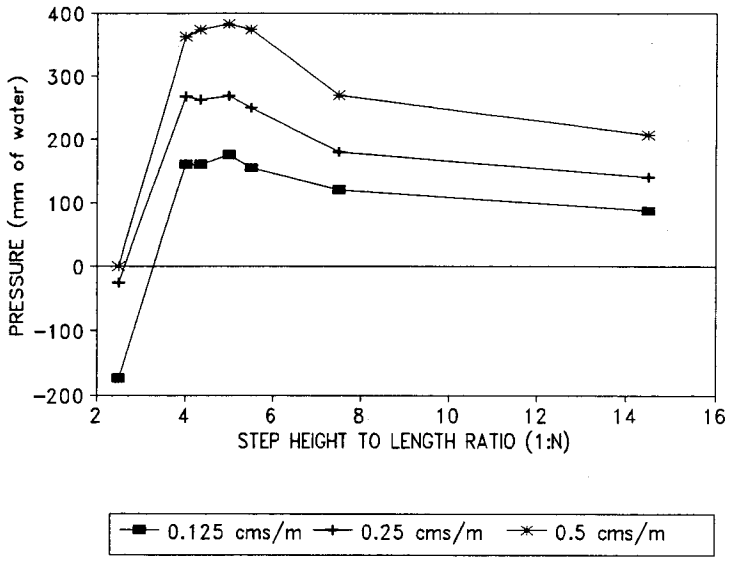

Figure 2.3. Impact Pressure as a Function of Step Height to Length Ratio (Baker, 1990) (1 mm of water = 0.04 inches of water, 1 cms/m = 10.8 cfs/ft)

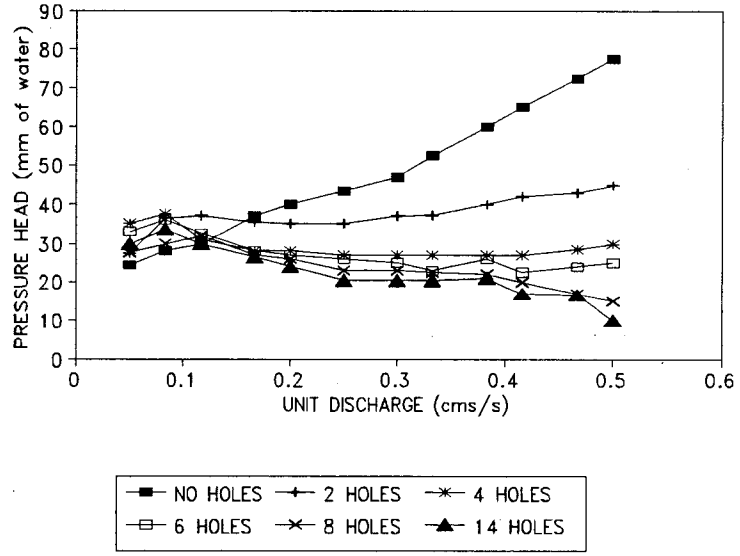

Figure 2.4. Drainage Layer Pressures as a Function of Unit Discharge and Drainage Hole Area (Baker, 1990)

explanation for this is that low discharges have correspondingly low velocities. Assuming that the recirculating flow in the separation can be modeled as a forced vortex, pressure reduction across the radius of the vortex is proportional to the square of the main flow velocity. Thus, the lower the velocity of the main flow, the smaller the pressure reduction across the vortex radius.

Inter-block and Frictional Forces

Lifting tests were performed on wedge blocks to quantify the restraining force of interblock friction. A wire was attached to the downstream face of a block, run over a pulley and weights attached to the other end until the block started to lift. As would be expected, the required lifting force increased with increasing unit discharge due to higher impact pressures and flow depths. It was determined that interblock friction increased the required lifting force by more than 30 percent.

The resistance of wedge blocks to sliding over the polyethylene fin drain was investigated by removing the toe restraint at the bottom of the flume. Both, overlapping and non-overlapping block panels slid down the slope if the flume was operated at very low flows. If the discharge was brought quickly up to a high value, though, overlapping blocks were stable with no toe restraint as long as the discharge was kept high. Non-overlapping wedge blocks did not exhibit this property. (CIRIA, 1992). The dynamic and static coefficients of friction for wedge blocks were found to be 0.72 and 0.83 respectively (Baker, 1990).

Performance of Wedge Blocks Under a Hydraulic Jump

The Salford University tests found that wedge blocks become unstable and fail at low discharges when subjected to the effects of a hydraulic jump. One problem is that wedge block geometry is designed for unidirectional flow. If that direction is reversed, as may occur in a hydraulic jump, the blunt step face of the block is exposed to impinging flow. In this case, blocks were found to fail by rotating backwards about their upstream ends. In other cases of observed failure, whole panels of blocks lifted up and waved about in the flow (Baker, 1990). Based on these tests, Baker concluded that wedge-blocks should not be used anywhere that the unidirectional flow regime is lost which occurs, for example, at bends, changes in channel shape or under hydraulic jumps.

U.S. Bureau of Reclamation, Denver, Colorado

As a precursor to the near-prototype testing that is the subject of this report, the U.S. Bureau of Reclamation conducted laboratory tests of wedge block protection systems. These tests were conducted in a 1.5 foot (0.46 meter) wide, plexiglass walled flume sloped at 2H:1V. The facility has a maximum discharge capacity of 14 ft^2/s (1.3 m^2/s) which is generated by a maximum overtopping head of 2.8 feet (0.85 meters). The total available vertical drop is 15.5 feet (4.72 meters).

Three different block geometries were investigated in an effort to establish which geometry provides the best balance of energy dissipation and separation zone pressure reduction characteristics. All block geometries were simulated by strips fixed to the floor of the flume. The first step geometry tested had a 4 inch (102 mm) long horizontal tread

surface and a 2 inch (51 mm) step height. For the second and third sets of tests, the tread surface of the steps were sloped downward from horizontal by 10 and then 15 degrees. It was found that the horizontal blocks provided the best energy dissipation but velocities close to the step were not high enough to produce the negative separation zone pressures deemed necessary for proper aspiration of the filter layer below. Aspiration is removal of fluid from beneath the overlay by suction. Ultimately, the 15 degree geometry was chosen for further testing on a near-prototype scale. This step had an exposed tread surface 4.14 inches (105 mm) in length and a step height of 0.93 inches (24 mm). These dimensions were scaled up by the factor 1:2.717 to arrive at the dimensions of the blocks that were tested at a near-prototype scale. Some results of the USBR model tests are presented in the following sections.

Pressure Profiles

Figures 2.5 and 2.6 present step pressure distributions recorded in the USBR model study at pairs of consecutive horizontal and 15 degree steps. Pressures at two locations in the flume where two consecutive steps were instrumented with pressure taps are presented for both step geometries. Each figure, therefore, shows four step pressure profiles. The 8 inch (203 mm) distance, shown on the horizontal axes of the two figures, corresponds to the combined tread surface length of two consecutive steps. The figures clearly show the two distinct pressure regions that develop on each step. The step's downstream portion is an area of impact with correspondingly high pressures and the upstream portion is an area of flow separation and low pressure. Comparing the two

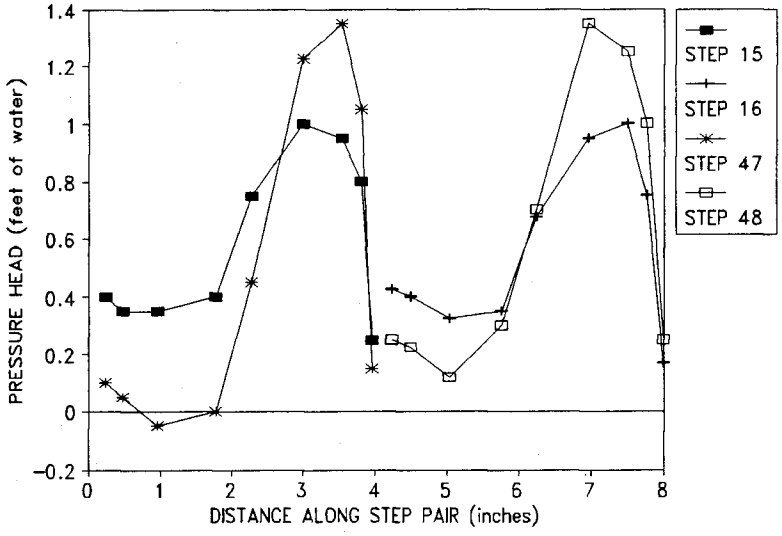

Figure 2.5. Pressure Profiles for Horizontal Steps, q = 6.71 ft^2/s (0.62 m^2/s), overtopping head = 1.67 feet (0.51 meters) (Frizell, 1992)

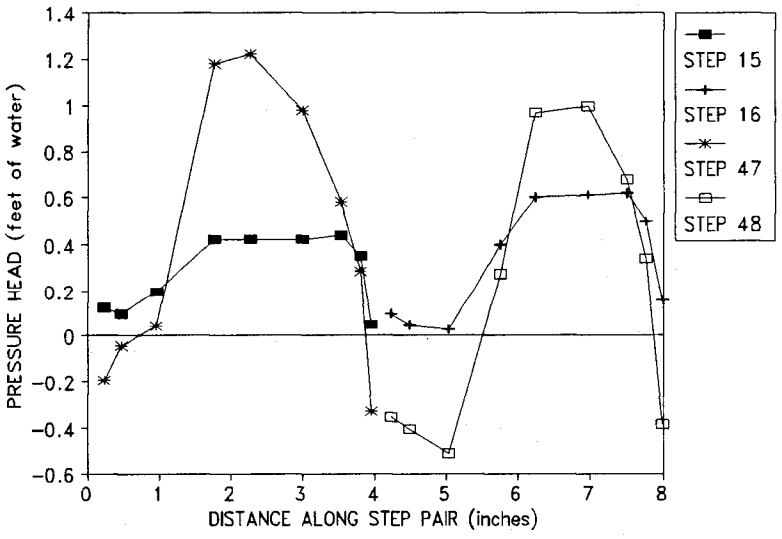

Figure 2.6. Pressure Profiles for 15 Degree Steps, q = 6.71 ft^2/s (0.62 m^2/s), overtopping head = 1.67 feet (0.51 meters) (Frizell, 1992)

figures also reveals that sloping the step tread downward by 15 degrees reduces the pressure in the separation zone at all steps, and at some point prior to steps 47 and 48 actually provides negative pressures. This reduction in pressure is the result of increased flow velocities that accompany the downward sloping of steps.

Velocity Profiles

The horizontal and vertical velocity components were measured at four locations in the flume, steps 3, 13, 23 and, 33, by laser-doppler anemometer. Velocity readings were taken from the tip of the step to as close to the water surface as possible. The resulting velocity profiles were checked against continuity using a known total discharge. If necessary to satisfy continuity, velocity profiles were adjusted by a constant which was typically in the range of 0 to 3 percent. Figure 2.7 shows corrected velocity profiles at a location corresponding to step 23 for a smooth surface, and stepped surfaces having horizontal and 15 degree sloping steps. As expected, horizontal steps provide the lowest velocities and a smooth surface provides the highest. From the figure, it is also evident that the greatest variations in velocity occur near the surface of the steps rather than higher in the flow profile. For this reason, changes in flow velocity have a large effect on the pressure in the separation zone.

Energy Dissipation

The energy dissipation characteristics of smooth surfaces and surfaces with horizontal and 15 degree steps were also investigated and compared. To do this,

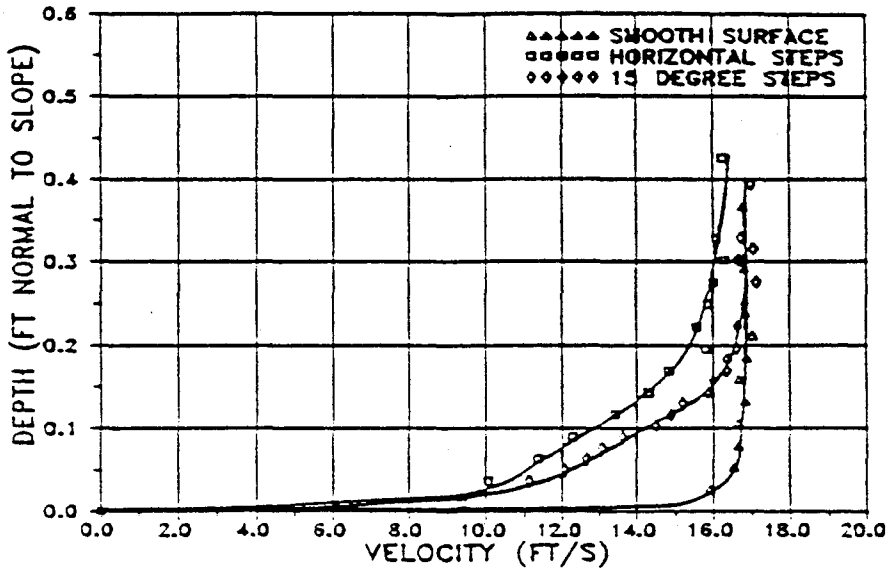

Figure 2.7. USBR Model Test Velocity Profiles, Step 23, q = 6.71 ft^2/s (0.62 m^2/s), Overtopping Head = 1.67 feet (0.51 meters) (Frizell, 1992)

corrected velocity profiles were used to compute the kinetic energy per unit volume of the flow. The ratio of this value to the total available head was then determined for different locations on the model embankment. The kinetic energy per unit volume was computed as $(1/2)\alpha\rho V^2$ and the total available head as the overtopping head plus the vertical distance from the crest down to the point in question. Figure 2.8 illustrates the results of these computations for a surface with 15 degree steps, which, was the geometry eventually chosen for near-prototype testing. The figure shows that the kinetic energy remaining in the flow generally increases as the unit discharge increases.

The variation of energy dissipation characteristics with surface type was also investigated. Figure 2.9 presents, for a single unit discharge, the ratio of kinetic energy to total available head for a smooth surface and surfaces with horizontal and 15 degree

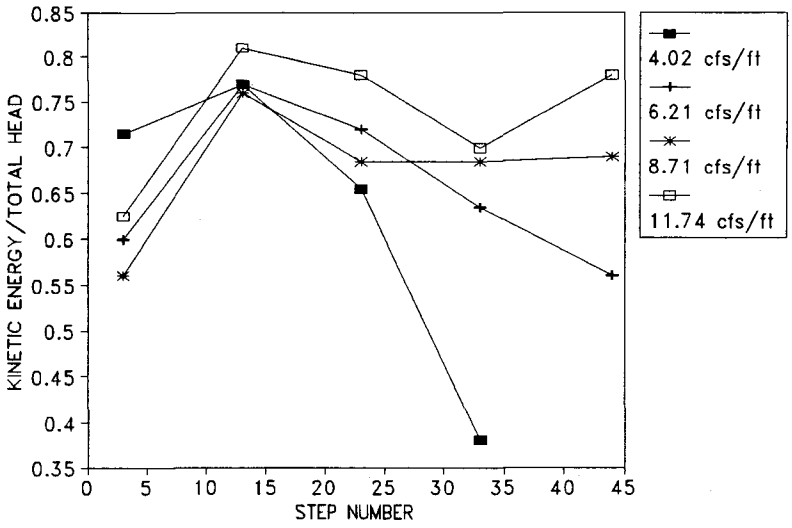

Figure 2.8. Variation of Energy Dissipation with Unit Discharge for 15 Degree Steps (Frizell, 1992)

steps. The figure shows that the ratio of kinetic energy to total head generally decreases in the downstream direction for both horizontal and 15 degree steps. For a smooth surface, it is evident that just the opposite is true, and the ratio of kinetic energy to total available head increases in the downstream direction. Additionally, it may be observed that the horizontal steps provide greater energy dissipation than the 15 degree steps.

In order to illustrate the economic benefits derived from the energy dissipating characteristics of stepped spillways, the required length of stilling basin was computed for a smooth surface, horizontal steps, and 15 degree steps. The calculations assume a 46 foot (14 meter) high embankment and a Type I basin which has no end sill to force the jump (Peterka, 1978). The experimental data in Figure 2.9 was used to compute the

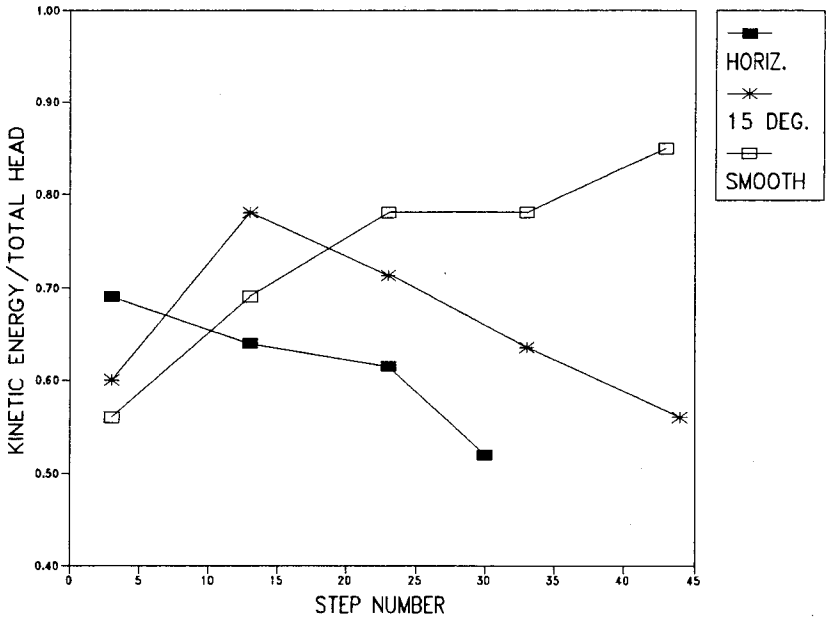

Figure 2.9. Comparison of Energy Dissipation Characteristics for Smooth Surfaces and Stepped Surfaces with Horizontal and 15 Degree Steps, q = 6.21 ft^2/s (0.62 m^2/s), overtopping head = 1.67 feet (0.51 meters) (Frizell, 1992)

flow velocity according to V_1 = (KE/H) X (embankment height) where KE/H is the ratio of kinetic energy to available total head. The depth entering the basin was computed as $D_1 = q/V_1$. Figure 6 in Peterka's USBR Monograph 25 was then used to compute the ratio of hydraulic jump length to the depth entering the basin. These calculations showed that 15 degree steps provide a 9 percent reduction in stilling basin length over a smooth surface and horizontal steps provide a 21 percent reduction over a smooth surface.

Russian Model Testing

Numerous laboratory studies of wedge block overtopping protection were carried out in the former USSR, but, detailed information concerning these tests is not readily

available. Many of the studies, such as those found in Table 2.7 by Nguen Dang Shon and M.E. Lunatsi, were conducted at the Moscow Institute of Civil Engineering (ICE) under the supervision of Professor Yuri Pravdivets. Available details on some of these tests are presented in the following paragraphs.

The tests conducted on blocks measuring 0.79 x 0.79 inches (20 x 20 mm) in plan were carried out in a 7.1 inch (180 mm) wide flume where a 1:100 scale coarse sand embankment was constructed. The downstream slope of the embankment was decreased toward the toe. At the toe itself, blocks were set on an approximately horizontal surface and angled slightly upward to deflect flow away from the bed.

Nguen Dang Shon carried out tests on a 1:100 scale model of a 104 foot (31.7 m) high embankment. The downstream side of the embankment had an initial slope of 2.86H:1V which was decreased to zero at the toe. Each of the two block sizes tested had 3 drainage holes, one on the block centerline and one on each vertical, longitudinal face. Both block sizes were stable on the sloping portion of the embankment at the maximum unit discharge tested. When a hydraulic jump was formed on the horizontal section of the embankment, though, both failed at lower unit discharges.

M.E. Lunatsi carried out further studies on the stability of wedge blocks under the influence of a hydraulic jump. His tests were carried out on a larger scale in a 18.1 inch (480 mm) wide flume using butt-jointed rather than overlapping wedge-shaped blocks. Unfortunately, details of this work are not readily available.

Another study was conducted in the design stages of Kolyma Dam. In order to choose a protection type, it was decided to carry out a comparison test between rip rap

and wedge block overtopping protection. A 1:10 scale model of the dam was constructed in a 16.4 foot (5 meter) high outdoor flume. The downstream face of the dam sloped at 2.5H:1V and the design discharge was 969 ft^2/s ($90m^2/s$). One half of the model embankment was covered by 6.6 x 6.6 foot (2 x 2 meter) scaled rip rap. The other half, with scaled 6.6 x 6.6 x 1.3 foot (2 x 2 x 0.25 m) stepped blocks. The rip rap failed quickly and the blocks performed satisfactorily but were undermined along the rip rap side because no dividing wall had been placed between the two. Despite their performance, stepped blocks were only used on a small appurtenant embankment rather than on the main Kolyma dam. The Kolyma information in Table 2.7 pertains to the model and the information in Table 2.8, to the small wedge block installation that resulted.

Table 2.7. Model Testing of Stepped Block Spillways (CIRIA, 1992)

Reference	Block Type	L (mm)	Lo (mm)	B (mm)	Hs (mm)	Ts (mm)	Hn (mm)	Tn (mm)	Flume Slope	qmax (m^2/s)	qfail (m^2/s)	Model "Scale"	Comments
El Khashab	BW	40	40		4				0.100				Fixed Strips
(1986,87)	BW	65	65		13				0.200				Fixed Strips
	BW	24	26	24			3	8.0	0.211	0.100	0.10?		
	BW	24	26	24			3	8.0	0.083	0.180			
Jiang (1985)	BW	63	63	63	12	12			0.200	0.180		1:20	Aluminum Blocks, S.G. = 2.7
	BW	53	63	53	13	19			0.250	0.241		1:40	
Norri (1985)	BW	40	40		4				0.100				Fixed Strips
	OS	65	85	63	13	13			0.200				Fixed Blocks
	BW	64	64	64	13	13			0.200		0.156		Aluminum Blocks, S.G. = 2.7
Simons, Li & Assoc. (1989)	WO	164	205	203			45	122.0	0.330 0.500	2.125			
Baker	BW	52		50			15	17.5	0.400				Sand/Cement Blocks, S.G. = 2.05
(1989,90,91)	WO	51	60	50			8	15.8	0.400	0.530			Trammel underdrain used
	WO	25	30	25			4	7.9	0.400				
	WO		180	150			28	51.1	0.400				
		200	240	200			40	60.0	0.286	0.480		1:5	Oman spillway model test. Blocks with side to side interlock.
Frizell, USBR	BW	102			51 - Vertical distance				0.500	1.090			Tread surface of step horizontal
(1992)	BW	103			33 - Vertical distance				0.500	1.090			Tread 10° down from horizontal
	BW	105			24 - Vertical distance				0.500	1.090			Tread 15° down from horizontal
Moscow ICE		20		20				3-6	0.170	0.100		1:30,50	S.G. = 2.4
		40		30				5.1	to 0.330			100,12 0	
Kolyma Dam		200		200		40			0.400	90.00		1:10	

Table 2.7 cont.

Reference	Block Type	L (mm)	Lo (mm)	B (mm)	Hs (mm)	Ts (mm)	Hn (mm)	Tn (mm)	Flume Slope	qmax (m^2/s)	qfail (m^2/s)	Model "Scale"	Comments
Nguen Dang	WO		25	20	3	7			0.370	0.100	0.030	1:100	Blocks did not fail on slope.
Shon (USSR)	WO	28		22	4	8			0.370	0.100	0.040		Values of qfail refer to failure under jump on horizontal toe.
Lunatsi (USSR)	BW	89					18	21.2	0				Tests with jump on horizontal channel. Froude number 4.5-6.6.
	BW	79					15	22.3	0				
	BW	62					12	23.9	0				
	BW	46					9	25.4	0				

KEY -

OS = Overlapping slabs
BW = Butt-joined and wedge-shaped
WO = Wedge-shaped and overlapping
L = Exposed assembled block tread surface length
Lo = Overall length of block
B = Width of block
Hs = Step height measured normal to block tread surface
Ts = Average thickness measured normal to block tread surface
Hn = Step height measured normal to flume slope
Tn = Average thickness of block measured normal to flume slope
qmax = Max. unit discharge tested
qfail = Unit discharge at which blocks failed

NOTE: 1 mm = .0397 in., 1 m^2/s = 10.764 ft^2/s

PROTOTYPE INSTALLATIONS OF STEPPED PROTECTION MEASURES

To date, the stepped block concept has been implemented only at sites in Russia and China. Since the mid-1970's, Russia has used stepped blocks as overtopping protection for cofferdams and as service and emergency spillways on embankment dams (Frizell et al, 1991). Available details of these installations and the one located in China are summarized in Table 2.8 and some additional information is given below. For further details, the report by CIRIA (1992) or the references in Table 2.8 should be consulted.

Dneiper Power Station, USSR

A section of gated spillway at Dneiper Power Station, 103.7 feet (31.6 m) long, 46.6 feet (14.2 m) wide, and sloped at 6.5H:1V, was used as a test section for large, overlapping wedge blocks. The test channel was operated for a total of 10 hours and withstood a unit discharge of 646 ft^2/s (60 m^2/s). Flow depths approaching the test section were less than normal (uniform flow) depth, though, and velocities experienced actually corresponded to uniform flow on that slope of 1400 ft^2/s (130 m^2/s). Inspection following the test revealed that only two blocks had been significantly displaced. The displacements were 1.6 to 2.3 feet (0.5 to 0.7 meters) vertically and downslope and were attributed to loss of filter material. The desired filter material size of 1.6 to 3.9 inches (40 to 100 mm) had not been available so 0.8 to 1.6 inch (20 to 40 mm) material was used instead. This material was small enough to pass through the drainage holes so a mesh was placed over them to retain the material. The mesh failed, though, when it was

distorted by the flow and consequently filter material was removed through the drains allowing the two blocks to be displaced.

One block in the test section was instrumented with 10 pressure taps on its top and bottom surfaces and a second block was equipped to measure vertical and horizontal forces. Standard deviations of pressures on the top and bottom surfaces of the first block were found to be 3.28 feet (1.0 meters) of water and 0.2 feet (0.06 meters) of water respectively. The second instrumented block indicated vertical downward forces to be 9900 pounds (4.5 metric tons) and horizontal forces to be 4400 pounds (2 metric tons).

Dneister Power Station, USSR

Another test section was constructed on a 66 foot (20 meter) wide section of a 820 foot (250 meter) long cofferdam at Dneister Power Station. The majority of the dam face was protected by concrete slabs measuring 14.8 feet long x 32.8 feet wide x 1.64 feet thick (4.5 x 10 x 0.5 meters). This contrasts with the stepped blocks placed in the test section whose thickness was only 0.82 feet (0.25 meters). The blocks have performed without incident, withstanding several floods and two ice-flows which occurred in 1978 and 1979.

Jelyevski Dam, USSR

At Jelyevski Dam, wedge blocks were used to construct a spillway on one of the abutments. The spillway was designed by a former student of Professor Pravdivets, but, without his supervision. Upon operation of the spillway, much of the underlying filter

material and soil was washed away causing the channel to become nearly horizontal. Professor Pravdivets investigated the failure and came to some conclusions. First, the filter layer had been incorrectly designed and had, thus, failed to protect the underlying soil. Second, the clay and sand from which the abutment was constructed were of poor quality. Further, he concluded that stepped block spillways should generally be constructed only on embankment sections of dams rather than on abutments because abutment materials are less carefully selected and placed.

RESULTS OF RUSSIAN MODEL AND PROTOTYPE TESTING

Step Height to Length Ratio

A number of the model studies and prototype trials that have been discussed in this chapter have led to the conclusion that a step height to length ratio between 1:4 and 1:6 is optimum for block stability (Pravdivets and Bramley, 1989 and Pravdivets and Slissky, 1981). Baker, at Salford University, reached the same conclusion. He found that flow failed to reattach to the next block downstream for step height to length ratios less than approximately 1:3.5 and that maximum impact pressures occurred for a ratio of approximately 1:5 (Baker, 1990).

Block Thickness

Laboratory experiments investigating wedge block stability were conducted by Grinchuk and Pravdivets (1977) and Pravdivets et al (1980). The results of these studies relate required block thickness to embankment slope and unit discharge. To obtain these

Table 2.8. Prototype Installations of Stepped Block Protection (CIRIA, 1992)

Location	Block Type	L,Lo (m)	Hs,Hn (m)	B (m)	Ts (m)	Channel Slope	Channel Width	Zt,Zo (m)	qd (m^2/s)	q (m^2/s)	V (m/s)	Date Built	Comments	References
Bolshevik (Russia)	OS	1.3,1.5		3	0.16	.12-.2	12	-11.5	3.3			1980	Farm Dam	Krest'yaninov & Pravdivets (1986)
Klinbeldin (Russia)	OS	1.3,1.5	0.2,-	3	0.16	0.159	15	7.5,5.5	3		7.5	1976	Farm Dam	Pravdivets(1987), Krest'-yaninov &
Maslovo (Russia)	OS	1.3,1.5	0.2,-	3	0.16	0.154	7.5	7.5,5.5	3			1981	Farm Dam	Pravdivets(1978) Krest'yaninov & Pravdivets (1978,86)
Sosnovski (Russia)	OS	1.3,1.5		3	0.16	0.167	12	13,11	3.3			1978	Farm Dam	Pravdivets et al.(1980), Krest'yaninov & Pravdivets (1986)
Luhovitsy (Russia)														Krest'yaninov & Pravdivets (1986)
Dneiper Power Station (Russia)	WO	2.6,3.0	0.5,-	3	0.8	0.154	14.2	37,-		63	25		Full-Scale Test Channel	Grinchuk et al.(1977), Pravdivets & Slissky (1981)
Dneister Cofferdam (Russia)	BW	1		1	0.25	0.222	20	7		13	8			Pravdivets (1978a), Pravdivets & Slissky
Kolyma (Rusia)	OS	2		2	0.25	0.5	6	20,-		90				(1981) Pravdivets et al.(1980), Pravdivets (1987)
Transbaikal (Russia)	WO					0.4	115	13,8.5	18					
Jelyevski (Russia)	WO	3		2	0.35	0.125	12		36.5				Failed	Pravdivets (1982)
Jaingshe Wanan (China)	BW	2.12	0.52,-	2.12	0.74	0.2								

KEY -

OS = Overlapping slabs
BW = Butt-jointed and wedge-shaped
WO = Wedge-shaped and overlapping
L = Exposed length of block top surface when assembled
Lo = Overall length of block
B = Width of block
Hs = Step height measured normal to tread surface of block
Ts = Average block thickness measured normal to block tread surface
Hn = Step height measured normal to flume slope
Zt = Vertical distance between upstream water level and spillway toe
Zo = Vertical distance between upstream and downstream water levels
qd = Design unit discharge
q = Max. unit discharge known to have occurred since construction
V = Max. velocity known to have occurred since construction

NOTE: 1 m = 3.281 ft, 1 m^2/s = 10.764 ft^2/s

relationships, the following approach was taken.

Block interlock and overlap forces were neglected. A factor of safety against block movement was then defined as follows.

$$F_s = \frac{N \tan\phi}{F} \qquad (2.1)$$

N is the minimum total normal force on the block, F is the sum of tangential forces acting to move the block, and ϕ is the friction angle between the block and an underlying granular material. The unit weight of concrete was taken to be 150 lb/ft^3 (2.4 metric tons/m^3). Values of ϕ used for clay were approximately 11 degrees and typical values used for granular drain materials were approximately 17 degrees. The flow related forces were determined from empirical data and appropriately conservative assumptions and are discussed by Pravdivets (1978). Flow forces were determined for different embankment slopes and unit discharges. Then, the average block thickness required for a safety factor of 1.5 was calculated. The resulting relationships differed slightly for the two sets of experiments and are presented in Figures 2.10 and 2.11. Note in the figures that the average block thickness is defined to be the total volume of the overlay divided by the total area.

Depth Calculations

Calculation of open-channel flow depths requires a value for Manning's n or Chezy's C depending on the rating equation used in the analysis. No reliable values for

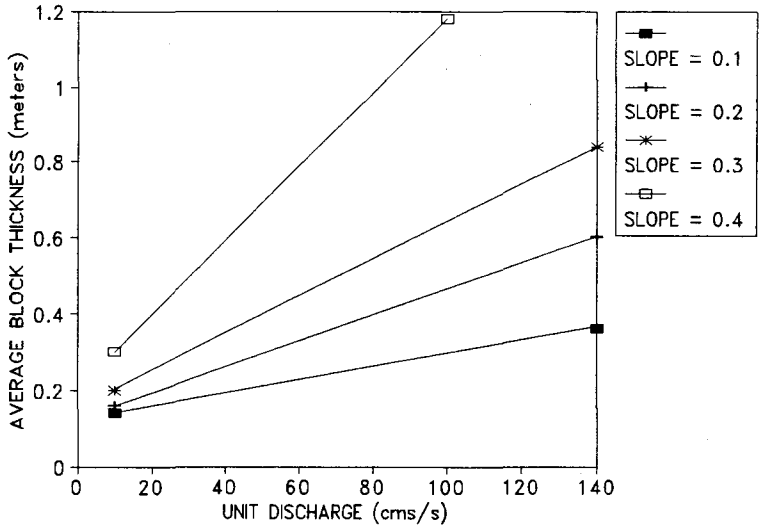

Figure 2.10. Recommended Average Block Thickness (Grinchuk and Pravdivets, 1977)

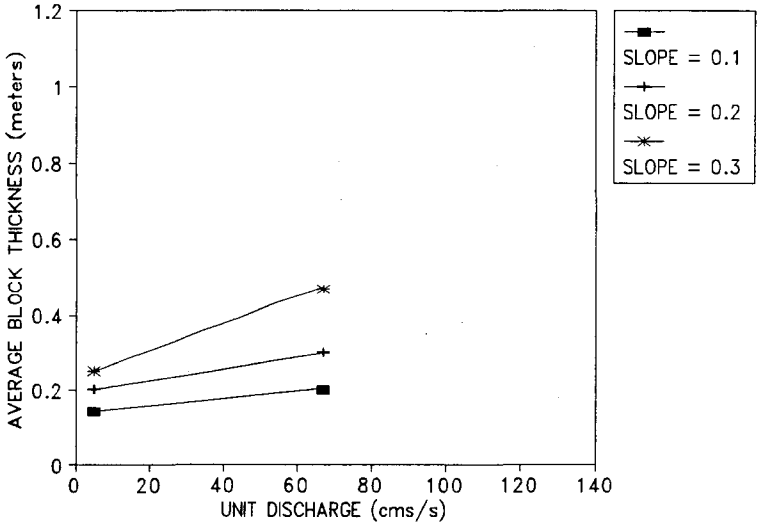

Figure 2.11. Recommended Average Block Thickness (Pravdivets et al, 1980)

these coefficients were available for stepped surfaces, so, an approach, was developed which makes use of a roughness factor called Φ (phi) (Pravdivets, 1989). The equation for unaerated flow depth is developed as follows. Consider an energy balance along the water surface between the crest and some downslope location. Assuming that friction losses are zero, all elevation head lost by the flow will be converted into velocity head and velocity will simply be a function of the change in elevation.

$$V = \sqrt{2g(P + H)} \tag{2.2}$$

P is the vertical distance below the crest and H is the overtopping head. Since friction losses have been neglected and are they are significant, the true velocity will not be as high as the above equation indicates. Therefore, multiply by a correction factor Φ which varies between 0 and 1 and decreases with increased distance downslope. Writing velocity as a function of unit discharge and flow depth yields an equation for unaerated flow depth that is valid for rectangular or very wide channels.

$$d = \frac{q}{\Phi \sqrt{2g(P + H)}} \tag{2.3}$$

The unaerated flow depth is d and q is the unit discharge. The correction factor Φ is based on model tests conducted in the USSR and the UK and curves for it as a function of position on the embankment are presented in Figure 2.12. These values for Φ are valid for water depths greater than twice the step height (CIRIA, 1992).

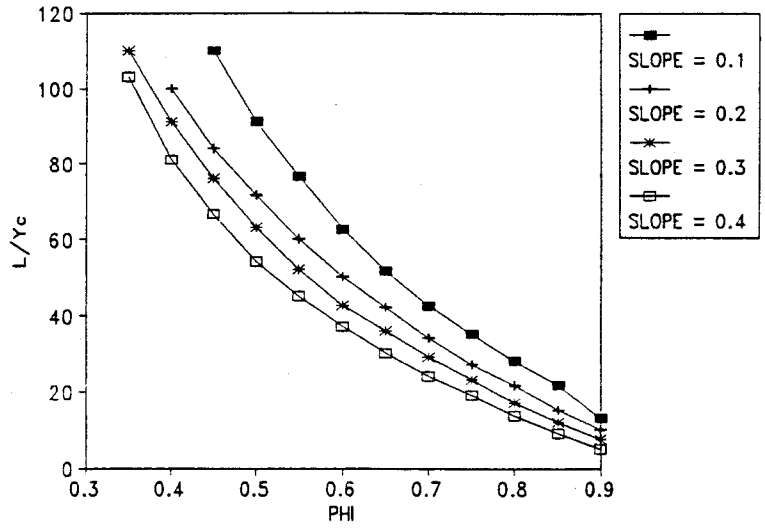

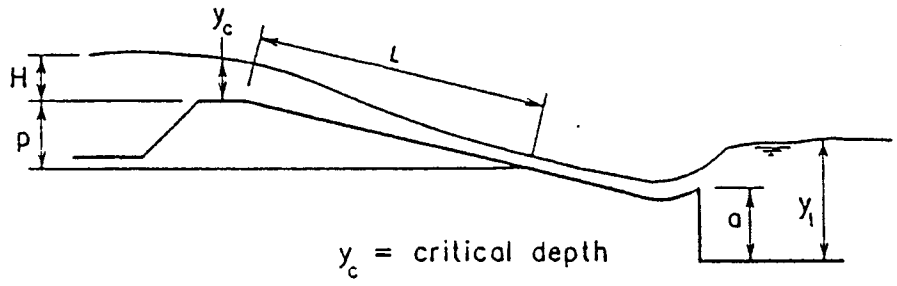

Figure 2.12. Correction Factor Φ Used for Stepped Spillway Depth Calculations, Yc = critical depth, L = downslope distance (Pravdivets and Bramley, 1989)

CHAPTER THREE

WEDGE BLOCK FLOW CHARACTERISTICS AND THEORETICAL CONSIDERATIONS

GENERAL CHARACTERISTICS OF FLOW OVER A WEDGE-BLOCK OVERLAY

An overtopping flow on an embankment dam produces large and potentially damaging velocities. The geometry of a wedge-block overlay is such that these high velocities are both mitigated and used to advantage. First, the stepped nature of the overlay provides more energy dissipation than would take place on a smooth overlay. This difference was quantified for a smooth surface and two different stepped geometries by the USBR in its stepped spillway model study (Frizell, 1992). Stepped spillways were shown to introduce significant cost savings over smooth spillways due to deceased stilling basin length requirements.

Energy dissipation is a desirable characteristic, but, only to a point in the case of a wedge-block overlay. Velocities on the overlay should remain high enough to produce very low pressures, negative if possible, in the separation zone. This separation/recirculation zone forms on every block in the recessed region below the pitch line of the slope. The pitch line is an imaginary line which has the same slope as the embankment and connects the tips of the steps on the slope. Flow over a section of wedge-block overlay is illustrated in Figure 3.1. Water moving through the recessed region encounters an abrupt expansion which causes flow separation. In this separated

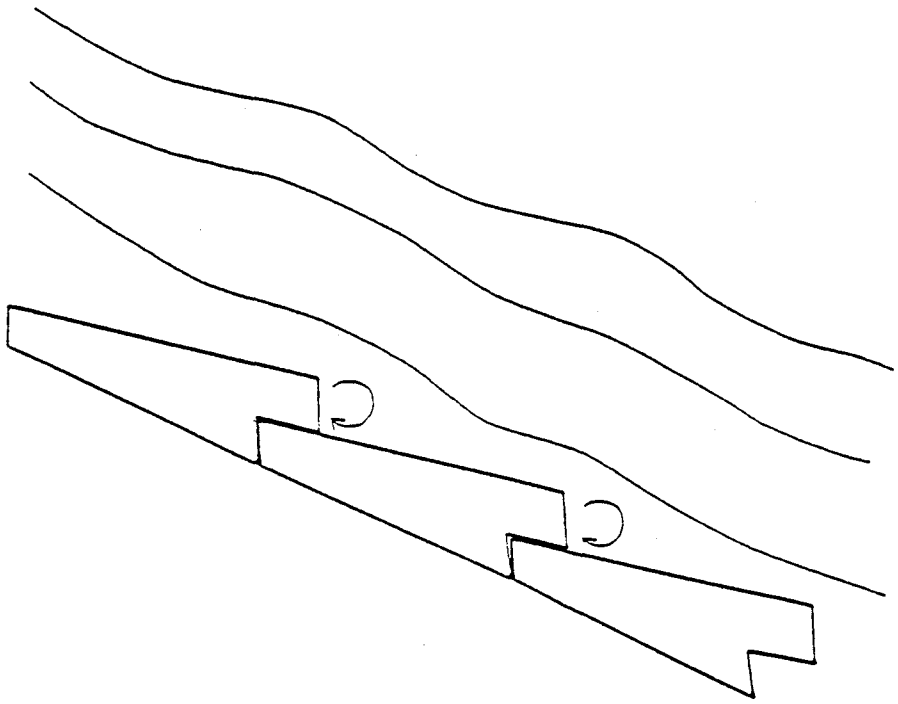

Figure 3.1. Flow Over a Wedge-Block Overlay

region a recirculating eddy or vortex forms as illustrated in Figure 3.1. The low pressure of this region is used to remove water, through drains, from the underside of the overlay thereby reducing uplift pressures. It is in this way that the high velocity of the flow has been used to advantage and is in fact necessary, to a certain degree, for proper functioning of the overlay.

Figure 3.1 illustrates one other important aspect of flows over stepped surfaces. As the flow leaves one step and proceeds on to the next, some liquid near the step surface splits off from the main flow and forms the recirculating eddy just discussed. Most of the flow near the surface, though, continues on and impacts the step on its downstream portion. Thus, a high pressure region is formed in this impact area on each

of the steps. As with the separation zone, the impact region of the step is a desirable characteristic of the flow. The downward pressures developed in this region help the overlay to resist uplift pressures which come from a variety of sources and are discussed later in this chapter.

THEORETICAL DISCUSSION OF RECIRCULATION REGION

In order to understand the physical reason for the low pressure which develops in the recirculation region, it is useful to model it as a forced vortex. More accurate models of eddies treat them as free vortices surrounding a forced vortex core but the explanation for the low pressure is the same, so, the more simple model will be used.

Because fluid in the forced vortex is spinning, it tends to move outward from the center which is consequently a region of low pressure. Examples of this phenomena, such as a stirred cup of coffee, are abundant. When stirred, the fluid surface at the center of the cup drops and near the walls of the cup it rises up. The center of the rotating coffee is thus observed to be the point of lowest pressure. Using the forced vortex approximation, we find that the magnitude of the low pressure which develops is a function of the pressure and velocity of the main flow. An analysis of the momentum equation in cylindrical coordinates with gravity neglected yields:

$$\frac{dP_r}{dr} = \rho r \omega^2 \qquad (3.1)$$

where ω is the angular velocity or V_r/r and P_r is the pressure along the vortex radius. This equation expresses a balance between the centripetal acceleration of the fluid and

the pressure force per unit mass exerted on the fluid. We may integrate this equation to obtain a pressure distribution:

$$P_r = P_c + \frac{\rho\omega^2 r^2}{2} \tag{3.2}$$

where the integration constant, P_c, is the pressure at the vortex center. Now a pressure at the center of the vortex may be obtained if the main flow pressure, P_o and V_o, are known. We assume that these occur at the edge of the vortex and thus get the desired result.

$$P_c = P_o - \frac{\rho V_o^2}{2} \tag{3.3}$$

This equation tells us that the drop in pressure head between edge and center of the vortex is equal to the change in velocity head between those two points. This, of course, assumes frictionless fluid flow. Equation 3.3 yields an important design insight. It indicates that the magnitude of the pressure drop in the recessed region is dictated by the main flow velocity and pressure. Note that there is a trade off. Higher flow velocities mean lower vortex pressures, but, they also mean more kinetic energy will have to be dissipated in the stilling basin. On the other hand, if flow velocities are not high enough, then vortex pressures will not be low enough to aspirate the subgrade. This trade off was investigated by the USBR in their laboratory model. Test results for steps with horizontal tread faces and faces sloped down 15 degrees were reported by Frizell in 1992. Velocity profiles showed horizontal steps provided lower velocities and thus greater energy dissipation down the slope. A sample calculation using these results

showed that horizontal steps resulted in a hydraulic jump at the base of the spillway that was 13.5 percent shorter than that obtained for the 15 degree steps. This translates into reduced stilling basin costs. But, for the horizontal steps, the recessed area pressures were deemed not low enough to aspirate. The 15 degree steps provided less energy dissipation but achieved the sub-atmospheric vortex pressures that were desired.

THEORETICAL DISCUSSION OF THE IMPACT REGION

The pressure resulting from the impact of flowing water may be analyzed in the following manner. Consider the principal of conservation of linear momentum for a parcel of water just before it strikes a step and just after. Neglecting pressure forces due to any overlying depth of water, a balance between the change in momentum due to impact and the force of impact is obtained.

$$F_y = \rho A(V_2 \sin\theta_2)^2 - \rho A(V_1 \sin\theta_1)^2 \qquad \textbf{(3.4)}$$

In this equation, F_y is the impact force normal to the block surface, A is the area of impact, and $V_1\sin\theta_1$ and $V_2\sin\theta_2$ are, respectively, the normal velocity components of the fluid parcel before and after it strikes the step. Equation 3.4 shows that impact pressures are directly proportional to density and the square of flow velocity. Aeration, which decreases the density of the flow, can, therefore, significantly reduce impact forces. From the above equation, it follows that while the flow remains unaerated, impact pressures should increase in the downslope direction due to increased velocities. Past the point at which aeration begins, though, impact pressures may decrease in the downstream direction as the degree of aeration increases depending the amount of

acceleration taking place. These theoretical trends can be clearly observed in experimental data presented in the following chapter.

THEORETICAL DISCUSSION OF OVERLAY FAILURE

Failures of any protective overlay fall into three general categories; erosional failures, geotechnical failures, and hydrodynamic failures.

Erosional failures occur when significant amounts of underlying drain or embankment materials are removed by flowing water. Erosion of the downstream face may be the result of overtopping flows or seepage flows beneath the overlay. Additionally, seepage flows, through or underneath the embankment, may erode significant cavities in a phenomenon called piping. The result of these erosional processes is usually a non-uniform settling of the embankment and overlay. In an overtopping flow, local scour will then cause further erosion at any depressions or discontinuities. For a concrete block overlay, especially a wedge-block version, there are the additional problems. Non-uniform settling changes the orientation of some of the blocks to the flow and may also reduce the degree of interlock. Exceptions to non-uniform settling are possible. Jelyevski Dam is an example. Here, the underlying drain and embankment materials eroded rather uniformly over the downstream face. Thus, the wedge-block overlay also settled uniformly and remained intact. Though the blocks remained together, the protection scheme as a whole failed because a portion of the spillway was reduced to a horizontal channel.

Geotechnical failures include the slumping or sliding downslope of portions of the

embankment due to failure along a weak plane or surface. Soil liquification is another possible geotechnical failure. This may be the result of vibrations induced by blasting or earthquakes or may result from significant upward seepage flows which suspend the soil particles.

Hydrodynamic failure occurs when the forces exerted by the fluid medium, which surrounds the protective overlay, unfavorably move or completely dislodge some portion of that overlay. The near-prototype testing carried out at Colorado State University did not examine the stability of a wedge-block overlay with regard to erosional or geotechnical failures. At most, some deductions about the settling and migration of drain materials may be made. Rather, hydrodynamic stability was the focus of the experiments. For the purposes of a stability analysis, it was reasoned that an equalization of forces normal to the slope would be a necessary prerequisite to failure. This idea and the stability analysis that stems from it are discussed further in Chapter Four, but, it is evident that three forces will dictate block stability. Two of these, impact forces and recirculation zone forces, have already been discussed. The final, and most important force, is the result of pressures which develop in the drainage layer. The possible sources of such pressures are discussed in the following sections.

Sources of Uplift Pressures

The first possible source of uplift pressure is the change in direction that the flow undergoes when moving from the crest to the sloped embankment face. Water moving across the crest of the embankment has horizontal momentum which cannot be

instantaneously redirected down the slope. Thus, there is a tendency for the flow to spring free as it leaves the crest. As a result, the portion of the slope directly below the crest is a region of low pressure, relatively speaking. An estimate of the magnitude of these low pressures may be obtained by superimposing on the actual embankment face geometry a nappe equation. The nappe equation describes, in terms of horizontal and vertical coordinates, the trajectory followed by a parcel of water which flows freely over and springs free from a weir. Superimposing the nappe equation on a spillway face and measuring the vertical distance between the two, gives the deviation of spillway pressure head from atmospheric. In other words, if the line corresponding to the nappe equation plots above the embankment face at some location, then, the vertical distance between the equation and the embankment face is an approximation of the negative pressure head that will develop at that location. It is evident that if the spillway face conforms well to the underside of the nappe, the pressure will everywhere be close to atmospheric, or zero-gage pressure. This reasoning has given rise to the well known ogee crest spillway.

One approach to obtaining a nappe equation is to start with the equations of rigid body motion. Such an analysis carried out in two dimensions yields the following water parcel trajectory:

$$Y = [\frac{-g}{2V_{ox}^2}]X^2 \qquad \textbf{(3.5)}$$

In the above equation, g is the acceleration due to gravity and V_{ox} refers to the velocity of the fluid parcel just as it leaves the crest. If the origin of the coordinate system is taken to be at the end of the crest, the equation yields coordinates defining the location

of the underside of the nappe (Clopper and Chen, 1988). This approach overestimates the negative pressures which develop for one major reason. In calculating the coordinates of the underside of the nappe the average flow velocity has been used. In reality, near the surface of the crest, velocity varies significantly with depth and goes to zero right at the crest surface.

The Bureau of Reclamation has standardized experimental nappe equations for the design of ogee crest spillways (USBR, 1974). The general form of their equation is given below.

$$\frac{Y}{H_o} = -K[\frac{X}{H_o}]^n \qquad (3.6)$$

The coefficient K and exponent n are chosen based on the approach velocity, the overtopping head and, the slope of the upstream face of the dam. Values for these coefficients can be found in the referenced text by the USBR (1974). The experimental curves for K and n, though, only cover vertical through 1H:1V upstream slopes. Thus, in the case of a long, horizontal crest, the significant horizontal momentum that the overtopping flow develops cannot be fully accounted for with the available curves for K and n. For this reason the USBR method, without further information on K and n, would tend to underestimate the low pressures developed. For purposes of checking the stability of the overlay, the more conservative rigid body approach was deemed most appropriate. An application of this method to the near-prototype embankment at a unit discharge of 31.6 ft^2/s (2.94 m^2/s), the worst case, produced the results illustrated in Figure 3.2. Velocity of flow, V_{ox}, was conservatively estimated to be the velocity of

flow at critical depth. It is evident that for the velocity considered, only a small portion of the embankment would be subjected to uplift pressures from this source. For larger approach velocities,the size of this region and the magnitude of the low pressures that develop in it would both be larger. It is important to the stability of the entire overlay, though, that this low pressure region, however small, be adequately anchored. The removal, by uplift, of even one block, could quickly cause the failure of the entire overlay. The reason is that if one block is removed, the block below it will have its vertical upstream edge and underside exposed to high velocity flow. This exposed block would easily be washed out, thus, exposing the block below it , and so on.

Another source of uplift pressure is the hydraulic connection of the reservoir head and the underside of the protective overlay. This is a potentially serious problem if the filter material and subgrade are inadequately drained. Consider the worst case scenario for a 50 foot (15.2 meter) high embankment just about to be overtopped. If there is seepage from the reservoir side of the embankment to the overlay side and there are no drains present to allow this seepage to escape, then, there could potentially be 50 feet (15.2 meters) of pressure head acting to uplift the blocks at the toe of the embankment. Even with an aspirating wedge block design there may still be some pressure buildup because the drains do not function well until low enough pressures are attained in the separation zone.

A final source of uplift arises from impact pressures which force water into the filter layer through the spaces between adjacent blocks. Again, with a wedge-block design, the drains can evacuate this water but not without some pressure buildup in the

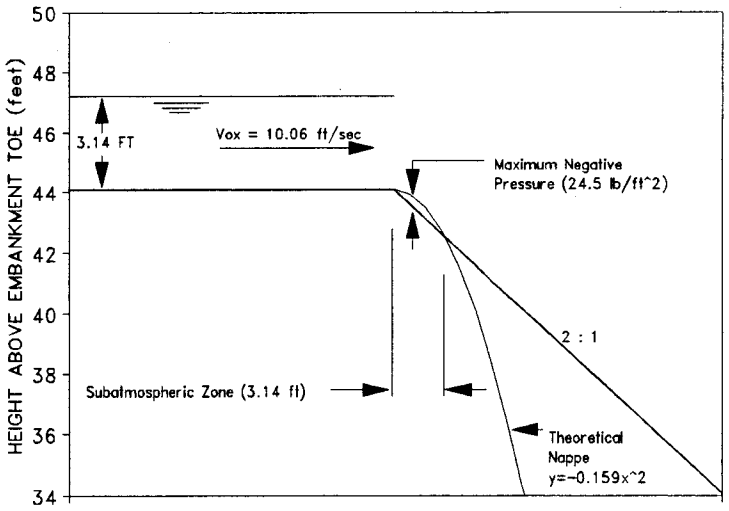

Figure 3.2. Theoretical Nappe Equation Superimposed on CSU Near-Prototype Embankment

filter. Pressures in the separation zone are determined by the velocity of the main flow and are thus, somewhat fixed at a given location. The more water that is forced into the filter layer, then, the higher filter layer pressures must rise to force it out through the drains. Such a pressure build up is likely to be most severe on upper sections of the slope where velocities are relatively low.

CHAPTER FOUR

DESCRIPTION OF NEAR-PROTOTYPE TESTING OF WEDGE-BLOCK PROTECTION

DESCRIPTION OF TESTING FACILITY

The CSU/USBR Dam Safety Overtopping Test Facility is located at the Engineering Research Center on the Foothills Campus of Colorado State University. The facility consists of a 10 foot-wide concrete flume constructed on a 2H:1V slope which provides approximately 50 feet (15 meters) of vertical drop. A plan view and longitudinal section of the facility are presented in Figures 4.1 and 4.2.

Water is delivered to the head box from Horsetooth Reservoir through a 36 inch (914 mm) pipeline. The reservoir can supply approximately 150 ft^3/s (4.25 m^3/s) depending on its stage. An additional 50 ft^3/s (1.42 m^3/s) is available from a pump which may be used to recirculate a portion of the flow. The pump is powered by an Aurora Diesel 8V-92T engine which delivers 435 BHP (325 KW) at 2100 rpm. This possible 200 ft^3/s (5.66 m^3/s) flow capacity corresponds to a unit discharge of 40 ft^2/s (3.72 m^2/s) and an overtopping head of approximately 5.4 feet (1.65 meters). A rating curve for the flume is given in Figure 4.3.

The flume is designed to model flows on a near-prototype scale. The advantage of the large size is that the inaccuracies inherent in hydraulic modeling are minimized.

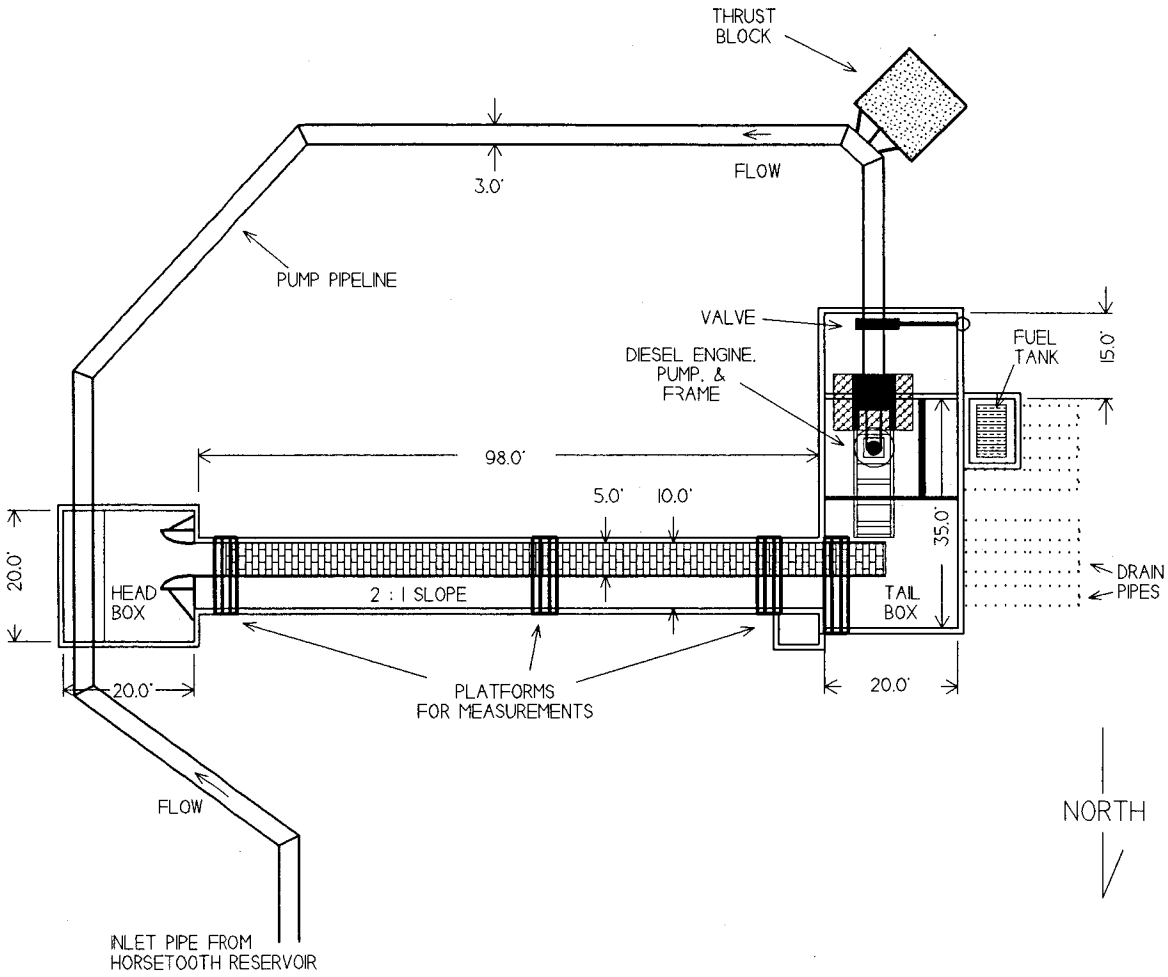

Figure 4.1. Plan View of CSU/USBR Dam Safety Overtopping Facility

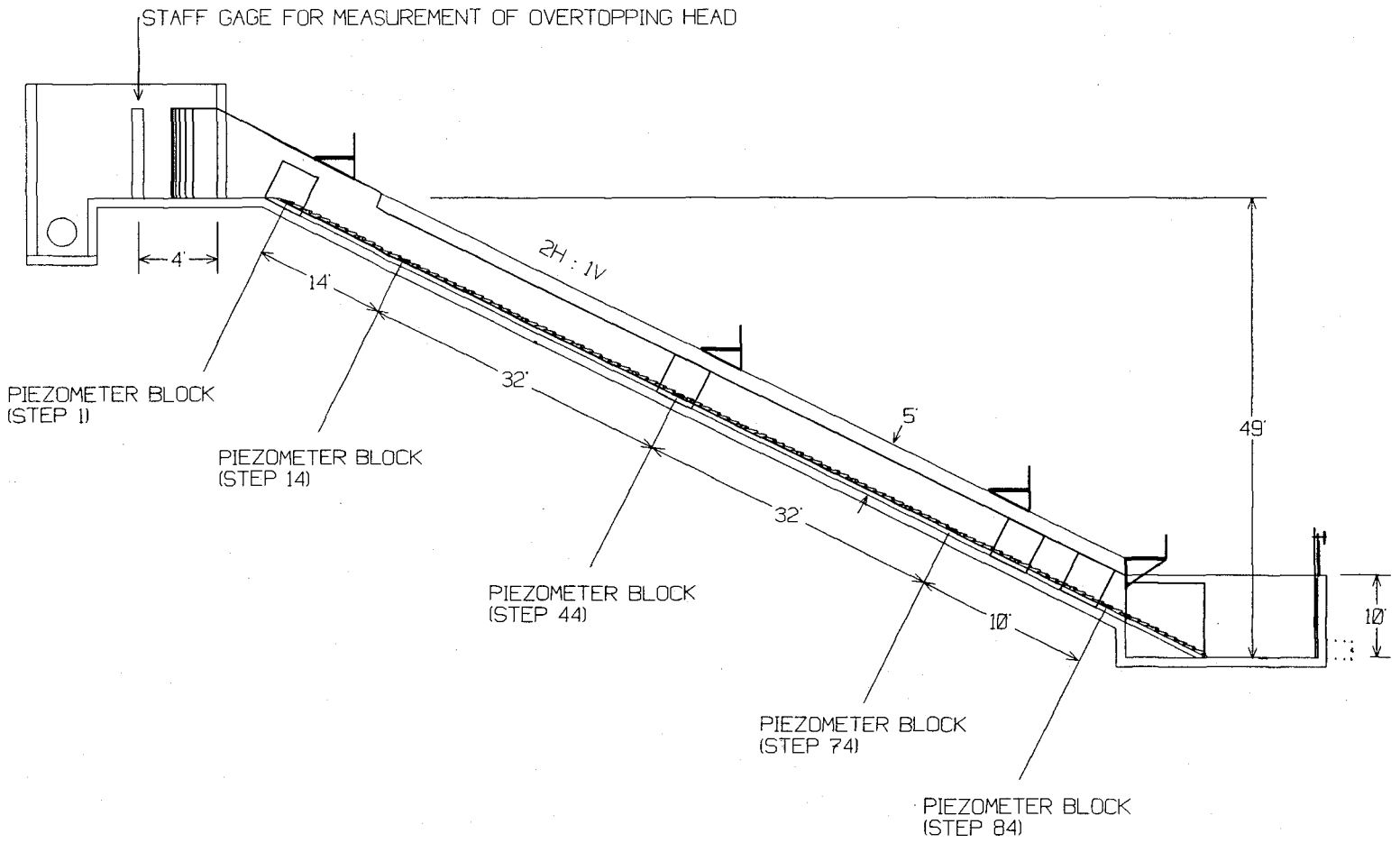

Figure 4.2. Profile of CSU/USBR Dam Safety Overtopping Facility

mm) redwood timbers were fastened to the flume's sidewalls. A 6 inch (152 mm) layer of aggregate, free of fines, was then put down on the concrete floor to serve as a drainage medium and bedding material for the wedge blocks. The aggregate was compacted, as it was put in, using hand tamps. The size distribution of drain material falls within the range defined by the two curves in Figure 4.4.

Rows of wedge blocks were laid directly on top of the drain material. Each row consisted of two, 2 foot (0.61 meter) wide blocks and one, 1 foot (.3 meter) wide block. The blocks were arranged in stretcher bond configuration where longitudinal joints between adjacent blocks in one row do not line up with the joints of the row above or below (Baker, 1990). The outside edges of the two blocks which butted up against the flume sidewalls, were set on top of the redwood timbers which were fastened there. In this way, the outside edges of each row were prevented from settling. The overlay and drainage layer were terminated at the toe of the embankment by a 6 x 6 x 3/8 inch (152 x 152 x 9.5 mm) piece of angle iron bolted to the floor of the flume.

In order to increase block interlock at the embankment toe where a hydraulic jump might form, 3 inch (76 mm) long pins were placed in holes located in the upstream and downstream block faces which butted up against each other. These pins were placed in the first ten rows up from the toe at 1 foot (0.3 meter) intervals across the width of the flume.

To lend further stability to the overlay, j-bolts, hooked to angle iron beneath the blocks, were used to secure the overlay to the embankment at four locations: immediately below the crest; at the toe of the slope; and at two middle locations such

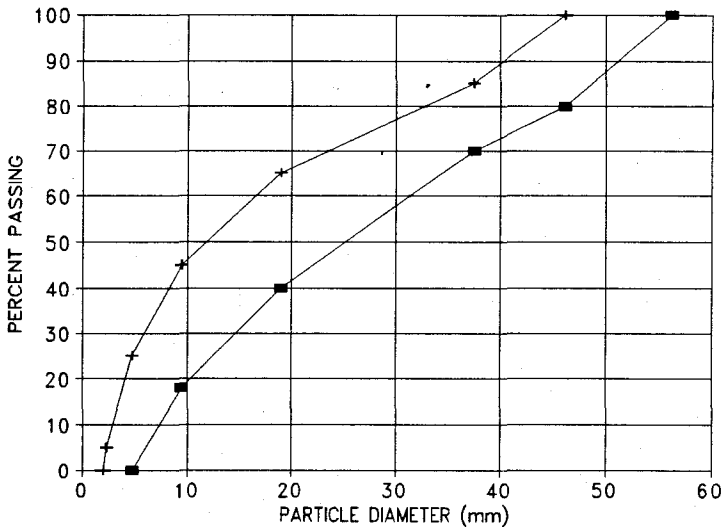

Figure 4.4. Drain Material Size Distribution Range

that the length of the slope was divided into approximate thirds. J-bolted rows of wedge blocks were then tightened down on to the filter material. Figure 4.5 illustrates how j-bolts were used to fasten the overlay to the embankment. Figure 4.6 is a photograph of the completed flume. Figure 4.7 is a photograph of the facility being operated at a unit discharge of 8 ft^2/s (0.74 m^2/s).

Discharge and Overtopping Head Measurements

The discharge in the pipeline from Horsetooth Reservoir was determined by a Mapco Nusonics sonic flow meter. The meter is advertised to be accurate within 1%.

Once the flow rate had been set to the desired value, the overtopping head was determined from two staff gages located on the north and south walls of the headbox.

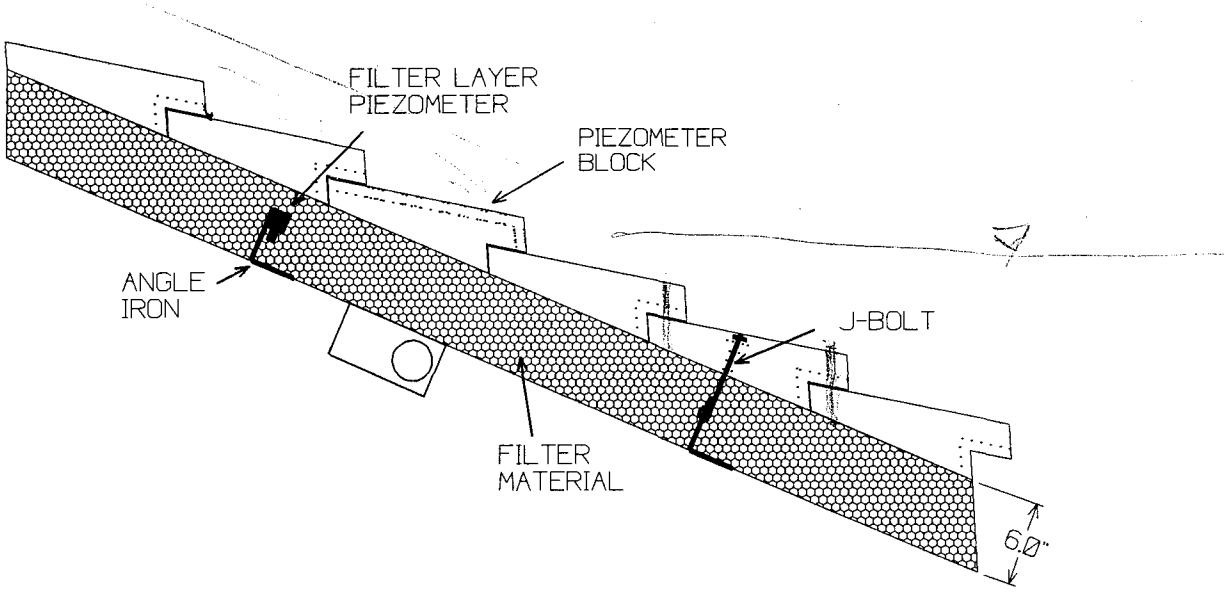

Figure 4.5. Typical Section of Wedge-Block Overlay and Drainage Layer

The staff gages were installed using a surveyor's level so that a zero reading on them corresponded to the elevation of the spillway crest.

The recirculating pump was used only to obtain the highest tested unit discharge which was 31.6 ft^2/s (2.94 m^2/s). The pump discharge was determined by subtracting the flow rate in the Horsetooth line, as determined by the sonic flow meter, from the total flow calculated from the flume rating curve given in Figure 4.3.

The unit discharges, overtopping heads, and test durations for the tests conducted at the CSU/USBR near-prototype facility are presented in Table 4.1.

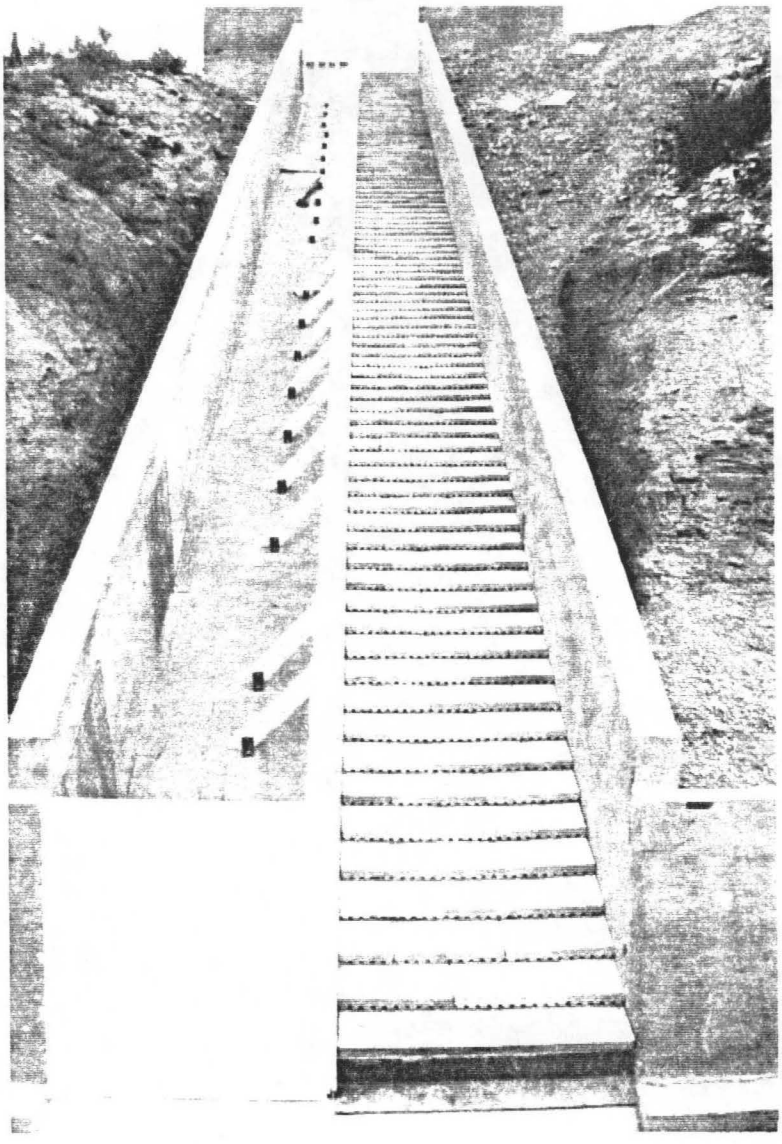

Figure 4.6. Completed CSU/USBR Dam Safety Overtopping Facility and Wedge-Block Overlay

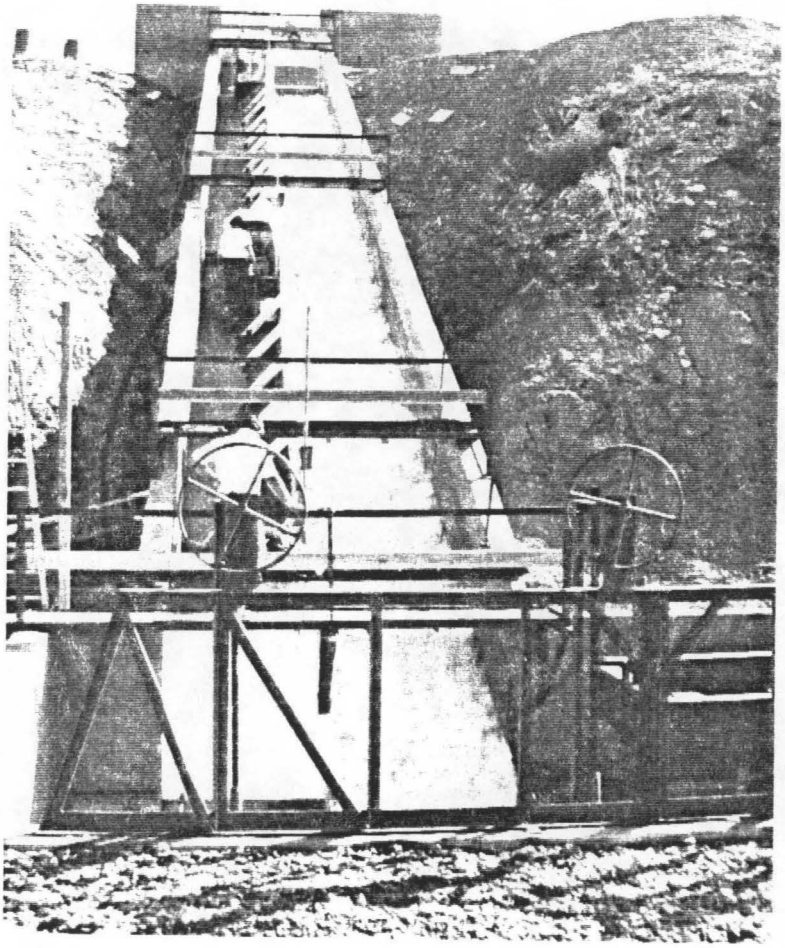

Figure 4.7. CSU/USBR Dam Safety Overtopping Facility Operating at a Unit Discharge of 8 ft^2/s (0.74 m^2/s)

Table 4.1. Five Discharges Tested at the CSU/USBR Near-Prototype Facility

Unit Discharge (ft^2/s)	Overtopping Head (feet)	Test Duration (hours)
2.8	1.0	4
8	1.9	4
14.8	2.9	4
22.8	3.7	4
31.6	4.7	4

Pressure Measurements

Five wedge blocks instrumented with 11 piezometer taps each, were placed at the flume locations indicated in Figure 4.2. The locations of the taps on the instrumented blocks are shown in Figure 4.8.

In order to measure pressures in the filter layer, piezometers were mounted to pieces of angle-iron at five locations in the drainage layer. Each one was located near the underside of one of the instrumented wedge-blocks. To avoid clogging, these piezometers were constructed out of blocks of aluminum with numerous holes in their top surface. With this design, if one or more holes did become clogged, others would still be open. All five of these drainage-layer piezometers functioned satisfactorily during the tests conducted.

Polyflow tubing, with an outside diameter of 3/8 inch (9.5 mm), was used for all piezometer lines. This large size was selected to prevent clogging. The twelve piezometer lines at each of the five instrumented locations were passed outside the flume

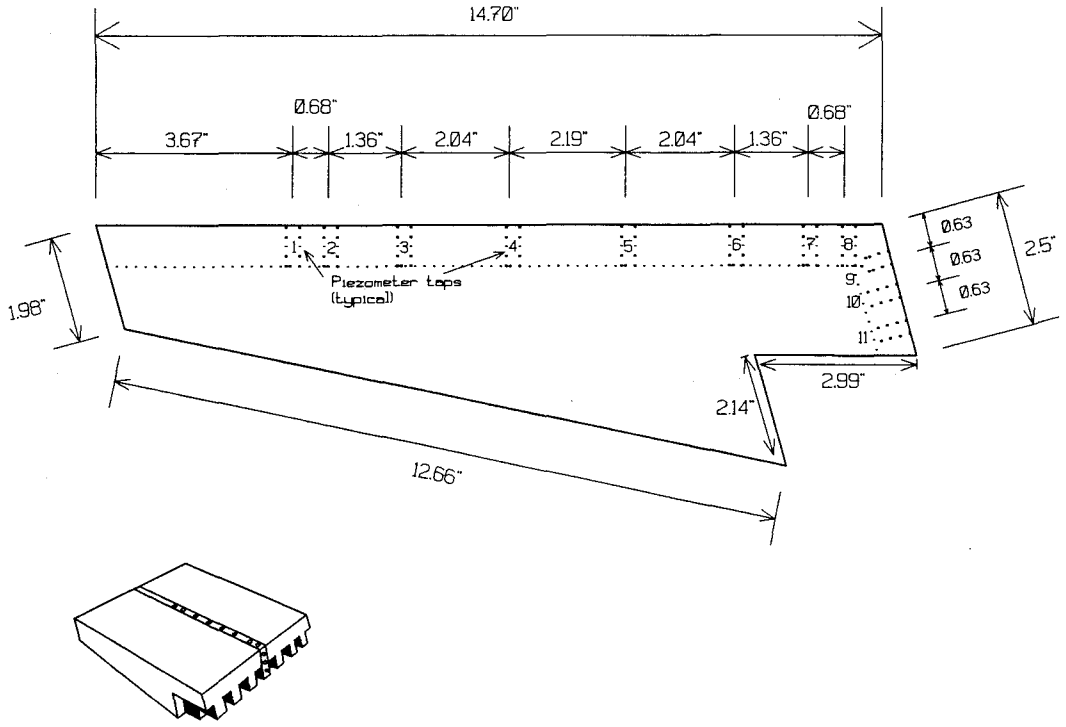

Figure 4.8. Wedge Block Dimensions and Tap Locations

through a piece of 6 inch (152 mm) conduit cast into the flume floor. All twelve lines were then attached, each with its own valve, to a manifold. A thirteenth valve on the manifold, used for bleeding the 12 lines, could be opened to allow connection with a water tank located on top of the embankment. A fourteenth and final valve located on each manifold provided connection with a pressure transducer. A different pressure transducer was used for each instrumented block and drainage layer piezometer combination. At the instrumented location nearest the crest, the pressure transducer used was a 2.5 lb/in^2 (17.2 KPa) Druck PDCR-22. This transducer was hooked directly up

to a digital recorder. For the lower four instrumented locations, 5 lb/in^2 (34.5 KPa) Pace PD-25 pressure transducers were used. These four were hooked up to a four channel, analog, strip-chart recorder. From the strip-chart recorder, the signals were also then sent to the digital recorder.

Before the first test run, zero transducer readings for each pressure tap were obtained. To obtain the zero reading for a particular pressure tap, the line was first bled, then, the transducer reading obtained when the water surface was flush with the block surface was recorded as the zero. The zero readings were checked against surveyed differences in elevation and subsequently used for all five test runs.

During testing, piezometer lines were bled using high pressure from the tank before each pressure reading. Pressures at the same tap number were read simultaneously for all five locations in the flume. For all taps, pressures were recorded continuously for one minute at a rate of 25 readings per second or at 25 hertz.

Depth Measurements

All depth measurements were recorded at the measurement platforms shown in Figures 4.1 and 4.2. Measurement of flow depths was complicated by the fact that over much of the length of the flume, for all discharges, the flow was extremely aerated. In an attempt to get as much information as possible, two different methods were used to obtain depths.

The first method employed was a standard point gage graduated to hundredths of a foot (0.25 mm). Point gages were mounted, normal to the slope, on each of the four

measurement platforms. At each of these four cross sections, depths were recorded every six inches (nine locations) by two different people. These two sets of nine depths were then averaged to obtain a single value for depth at the cross section.

At the platform nearest the head box and transition structure, surges and lateral waves created an uneven water surface. To improve measurement accuracy at this station, the procedure discussed above was followed, and in addition, the number of depth readings was doubled. Each of the two people reading depths at this station, recorded two values every six inches rather than one; a "high" and a "low". For the high reading, a depth was recorded where the tip of the point gage was generally unsubmerged, but, would be touched intermittently by the water surface. For the low reading, a depth was recorded where the tip of the point gage generally remained submerged, but, the water surface would intermittently drop below it. These two sets of nine high and nine low values were then averaged to obtain a single value for depth in the cross section.

At the bottom three measurement stations, for all discharges tested, the flow was aerated to some degree. Depth measurements in such a flow are difficult because the water surface is not well defined. For the present testing program, it was decided that when taking point gage measurements in an aerated section of the flume, the intention would be to measure the depth of the underlying "solid" layer of flow. Generally, such a layer could be distinguished, partially by feel and partially by sight, from the less dense overlying spray. It was found that this technique yielded depths comparable to unaerated flow depths calculated according to the procedure discussed in Chapter Two.

The second method employed to measure depths was an ultrasonic distance meter, model DMI, manufactured by CONTAQ Technologies. This instrument has a range of 2 inches (51 mm) to 60 feet (18.3 meters) and is advertised to be accurate within 1%. Depths at each of the four measurement platforms were recorded only at the center of the flume with the DMI, but, readings were taken several times to assure repeatability. The DMI consistently interpreted the uppermost limit of spray as the water surface. Thus, depths obtained with distance meter include the entire depth of aerated flow.

Velocity Measurements

Determination of velocities was hindered by the fact that they were quite high and water depths were not well defined due to aeration. Two different meters were tried and both were damaged by the high velocities. All velocity measurements were taken from the four measurement platforms shown in Figures 4.1 and 4.2.

An Ott Meter, using propeller number 4 (serial number 71952), was the first meter tried. Velocities were recorded on the center line of the flume at each of the four measurement platforms using the six-tenths depth method. Each velocity measurement was carried out four times to ensure repeatability. At the lowest unit discharge, 2.8 ft^2/s (0.26 m^2/s), depths were too shallow at all but the first station to obtain velocities with the Ott Meter. For unit discharges of 8 and 14.8 ft^2/s (0.74 and 1.37 m^2/s), velocities were obtained at all four stations. These readings, though, ranged from 12 to 34 ft/s (3.66 to 10.36 m/s) and the calibration equation supplied with the meter for propeller

number 4 was recommended by the manufacturer only for velocities between 0.2 to 16.4 ft/s (0.06 to 5 m/s). Nevertheless, this equation was used to compute velocities and, therefore, they should be viewed with caution. Velocity readings were also tried with the Ott meter at a unit discharge of 22.8 ft^2/s (2.12 m^2/s). Unfortunately, the propeller was lost at the second station down from the crest and another was not available. For this reason, no further measurements were taken with the Ott Meter.

The Global Flow Probe, manufactured by Global Water of Fair Oaks, California was then tried as an alternative. The Flow Probe utilizes the same principal as the Ott Meter. It consists of a propeller mounted inside a protective housing which is attached to a telescoping arm. One blade of the propeller contains a magnet which generates an electrical impulse as it moves past the top of the protective housing. Velocities are read directly from a digital display mounted on top of the telescoping arm. Once the probe is inserted into the flow a running average of velocities, accurate to 0.1 ft/s (0.03 m/s), is stored by the probe and displayed along with an instantaneous velocity, accurate to 0.5 ft/s (0.15 m/s). The advertised range of applicability for the probe is from 0 to 25 ft/sec (0 to 7.62 m/s). The Flow Probe was tried at a unit discharge of 31.6 ft^2/s (2.94 m^2/s). Measurements were obtained at the top two stations, but, at the third station, the two plastic blades of the propeller were torn from their shaft. No further measurements were taken with the Flow Probe. It should be noted that, although a velocity reading was obtained with the probe at the second station for 158 ft^2/s (14.7 m^2/s), that reading was out of the probe's specified range of applicability and should be viewed with caution.

CHAPTER FIVE

RESULTS OF NEAR-PROTOTYPE TESTING OF WEDGE-BLOCK PROTECTION

ANALYSIS OF PRESSURE DATA

Pressure Forces on a Block

The pressure forces which develop on a wedge block during an overtopping event may be divided into three general categories:

1. Pressure forces due to the impact of flowing water.
2. Pressure forces that result from flow separation and subsequent vortex formation.
3. Pressure forces beneath the overlay which are the result of hydraulic connection with the overtopping head and impact forces acting at the longitudinal joints between adjacent blocks.

All of these pressure forces vary with location on the embankment and unit discharge or overtopping head. An investigation of these variations and their causes is merited by their influence on the stability of the overlay and, therefore, on its design. Additionally, identification of trends also provides for some extrapolation of experimental results, at least in a qualitative sense, to larger embankments.

Impact and Separation Zone Pressures

Average Pressure Values

The variation of step pressure head profiles with location for five different unit discharges is presented in Figures 5.1a - 5.5a. The differences between maximum and minimum pressure heads and averages are given in Figures 5.1b - 5.5b. Values on the horizontal axis correspond to the location of the eleven pressure taps on the top surface of the block. In each of these figures, two distinct pressure zones are evident: a low pressure region on the upstream portion of the step where flow has separated; and a high pressure region on the downstream portion where flow is impacting the step.

The data presented in Figures 5.1a - 5.5a shows that the maximum impact pressures recorded in the flume consistently occur at the third instrumented block which is approximately 43 feet (13.1 meters) downslope from the crest. Further, the figures show that, for all discharges, impact pressures are generally rising between the crest and the region of step 44 and generally falling from that point on down. This behavior is explained by the fact that impact pressures are proportional to both water density and flow velocity. On the upper portion of the slope, the flow is experiencing large accelerations as it tries to attain an equilibrium state. Here, the velocity increases are large enough to outweigh the effects of decreased flow density due to air entrainment. On the lower portion of the slope, accelerations are much smaller as the flow nears normal depth and the effects of air entrainment become the dominant factor. These trends have been quantified in Figure 5.6 where the total impact force per unit width of the block has been plotted as a function of location and unit discharge. Values on the

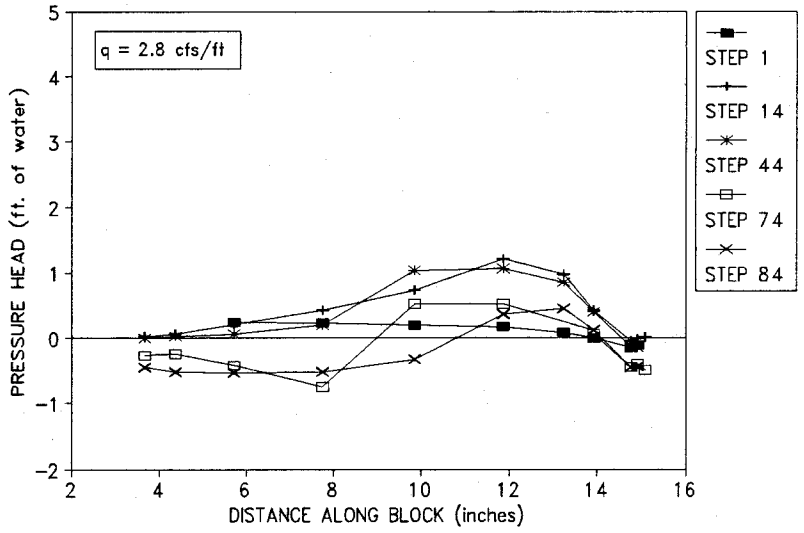

Figure 5.1a. Average Step Pressure Distributions, Unit Discharge = 2.8 ft^2/s (0.26 m^2/s)

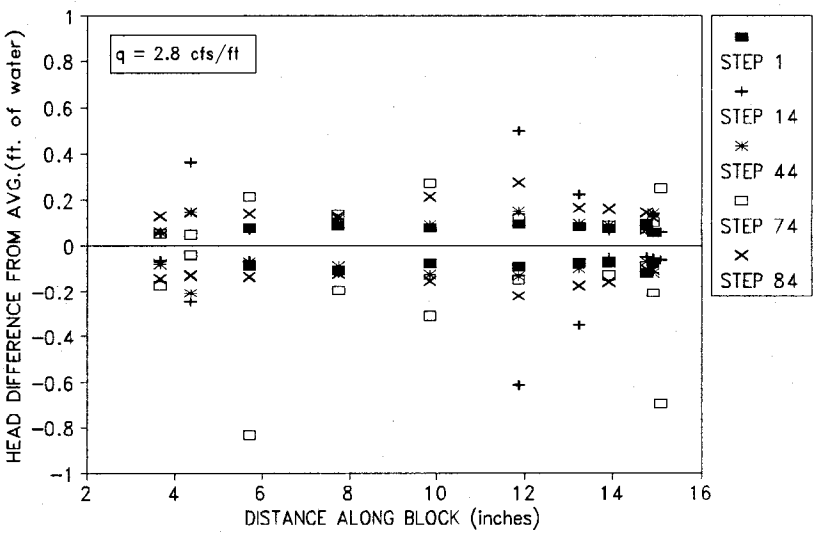

Figure 5.1b. Differences of Maximum and Minimum Step Pressure Heads from Average Values, Unit Discharge = 2.8 ft^2/s (0.26 m^2/s)

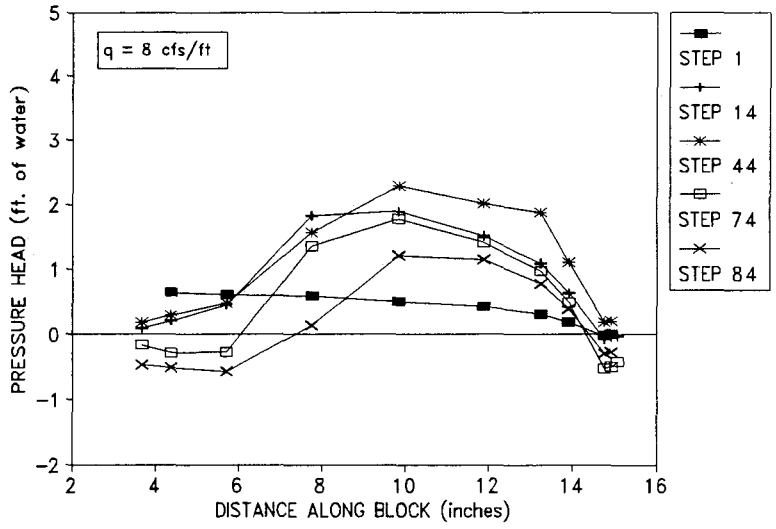

Figure 5.2a. Average Step Pressure Distributions, Unit Discharge = 8 ft^2/s (0.74 m^2/s)

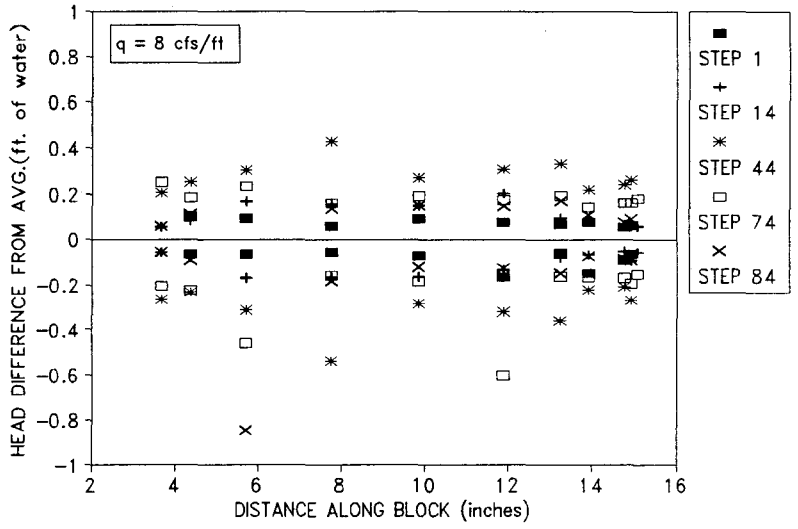

Figure 5.2b. Differences of Maximum and Minimum Step Pressure Heads from Average Values, Unit Discharge = 8 ft^2/s (0.74 m^2/s)

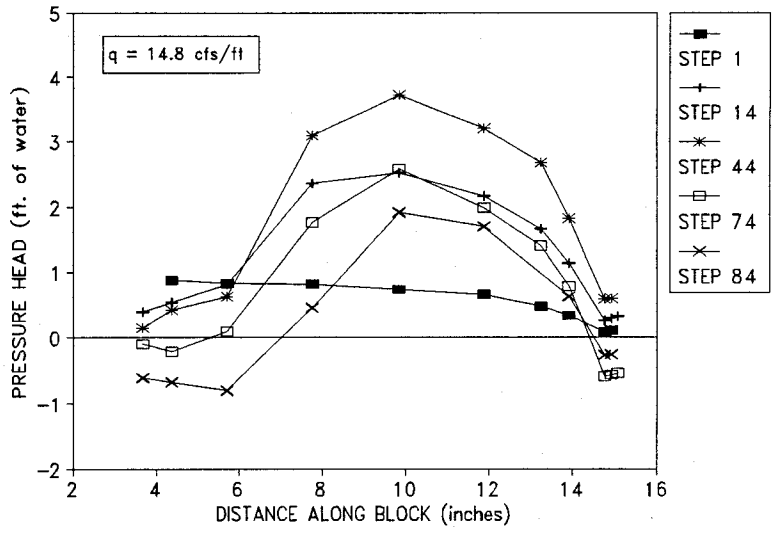

Figure 5.3a. Average Step Pressure Distributions, Unit Discharge = 14.8 ft^2/s (1.37 m^2/s)

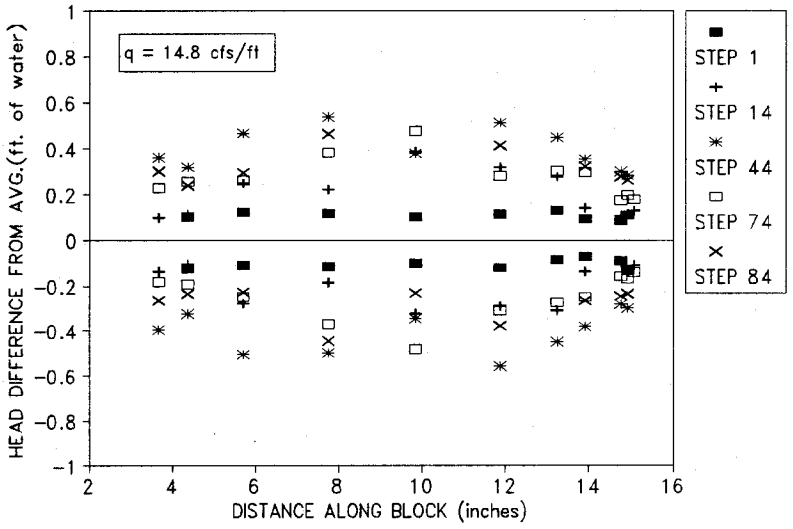

Figure 5.3b. Differences of Maximum and Minimum Step Pressure Heads from Average Values, Unit Discharge = 14.8 ft^2/s (1.37 m^2/s)

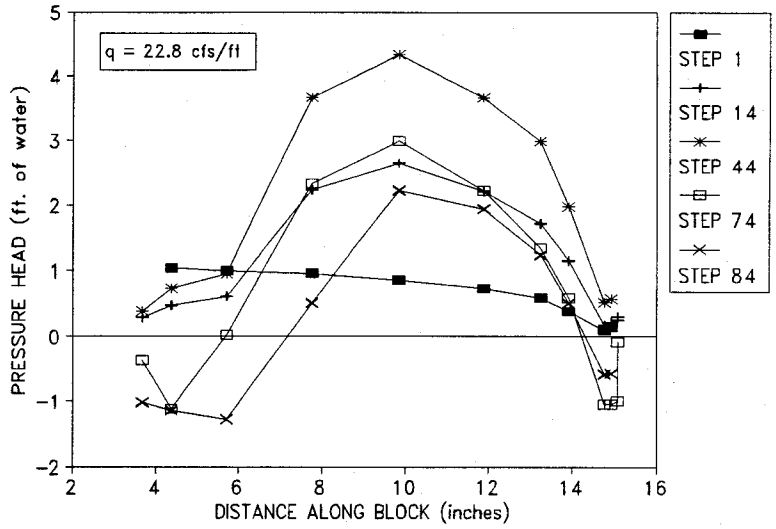

Figure 5.4a. Average Step Pressure Distributions, Unit Discharge = 22.8 ft^2/s (2.12 m^2/s)

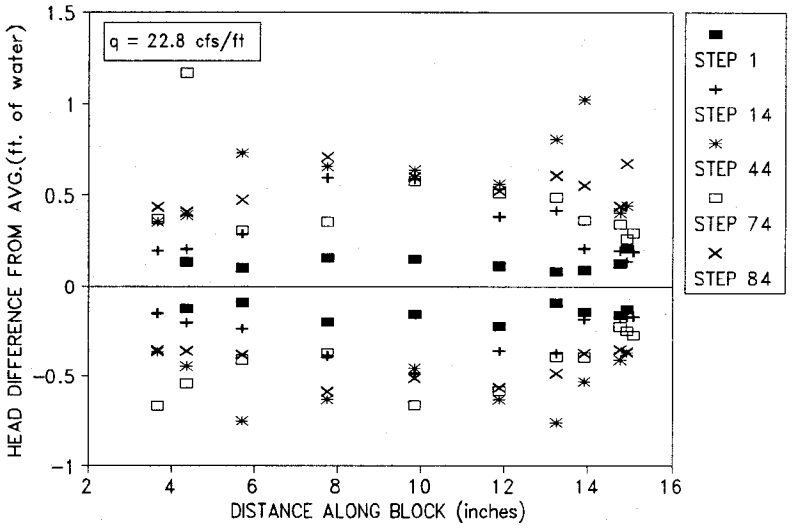

Figure 5.4b. Differences of Maximum and Minimum Step Pressure Heads from Average Values, Unit Discharge = 22.8 ft^2/s (2.12 m^2/s)

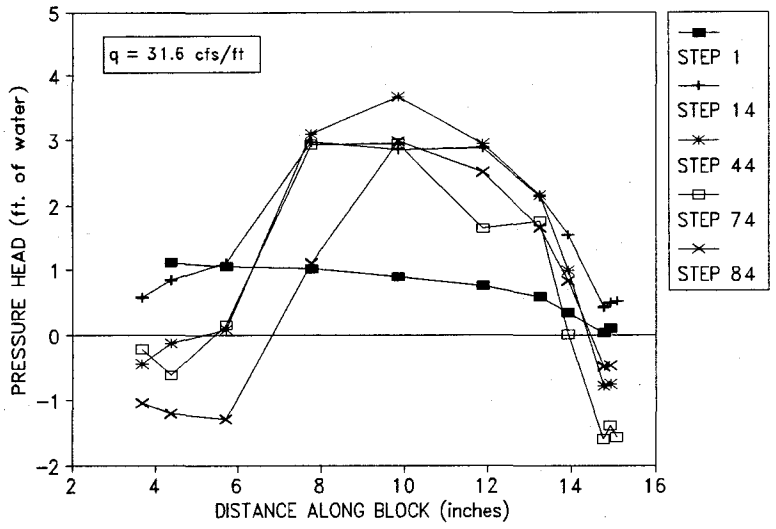

Figure 5.5a. Average Step Pressure Distributions, Unit Discharge = 31.6 ft^2/s (2.94 m^2/s)

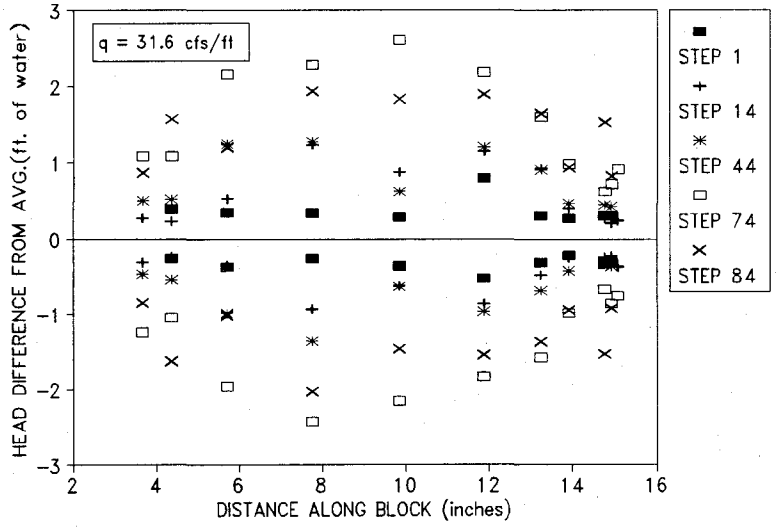

Figure 5.5b. Differences of Maximum and Minimum Step Pressure Heads from Average Values, Unit Discharge = 31.6 ft^2/s (2.94 m^2/s)

vertical axis of Figure 5.6 correspond to computed areas under the positive portions of the pressure profiles presented in Figures 5.1a - 5.5a.

Another characteristic of impact pressures can be discerned from Figures 5.7 and 5.8. These graphs show that, regardless of location on the slope, impact pressures increase as the unit discharge increases.

Pressures in the recirculation region of the step were also found to vary both with location and unit discharge. It is evident from Figure 5.7 that, on the upper portion of the slope, separation zone pressures increase as the unit discharge increases. Depth data indicate that these increases in separation zone pressures are roughly equal to the increases in depth that accompany larger discharges. Using the forced vortex approximation, though, mean flow velocity and depth data for the two unit discharges, 8 ft^2/s (0.74 m^2/s) and 14.8 ft^2/s (1.37 m^2/s), indicates that a pressure reduction in the separation zone of approximately 6 feet (1.83 meters) should have accompanied the increase in discharge. Some of the difference is due to the inaccuracy of the forced vortex model. It assumes no friction, a circular shape, and that the velocity at the outer edge of the vortex equals the main flow velocity at that point. An additional inaccuracy is that the average flow velocity has been used as the value for velocity at the outer edge of the separation zone. In actuality, velocities near the step surface are significantly smaller than the average. For all these reasons the forced vortex approximation overestimates pressure reductions. In spite of these factors, some reduction of pressures would be expected and none is observed. Apparently, on the upper portion of the slope, a well developed recirculation flow does not exist in the separation zone. Higher

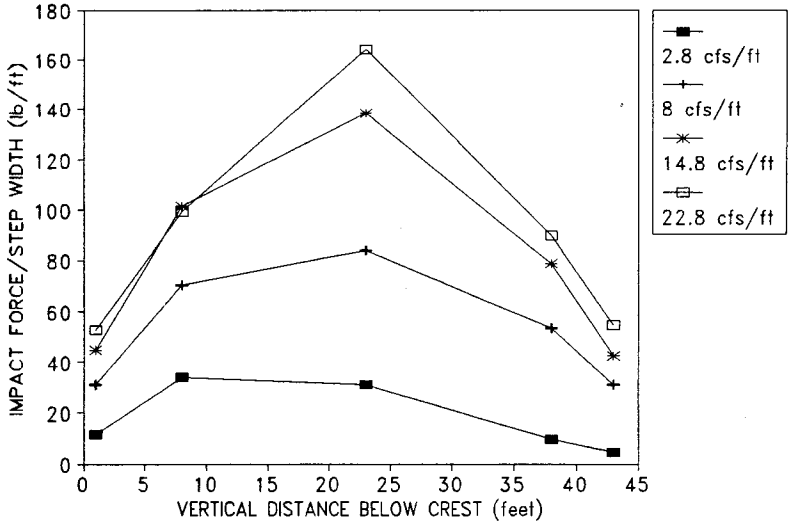

Figure 5.6. Impact Force Per Unit Step Width

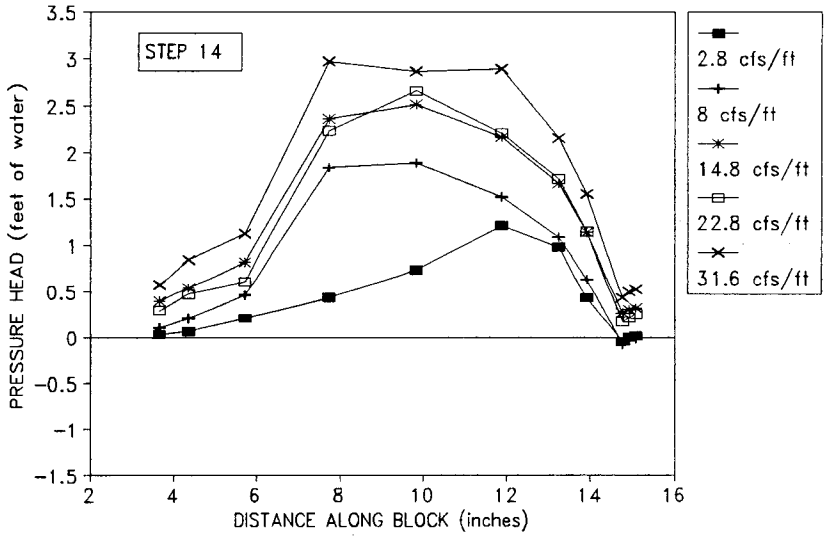

Figure 5.7. Variation of Pressure Distribution with Unit Discharge at Step Number 14 Below the Crest

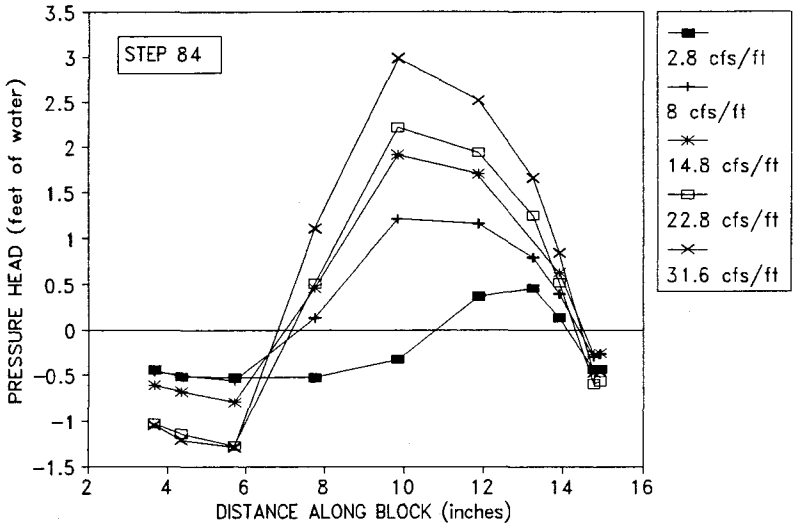

Figure 5.8. Variation of Pressure Distribution with Unit Discharge at Step Number 84 Below the Crest

velocities than are present must be required for pressure reduction because of the influence of a number of factors. These factors include:

1. Friction at the boundaries.
2. Energy losses at the interface of the main flow and the separation region.
3. Flow through the drains interfering with vortex formation.
4. Flow through the longitudinal joints between adjacent blocks interfering with vortex formation.
5. Transfer of positive underdrain pressures through the drain openings to the separation zone.

On the lower portion of the embankment, this trend is reversed and separation zone

pressures drop, as expected, with increasing unit discharge. Figure 5.8 illustrates this drop in separation zone pressures with increasing unit discharge at step 84. The reversal in behavior occurs because the velocities on the lower portion of the embankment have become high enough to overcome the restraints discussed above and develop a significant rotation in the separation zone.

Pressure Deviations from the Average

At any given time, the value of pressure at a given location consists of two components. The first of these is a time mean value. The second is a fluctuating component. Hydrodynamic failure of an overlay would be a stocastic event that occurs when fluctuating forces combine in an undesirable manner (Baker, 1990). Thus, when considering the stability of a proposed wedge-block overlay, fluctuating pressure components should be considered. To help facilitate this, the difference of maximum and minimum pressure heads from average values are presented in Figures 5.1b - 5.5b. Data points above zero correspond to the difference between maximum and average observed heads. Data points below zero correspond to the difference between minimum and average observed pressure heads. Note from these figures that pressure deviations from the average increase as the unit discharge increases. Also note that the deviations generally rise toward midslope and fall there after, tracking the rise and fall of impact pressures.

Drainage Layer Pressures

Average Pressure Values

Pressures developed in the drainage layer constitute the final force that will be considered in the block stability analysis. In order to measure drainage layer pressures, piezometers were installed near the underside of each of the five instrumented blocks. The average pressures recorded for each of the five flow rates tested are presented in Figure 5.9a as functions of the location on the slope. Due to the limited number of data points available, the lines connecting these points should be viewed with caution. They were included only to emphasize the general trends that are observed in the data. Figure 5.9b presents the differences between maximum and minimum pressure heads and average values.

Figure 5.9a shows that a general rise in filter pressures occurs between the crest and mid-slope of the near-prototype. At all locations on the embankment, water is driven into the drainage layer through gaps in the overlay by flow depths and impact pressures. On the upper portion of the slope, though, flow velocities are still low and water depths high. These factors combine to prevent large pressure reductions in the separation zone and, thus, precipitate the observed buildup of drainage layer pressures.

Figure 5.9a indicates that after approximately mid-slope, filter layer pressures begin to decline. In this region of the slope, velocities are high enough to produce large separation zone pressure reductions. This allows water in the drainage layer to be removed through the drains in the overlay with less pressure buildup beneath the blocks.

The final characteristic of the filter pressures evident in Figure 5.9a is the rise in

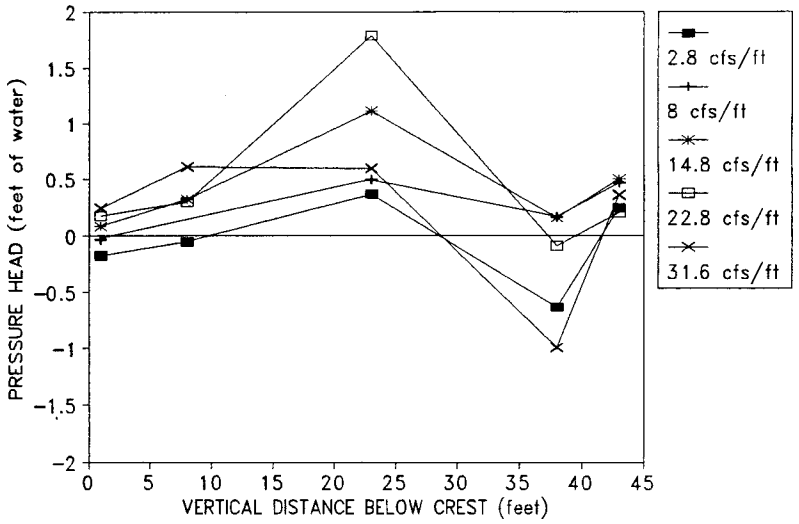

Figure 5.9a. Average Drainage Layer Pressures

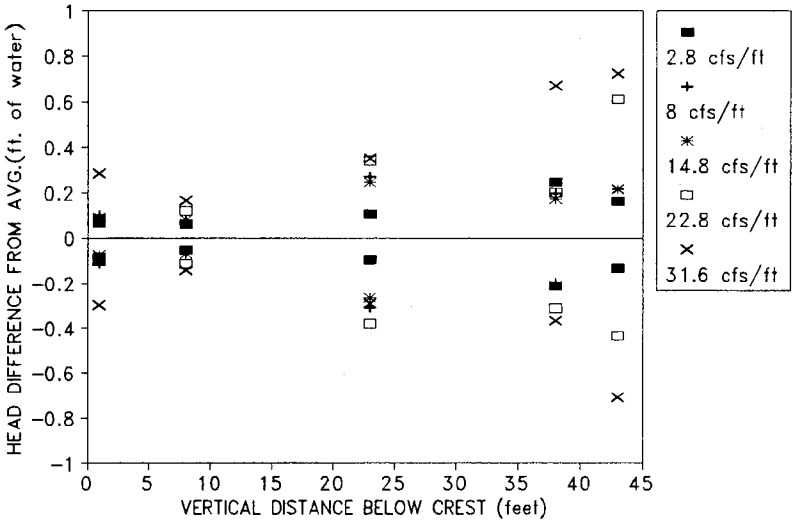

Figure 5.9b. Differences of Maximum and Minimum Drainage Layer Pressure Heads From Average Values

pressure that occurs near the toe of the slope. This rise may be attributed to poor drainage of the filter layer at its termination structure. At the CSU/USBR test facility, a solid piece of angle-iron anchored to the flume floor terminated the overlay and filter layer. Placement of drains in this structure would have helped alleviate the stagnation pressure that developed there.

Pressure Deviations from the Average

The possible magnitude of drainage layer pressure deviations from their average values should be considered when analyzing the hydrodynamic stability of a wedge block. To help facilitate this, the differences between maximum and minimum pressure heads and average values are presented in Figure 5.9b. Note that the magnitude of deviations from the average tend to increase with increasing unit discharge and with increasing downstream distance.

Analysis of the Hydrodynamic Stability of Wedge Blocks

Failure modes of a wedge-block overlay fall into three general categories. The first of these is the removal of a block or blocks due to hydrodynamic instability. A given block would be hydrodynamically unstable if the forces acting to dislodge it were greater than the forces acting to hold it in place. The other two failure modes are geotechnical and erosional failures. The current experimental setup of the CSU/USBR near-prototype facility does not allow the stability of underlying materials to be examined fully because the drainage layer was set directly on the flume's concrete floor. On the

other hand, the setup does permit conclusions to be drawn concerning the hydrodynamic stability of the blocks. An analysis of block stability has been carried out with the intention of providing qualitative and quantitative information about where on an embankment the block overlay tends to be less stable.

Numerous modes of movement can be envisioned for a wedge block including lifting, rotation about various points, and combinations of these. In the following analysis it was decided that an equalization of forces normal to the slope was a necessary prerequisite to failure. The normal direction was selected because the most significant dislodging forces, drainage layer pressures, exert their greatest influence in this direction. Additionally, as long as there is a net downward force, normal to the slope, block overlap forces make rotations unlikely. Thus, for this analysis, failure is assumed to occur when the forces acting to push a block away from the slope in a normal direction become large enough to equal forces acting to hold the block down.

Addressing the question of hydrodynamic stability is complicated by the fact that overlap and interlock forces, which are difficult to quantify, play a significant role. One approach to the problem is to ignore these forces altogether and consider them to be an added measure of safety. This approach has been adopted for the current analysis. The forces that remain to be dealt with are illustrated in Figure 5.10.

In order to determine the weight per unit width of a wedge block, a unit weight for concrete of 150 lb/ft^3 (2356 n/m^3) has been used. Using this value, the submerged weight per 1 foot (0.3 meters) of block width was determined to be 25 pounds (111 Newtons).

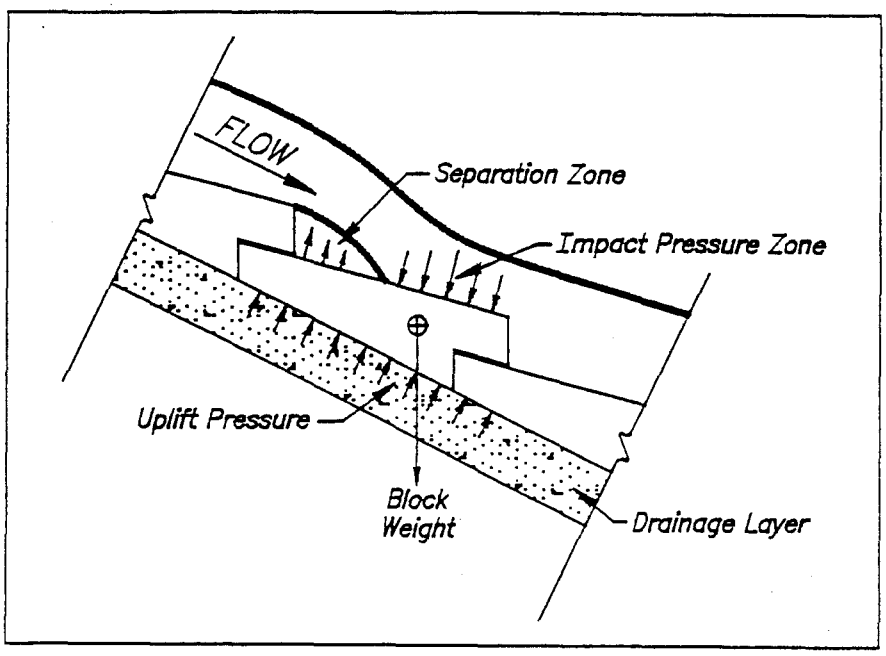

Figure 5.10. Block Pressure Forces Considered in Stability Analysis

In order to determine the pressure forces per unit width acting on the tread surface of the block, both negative and positive areas under each pressure profile in Figures 5.1a - 5.5a were computed and then summed up. The results of these calculations are presented in Figure 5.11.

Pressures in the filter layer were obtained from the piezometers located underneath each of the five instrumented blocks. These pressures, which have already been presented in Figure 5.9a, were multiplied by the length of the underside of the block to obtain values for the uplift force per unit width. Pressures acting beneath the overlapping block lip cancel because they act downward on the upstream end of the block and upward on the downstream end.

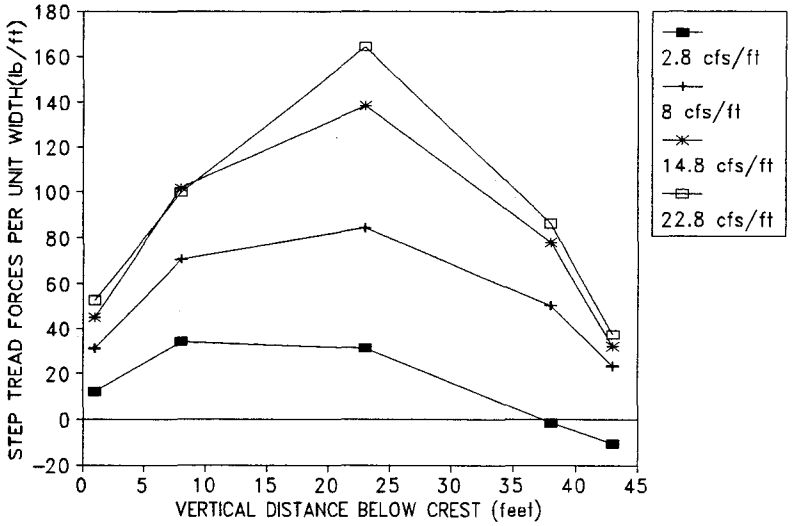

Figure 5.11. Summation of Step Tread Pressure Forces Per Unit Width

A sign convention was adopted for the forces. Restraining forces, which act toward the slope, were considered positive and dislodging forces, which act away from the slope face, were considered negative.

The assumptions made in the stability analysis may be summarized as follows:

1. The failure mode is assumed to be lifting normal to the slope.

2. The forces that have been considered are: impact pressure forces; separation zone pressure forces; the submerged weight of the block; and drainage layer pressure forces.

3. The restraining forces offered by block overlap, block interlock through pins, and anchoring of the overlay have been neglected and constitute an added measure of safety.

All normal forces were summed up for each instrumented block at each unit discharge to create Figure 5.12. If the summation of all normal forces is positive, then a net downward force acts on the block and it is stable. If that summation is negative, a net upward force is being sustained and the block is unstable. Figure 5.12 is essentially a plot of the hydrodynamic stability of blocks as a function of their location and the unit discharge. A number of conclusions may be drawn from the figure:

1. For the range of discharges tested at the CSU/USBR facility, the wedge-block overlay appears, in general, to be quite stable.
2. The stability of the wedge blocks tends to increase with increasing unit discharge. This may be explained as follows. As the unit discharge increases, stabilizing impact forces do also. Additionally, as unit discharge increases, separation zone pressures decrease, thus, improving aspiration of the subgrade and reducing uplift pressures.
3. There appears to be only one possibly unstable situation for the blocks and that is the toe region at very low discharges. At very low discharges, stabilizing impact pressures are low and a cascading type flow develops which does not separate or recirculate in the recessed portion of the step. Also contributing to the instability are the stagnation pressures which developed in the drainage layer due to poor drainage through the termination structure. Note that, although the last instrumented block appears unstable at the lowest discharge, no failure occurred due to the restraining forces which have not been considered.

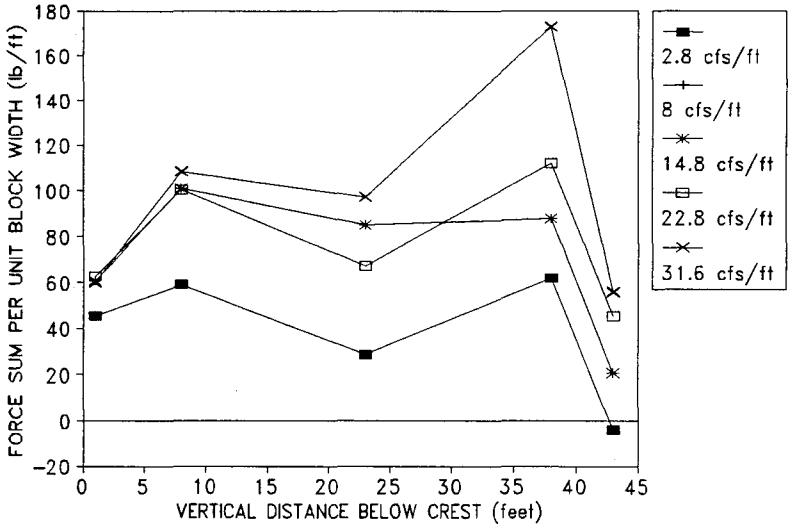

Figure 5.12. Summation of All Pressure Forces Per Unit Width Acting on Wedge Blocks

4. The crest and midslope regions are areas where the stability is not low in an absolute sense, but, tends to be lower relative to other areas of the embankment. These situations may be explained in the following way. Near the crest, velocities are low, therefore, stabilizing impact pressures are also low. Low velocities also mean that large pressure reductions will not occur in the separation zone which results in poor aspiration of drainage layer. Additionally, the horizontal momentum of flow at the crest may be causing some general reduction of pressures in the area. Near the midslope region, stability tends to decrease because this is the area of highest drain pressures.

Aspiration Characteristics

In order to get a qualitative look at the variation of aspiration along the embankment face, pressures underneath the instrumented blocks were compared to pressures recorded in the separation zone. For the separation zone, pressures recorded at tap 10 were used for the piezometer blocks located at step numbers 1, 44, and 84. Pressures at tap 11 were used for the piezometer blocks at steps 14 and 74. Tap 11 was preferred because it was closest to the drain opening, but, it was not functioning at three of the instrumented locations. For each of the tested discharges, filter layer and separation zone pressures have been plotted as functions of location on the embankment face in Figures 5.13 - 5.17. The data in these figures indicate that, over the majority of the embankment face, for all discharges tested, the direction of flow through the drains is out of the drainage layer. Thus, the drains appear to be working as desired. Exceptions to this appear to occur on the upper portion of the embankment, within a distance of approximately 20 feet (6.1 meters) downslope of the crest. Pressure differences between the top and bottom surfaces of a block are generally much smaller in this area than seen elsewhere on the embankment. In fact, Figure 5.13 shows that at a unit discharge of 2.8 ft^2/s (0.26 m^2/s), pressures on the top surface of the block are slightly higher than pressures on the bottom of the block. This indicates that water may actually be moving into the drain, rather than out, in this area of the overlay.

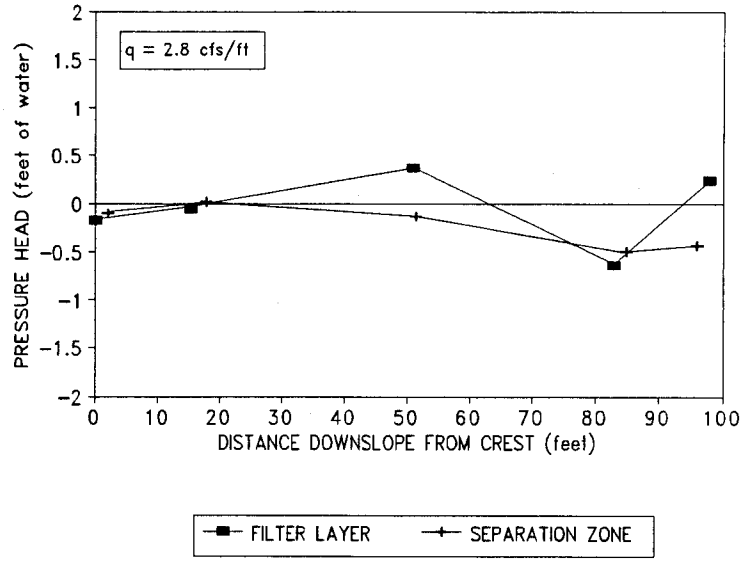

Figure 5.13. Pressure Head Difference Between Bottom and Top Block Surfaces Near the Overlay Drains, Unit Discharge = 2.8 ft^2/s (0.26 m^2/s)

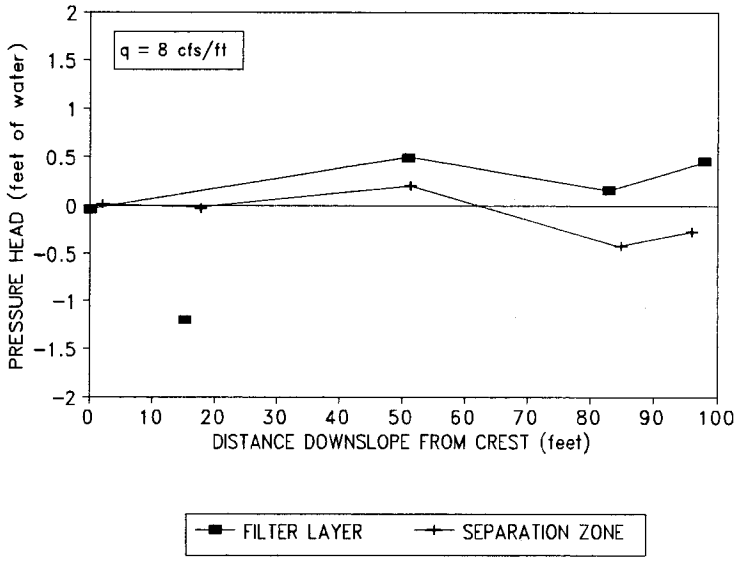

Figure 5.14. Pressure Head Difference Between Bottom and Top Block Surfaces Near the Overlay Drains, Unit Discharge = 8 ft^2/s (0.74 m^2/s)

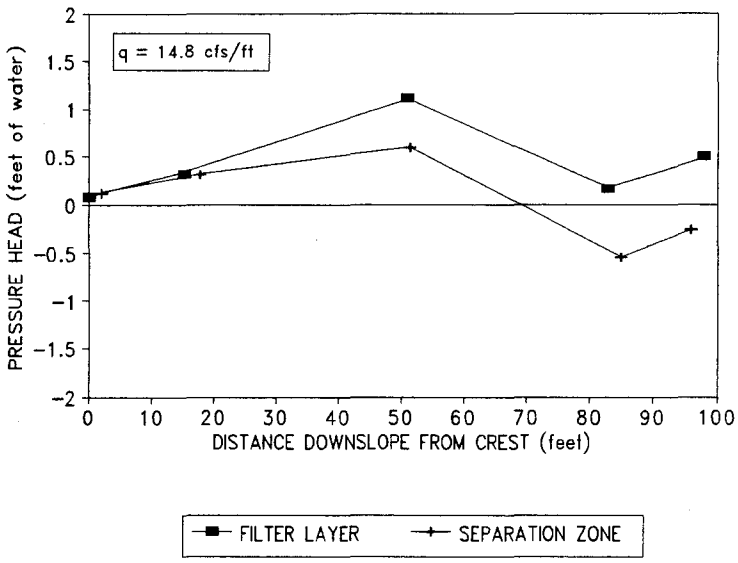

Figure 5.15. Pressure Head Differences Between Bottom and Top Block Surfaces Near the Overlay Drains, Unit Discharge = 14.8 ft^2/s (1.37 m^2/s)

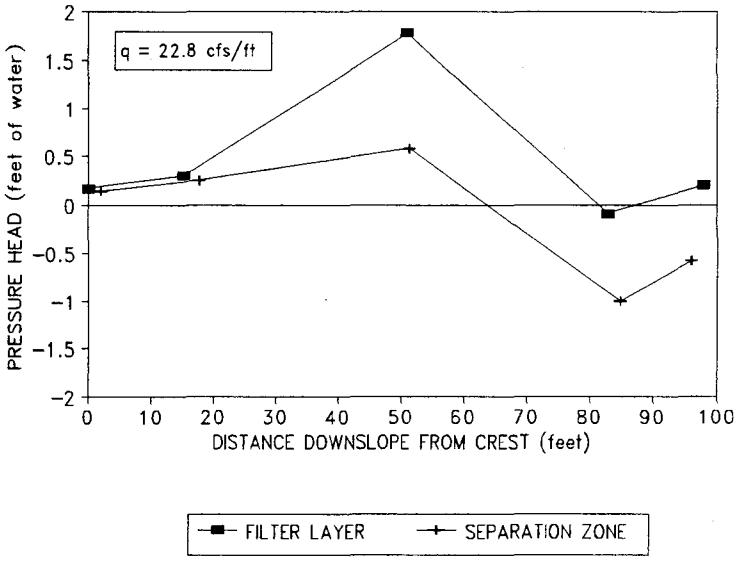

Figure 5.16. Pressure Head Differences Between Bottom and Top Block Surfaces Near the Overlay Drains, Unit Discharge = 22.8 ft^2/s (2.12 m^2/s)

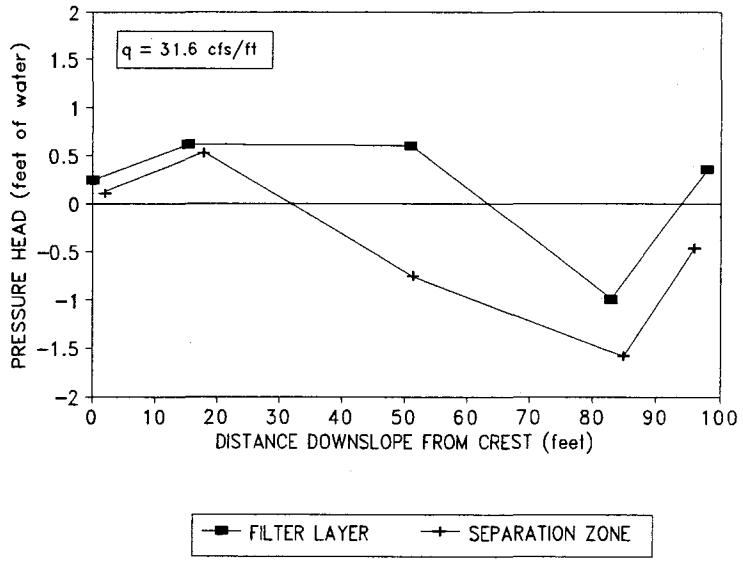

Figure 5.17. Pressure Head Differences Between Bottom and Top Block Surfaces Near the Overlay Drains, Unit Discharge = 31.6 ft^2/s (2.94 m^2/s)

Flow Reattachment

The point of flow reattachment on a row of wedge blocks is important because it has a large effect on stability. It would be undesirable for this point to be located on the far downstream end of a block's tread surface because the total impact force on the block would tend to be small. These impact forces are a major source of stability for the block which is subject to uplift pressures from the drainage layer. Research has shown that the step height to length ratio of blocks has a major influence on the point of flow reattachment. For ratios less than approximately 1:3.5, flow has been shown to reattach only to every other row of blocks (Baker, 1990). In this case a low pressure zone forms over the entire block and it becomes very vulnerable to uplift pressures.

The geometry of wedge blocks tested in the CSU/USBR facility is such that the step height to length ratio is 1:4.6 and the tread surface slopes downward from the horizontal by 15 degrees. From the standpoint of flow reattachment, this geometry seems quite good. The highest impact pressures, which correspond to the main point of flow reattachment, consistently occur in the vicinity of tap number 5 which is located 60 percent of the distance down the exposed tread surface of the block. Thus, large areas of the block are subjected to the stabilizing effects of impact forces. This point of flow reattachment varied little with location on the embankment or unit discharge. Significant movement of the reattachment point was observed only in two cases: at the piezometer block located immediately downstream of the crest and at the lowest tested unit discharge which produced a cascading or tumbling flow. In both cases, the highest impact pressures were instead recorded at tap number 6 which is located 77 percent of the distance down the exposed tread surface of the block.

Separation Zone Size

The size of the separation zone is important because it dictates where on an individual block drains must be placed to be effective. The block design tested in the CSU/USBR facility, had drainage holes cast into the underside of the overlapping lip of each block. Designs tested by researchers in the USSR and the UK, though, had drainage holes placed through the tread surface of each block. Reports on experiments conducted with the later design type indicate that drains should be placed no more than 1.5Δ to 2Δ downstream from the step face of the previous block, where Δ is the step

height (Baker, 1990 and CIRIA, 1992). Table 5.1 presents, for the two blocks which consistently exhibited negative separation zone pressures, the distances downstream from the step face over which negative pressures prevail. The table shows that, generally, at a given location, the length along a block over which negative pressures prevail remains somewhat constant. It is evident that at very low discharges the zone of negative pressure is elongated considerably, but, higher discharges present the limiting case for placement of drains. The height of steps tested in the CSU near-prototype facility was 2.5 inches (63 mm). Therefore, the results in Table 5.1 indicate that drains should be placed no further downstream of a step than 1Δ. For the tested geometry, locating drain holes any further downstream than 1Δ would fail to take maximum advantage of separation zone's low pressure.

Table 5.1. Negative Pressure Zone Size as a Function of Unit Discharge

Unit Discharge (ft^2/s)	Length of Negative Pressure Zone	
	Block Number 74 (in)	Block Number 84 (in)
2.8	6.0	7.8
8	3.1	4.4
14.8	2.3	4.0
22.8	2.7	4.2
31.6	2.5	3.9

DEPTH DATA

Flow depths measured with the DMI distance probe were compared to calculated depths in order to quantify the bulking due to air entrainment. Figure 5.18 presents the unaerated water surface profiles calculated by the method discussed in Chapter Three. Flow depths recorded with the distance probe at the bottom three platforms provided aerated depths for comparison. It was found that DMI flow depths were between 1 and 2 times the calculated depths and that the average was 1.5. These comparisons indicate that, on average, flows were undergoing a bulking of 50 percent due to air entrainment. Note that the DMI consistently interpreted the upper most limit of spray as the water surface. The flow depths recorded with the distance probe are presented in Figure 5.19.

Flow depths, measured by point gage, were also compared to the calculated depths. In general these two values compared quite well. Point gage depths were between 0.9 and 1.2 of the calculated depths and the average was 1.06. The flow depths obtained with point gages are presented in Figure 5.20.

VELOCITY DATA

The velocities determined using the Ott Meter and the Global Flow Probe are presented in Table 5.2. Rough continuity checks using measured depths and discharges indicate that all measured velocities are at least reasonable. Note, though, that many of the values must be viewed with caution for two reasons: many do not fall within the meter manufacturer's specified range of applicability; and the six-tenths depth rule was difficult to apply to the highly aerated flow.

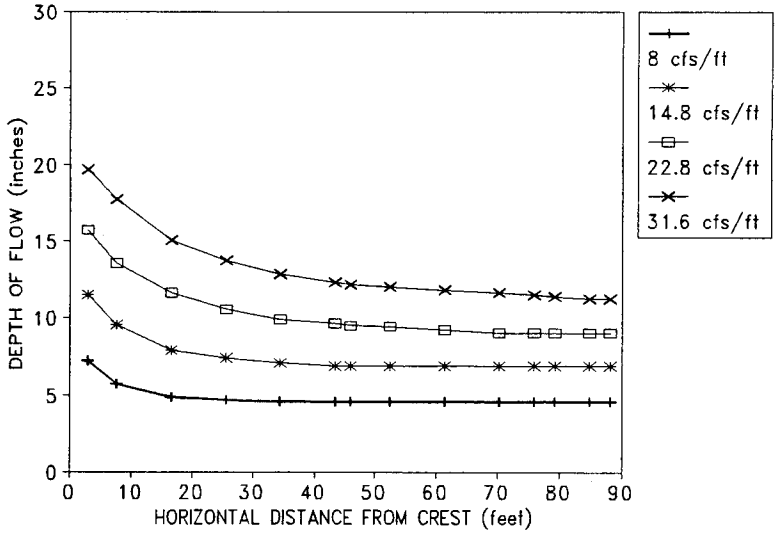

Figure 5.18. Calculated Unaerated Flow Depths

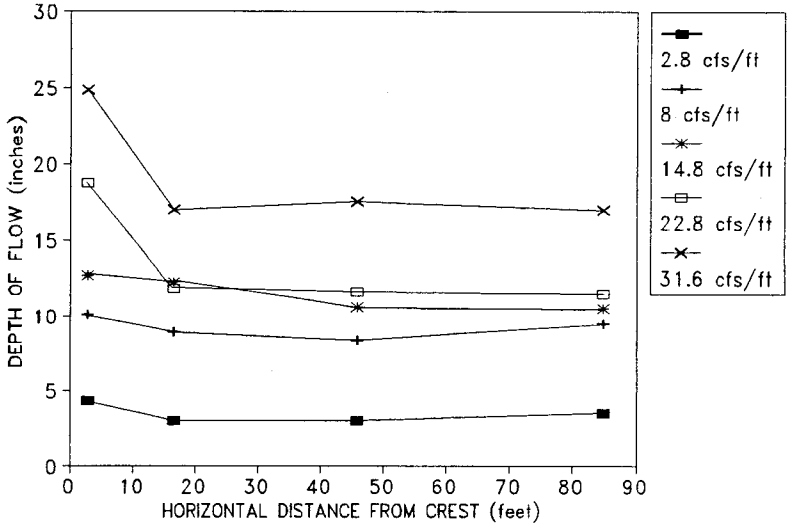

Figure 5.19. Flow Depths (Aerated) Obtained Using the DMI Distance Probe

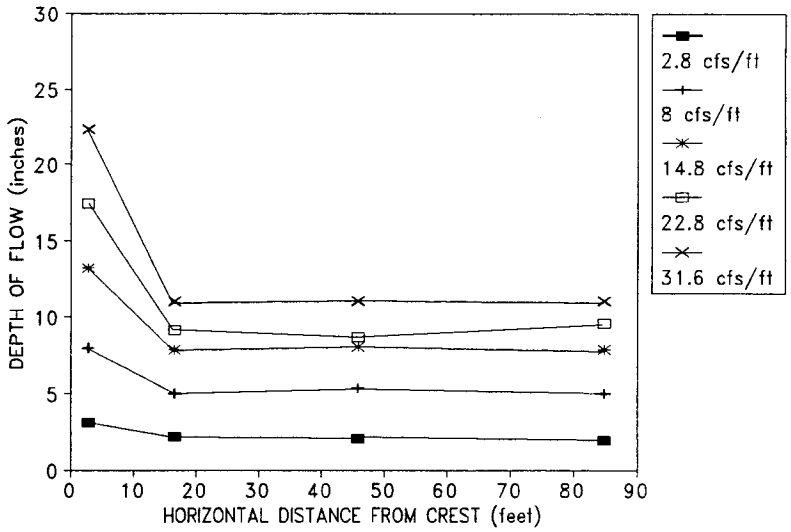

Figure 5.20. Flow Depths Obtained By Point Gage

Table 5.2. Measured Flow Velocities

Station	Velocity (ft/s)				
	2.8 ft^2/s	8 ft^2/s	14.8 ft^2/s	22.8 ft^2/s	31.6 ft^2/s
1	9.7	11.7	13.5	14.3	23.7
2		24.0	31.1		38.0
3		24.6	33.1		
4		27.2	33.5		

BLOCK MOVEMENTS

Block movements up or down change the orientation of the blocks to the flow and may decrease the amount of interlock a block has with its neighbors. Such changes, even

at one block, adversely effect the stability of the entire overlay.

The maximum possible values for up and down block movements were obtained by laying a string line from one flume sidewall to the other across the top surfaces of the blocks. This was possible because at the flume walls, 2 x 6 inch (51 x 152 mm) redwood boards prevented the settling of block edges. Deviations from horizontal were recorded for all four corners of the worst case block in a row. This procedure was carried out at approximately every fifth row of blocks on the slope after all five test runs had been completed. Essentially no upward movement of the blocks was observed on the slope and all downward movements were less than 0.55 inches (14 mm). Note that since the drainage layer sat on top of a non-erodible material a potentially important mechanism for block movement has not been investigated.

COMPARISON OF MODEL AND NEAR-PROTOTYPE RESULTS

A comparison of pressure data obtained by the USBR in their model study of wedge-block protection and pressure data obtained from testing at the near-prototype facility was carried out. When model unit discharges were scaled up by Froude criterion, they fell between the unit discharges tested at the near-prototype facility. Model pressure profiles from step numbers 15 and 47 were compared to near-prototype pressure profiles from step numbers 14 and 44. Figure 5.21a illustrates a typical comparison of scaled up model pressures at step 15 and near prototype pressures at step 14. If Froude criterion modeling was completely accurate, model pressures would be expected to fall in the vicinity of a curve, interpolated on the basis of unit discharge,

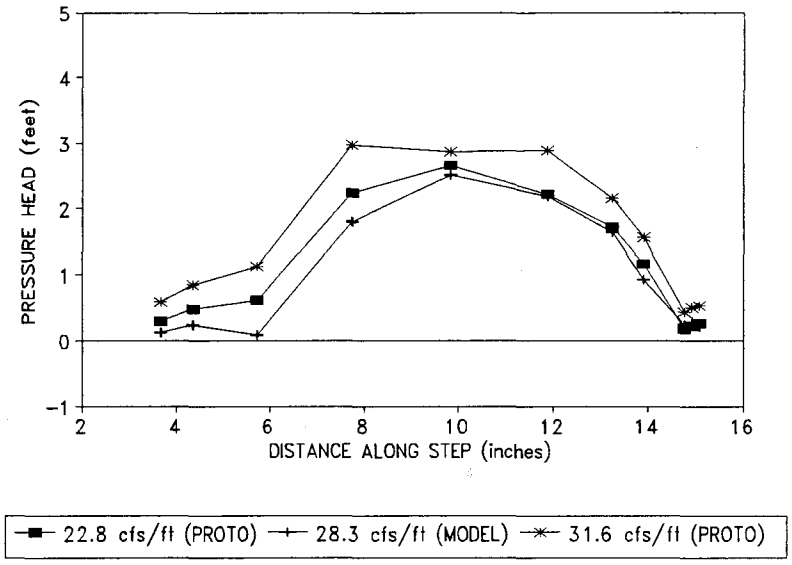

Figure 5.21a. Comparison of Model Pressure Profile at Step 15 With Bracketing Near-Prototype Profiles at Step 14

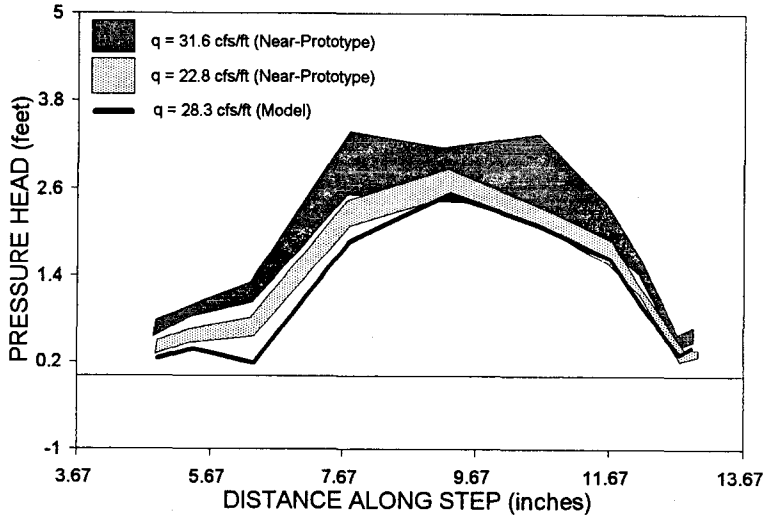

Figure 5.21b. Comparison of Model Pressure Profile at Step 15 With Bracketing Near-Prototype Pressure Fluctuation Bands at Step 14 (Band Width = 2 Standard Deviations)

between the two bracketing unit discharges of the near-prototype facility. This figure is typical of ones that may be obtained for other discharges at the same two steps in that the model pressure distribution is lower than would be expected. Figure 5.21b presents the same comparison but near-prototype profiles are presented as pressure fluctuation bands. The width of these bands is equal to twice the standard deviation of the pressure readings. Standard deviations for model pressures were not available. Figure 5.21b shows that there is some overlap of pressure readings, but, it is not large enough to question the conclusion that model pressures are lower than would be expected. The difference between the expected pressure distribution (the interpolated line) and the distribution given by Froude scaling of model data has been found to be fairly constant regardless of the flow rate or location on the step. Figure 5.22 illustrates this showing that when scaled up model pressures are subtracted from the expected pressures, model pressures are consistently low by between 0 and 1 foot (0 and 0.3 meters) of water with an average value of 0.4 feet (0.12 meters). This fairly constant difference between model and near-prototype pressures for different locations on the step illustrates the good correspondence obtained between the shapes of pressure distributions.

Figures 5.23a and 5.23b illustrate the similar comparisons for model step 47 and near-prototype step 44. Again, model pressure heads have been scaled up by Froude criterion and are plotted along with near-prototype pressures for bracketing discharges. For this location the model pressure distribution is again lower than would be expected and this is typical of plots that may be obtained for other discharges. Figure 5.24 presents the difference between the expected pressures and scaled up model

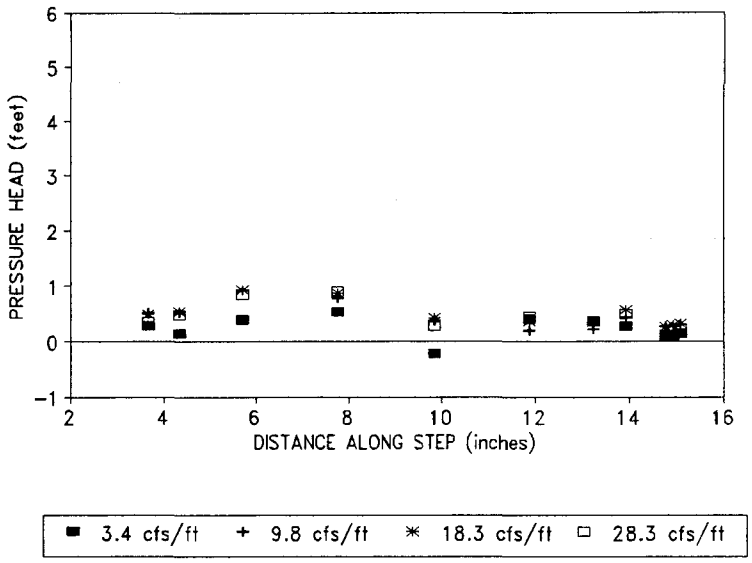

Figure 5.22. Difference Between Expected Model Pressures and Those Actually Recorded at Model Step 15 for Four Scaled up Model Unit Discharges

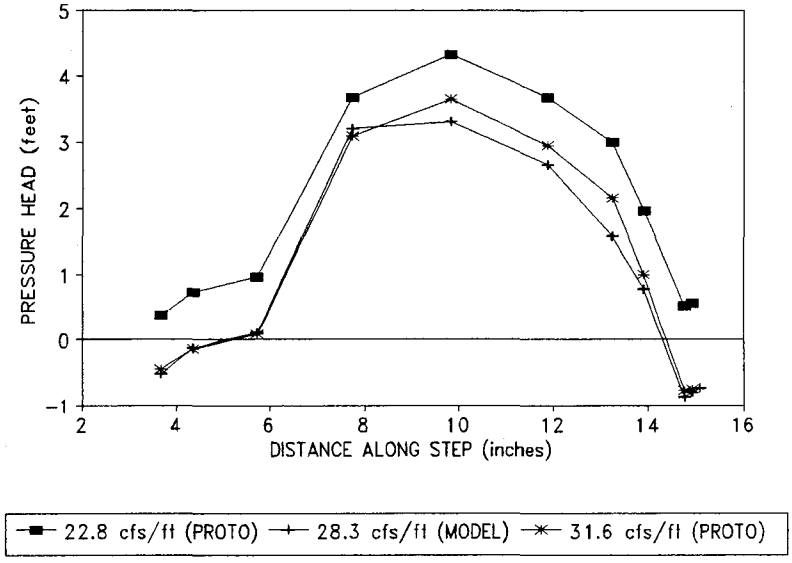

Figure 5.23a. Comparison of Model Pressure Profile at Step 47 With Bracketing Near-Prototype Profile at Step 44

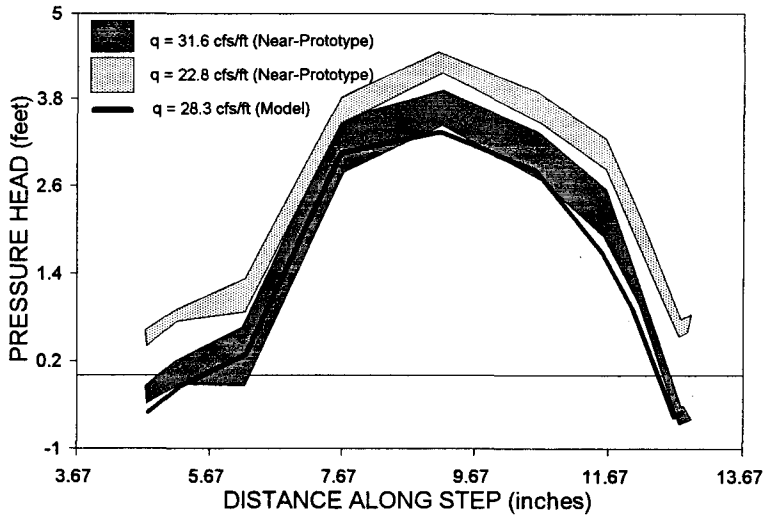

Figure 5.23b. Comparison of Model Pressure Profile at Step 47 With Bracketing Near-Prototype Pressure Fluctuation Bands at Step 44 (Band Width = 2 Standard Deviations)

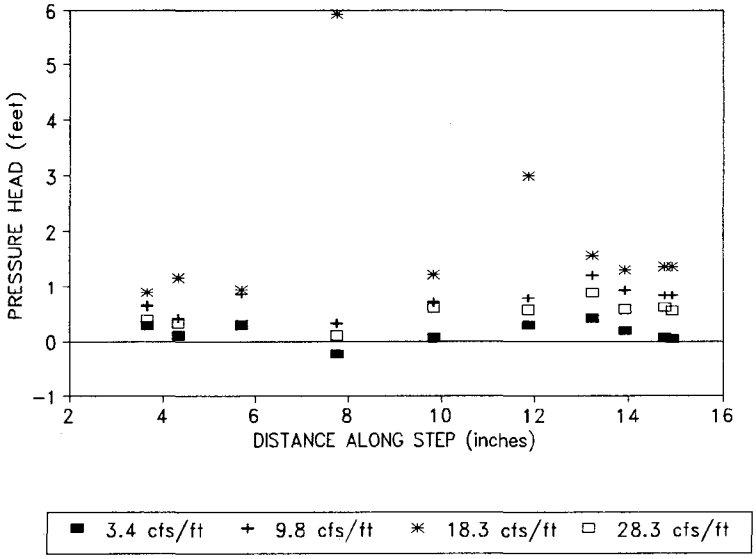

Figure 5.24. Difference Between Expected Model Pressures and Those Actually Recorded at Model Step 47 for Four Scaled up Model Unit Discharges

pressures. Model pressures are observed to be low by an average value of 0.7 feet (0.21 meters) of water.

The comparisons of model and near-prototype data discussed above indicate that although Froude criterion modeling of stepped spillways is not completely accurate, it may be sufficiently so to allow reasonable extrapolations of model or near-prototype data to larger embankments. From the data available it appears that scaling up pressures by Froude number produces a distribution that is low over the entire tread surface of a given block.

CHAPTER SIX

SUMMARY AND CONCLUSIONS

At the present time there are thousands of embankment dams in the U.S. that have the potential to be overtopped. The two most obvious solutions to this problem are to raise dam heights or increase spillway capacities. Both measures, though, are often prohibitively expensive. A promising alternative to these measures is to install a protective overlay on the downstream face of the dam which will allow it to be safely overtopped.

A variety of such overlay types have been tested and, to date, aspirating stepped designs appear to be the most stable alternative for high embankment dams. There are two basic reasons for this. One is that stepped overlays provide greater amounts of energy dissipation than their smoother counterparts. This translates into reduced stilling basin costs. The second is that the geometry of a stepped overlay is an inherently stable shape which is further improved by the inclusion of drains in the separation zone of each step. The superiority of stepped overlays is evidenced by the research that is discussed in Chapter Two. Consider the following conclusions which may be drawn from that chapter.

1. Stepped overlays, especially aspirating wedge-block designs, have been successfully tested under much more severe conditions than other protection forms. In the most extreme example, a test channel at Dneiper Power Station was protected with 1.6 foot (0.5 meter) thick overlapping wedge blocks. The overlay withstood a unit

discharge of 646 ft^2/s (60 m^2/s) and maximum velocities of 82 ft/s (25 m/s) for ten hours with only minor displacements of two blocks. Even this would probably have been avoided had the correct size of drain material been available.

2. Including the present near-prototype investigation, there have been at least ten separate model tests of wedge-block protection. Out of these, only one failure has been reported (Noori, 1985) and it apparently was not the result of hydrodynamic instability of the blocks.

3. Aspirated wedge-blocks and overlapping slabs have been used in ten prototype installations to date. The oldest of these has been in service since 1978. There has only been one failure, Jelyevski Dam, and it was attributed to poor embankment materials and a poorly designed drainage layer rather than to any hydrodynamic instability of the blocks themselves. In fact, the block overlay remained intact even though the embankment below was severely eroded.

Chapter Three discussed some theoretical considerations of wedge-block flow characteristics and embankment overtopping. The main points developed in that chapter are summarized below.

1. Recirculating flow in the separation zone may be roughly modeled as a forced vortex. The model indicates that the magnitude of pressure drop which occurs in the separation zone is a function of the velocity and pressure of the main flow at the outer edge of the vortex.

2. The principal of conservation of linear momentum may be used to analyze the

impact forces which act on the step tread. It was shown that impact pressures are directly proportional to water density and also a function of the square of the flow velocity. 3. Sources of uplift pressure on an embankment overlay include: changes in momentum at the crest; hydraulic connection of the overtopping head and the underside of the overlay; and impact forces acting at the spaces between adjacent blocks.

In Chapter Four, the results of wedge-block testing at the CSU/USBR near-prototype facility were discussed. A number of conclusions can be drawn from those tests.

1. On approximately the upper one half of the embankment, where accelerations are large, impact pressures generally rose in the downstream direction as a result of increased velocities.

2. On approximately the lower one half of the embankment, impact pressures generally decreased in the downstream direction due to increasing air entrainment and the lack of significant acceleration.

3. At any given location on the slope, impact pressures rise with increasing unit discharge.

4. On the upper quarter to one-half of the embankment, flow velocities were generally not high enough to produce a well developed recirculation flow for the range of discharges tested. Thus, separation zone pressures on the upper portion are generally positive and increase in proportion to increases in depth.

5. On the lower quarter to one-half of the embankment, velocities are high

enough to produce a well developed recirculation flow. Separation zone pressures are consistently negative and these pressures decrease with increasing unit discharge.

6. It was found that drainage layer pressures rise to a maximum value at approximately midslope and then begin to decline in the downstream direction. A poorly developed recirculating flow in the recessed portion of the step may explain the pressure buildup.

7. High drainage layer pressures were also found at the toe of the embankment. These pressures were probably due to poor drainage through the toe structure and subsequent development of a stagnation pressure.

8. An analysis of the hydrodynamic stability of individual wedge blocks indicates that, under the conditions tested, they are very stable.

9. In only one situation did analysis show the stability of the blocks to be questionable. This occurred at the toe of the embankment at a very low unit discharge. Better drainage though the toe structure would probably have greatly increased block stability at the toe by alleviating the stagnation pressure which developed in the drain there.

10. A comparison of drainage layer and separation zone pressures indicates that, over the majority of the embankment face, pressures are higher in the drain than the separation zone. Thus, water is generally moving out of the drainage layer and the overlay drains, therefore, appear to be working as desired.

11. Step geometry appears quite good from the standpoint of flow reattachment. Generally the main point of reattachment is located 60 percent of the

distance down the exposed tread surface of the block and does not move significantly with discharge or location. As a result, large areas of the blocks are consistently subjected to the stabilizing effects of impact forces.

12. Separation zone pressures show that, for the particular step geometry tested, drains should be located no further than 1Δ downstream of the vertical step face for maximum effectiveness.

13. A comparison of measured (recorded with the DMI) and calculated depths indicates that the flow undergoes an average bulking due to aeration of 50 percent.

14. No significant displacements of blocks or drain material were observed after the completion of all tests. During these tests, a total overtopping flow of more than 132 acre-ft (163,000 m^3) was delivered over a period of 16 hours.

15. A very good correspondence of block pressure profile shapes was observed in a comparison of model and near-prototype results.

16. Actual model step pressures tended to be lower than expected when scaled up and compared to near-prototype pressures. These differences averaged 0.4 feet (0.12 meters) and 0.7 feet (0.21 meters) of water, respectively, at two locations on the embankment.

REFERENCES

1. ASCE/USCOLD, (1975), "Lessons from dam incidents, USA."

2. Baker, R., (1989), "Pre-cast concrete blocks for dam spillways," Water Power and Dam Construction, July.

3. Baker, R., (1990), "Precast concrete blocks for high-velocity flow applications," Journal of the Institute of Water and Environmental Management, Vol. 4, No. 6, December, pp 552-558.

4. Baker, R., (1991), "Performance of wedge-shaped blocks in high-velocity flow," Laboratory study - stage 2, CIRIA.

5. Bivins, W., (1984), "Dam safety - An overview of a risky business," ASCE, Frontiers of Hydraulic Engineering.

6. Chen, Y.H., and Anderson, B.A., (1986), "Development of a methodology for estimating embankment damage due to flood overtopping," *Final Report*, by Simons, Li & Associates, Inc., for Federal Highway Administration and Forest Service, Contract Number DTFH61-82-00104, SLA Project Number DC-FHA-01, Washington D.C.

7. CIRIA, (1992), "Design of stepped block spillways," *Final Draft*, by Rofe, Kennard & Lapworth, Consulting Engineers, CIRIA Research Project 407, Surrey, U.K.

8. Clopper, P.E. and Chen, Y.H., (1988), "Minimizing embankment damage during overtopping flow," *Final Report*, by Simons, Li & Associates, Inc., for Federal Highway Administration, Washington D.C. and Bureau of Reclamation, Contract Number DTFH61-85-C-00131, SLA Project Number DC-FHA-03, Denver, CO.

9. Clopper, P.E., (1989), "Hydraulic stability of articulated concrete block revetment systems during overtopping flows," by Simons, Li & Associates, for Federal Highway Administration, U.S. Bureau of Reclamation, Soil Conservation Service, and Tennessee Valley Authority.

10. Dodge, R.A., (1988), "Overtopping flow on low embankment dams - Summary report of model tests," U.S. Bureau of Reclamation Report Number REC-ERC-88-3, Denver, CO.

11. El Khashab, A.M., (1986), "From drag resistance of two-dimensional stepped steep open channels," Canadian Journal of Civil Engineering, Vol. 13, pp 523-527.

12. El Khashab, A.M., (1987), "Materials for protecting earth weirs," Proceedings 1987 National Conference on Hydraulic Engineering, ASCE, Williamsburg, USA, pp 577-581.

13. Frizell, K.H. et al., (1991), "Embankment dams: Methods of protecting during overtopping," Hydro Review, Vol. X, No. 2, pp 19-30.

14. Frizell, K.H., (1992), "Hydraulics of stepped spillways for RCC dams and dam rehabilitations," Roller Compacted Concrete III, ed. by Hansen, K.D. and McLean, F.G.

15. Grinchuk, A.S. and Pravdivets, Y.P., (1977), "Pre-cast reinforced-concrete revetment of earth slopes used for discharging water," (translated from Russian), Gidrotekhnicheskoe Stroitel'stvo, No. 7, July, pp 25-28.

16. Grinchuk, A.S. et al., (1977), "Test of earth slope revetments permitting flow of water at large specific discharges," (translated from Russian), Gidrotekhnicheskoe Stroitel'stvo, No. 4, April, pp 22-26.

17. Hewlett, H.W.M. et al., (1987), "Guide to the design of reinforced grass waterways," *CIRIA Report 116*, London, U.K.

18. Kresty'sninov, A.M. and Pravdivets, Y.P., (1978), "Improved flood spillways for embankment dams," (in Russian), Godrotekhnicha e Melioratsiya, No. 4, pp 44-50.

19. Kresty'sninov, A.M. and Pravdivets, Y.P., (1986), "Stepped spillways for small dams," (in Russian), Godrotekhnicha e Melioratsiya, No. 8, pp 27-30.

20. Noori, B.M.A., (1985), "Investigation of stepped blocks protecting weir slopes," Phd thesis, University of Southampton, U.K.

21. NRC, (1983), "Safety of existing dams; evaluation and improvement."

22. Powledge, G. et al., (1989), "Mechanics of overflow erosion on embankments. I: Research activities," Journal of Hydraulic Engineering, ASCE, Vol. 115, No. 8.

23. Pravdivets, Y.P., (1978), "Conjunction of jet and tailwater with a surface hydraulic jump," (in Russian), Energeticheskoe Stroitel'stvo, No. 2, pp 23-27.

24. Pravdivets, Y.P. et al., (1980), "Value for money in the construction of an earth dam spillway on erodible foundations," (in Russian), Energeticheskoe Stroitel'stvo, No. 3, pp 10-14.

25. Pravdivets, Y.P. and Slissky, S.M., (1981), "Passing floodwaters over embankment dams," Water Power and Dam Construction, July.

26. Pravdivets, Y.P., (1982), "Peculiarities of work on spillways of precast concrete blocks," Godrotekhnicha e Melioratsiya, No. 1, January, pp 23-25.

27. Pravdivets, Y.P., (1987), "Industrial design of an earth overflow dam," (translated from Russian), Gidrotekhnicheskoe Stroitel'stvo, No. 12, pp 15-18.

28. Pravdivets, Y.P. and Bramley, M.E., (1989), "Stepped protection blocks for dam spillways," Water Power and Dam Construction, Vol. 41, No. 7, July.

29. U.S. Army Corps of Engineers, (1982), "National program of inspection of non-federal dams," *Final Report to Congress*, Washington, D.C., May.

30. USBR, (1974), "Design of small dams."